NOVEL CONCEPTS IN MDM2 PROTEIN REGULATION

Erin G. Worrall B.Sc (Hons)

Thesis submitted to The University of Edinburgh for the degree of

Doctor of Philosophy

November 2008

“Basic research is like shooting an arrow into the air and, where it lands, painting a target.”

Homer Burton Adkins

“I have yet to see any problem, however complicated, which, when you looked at it the right way, did not become still more complicated.”

Paul Alderson

“The most exciting phrase to hear in science, the one that heralds new discoveries, is not "Eureka!" ("I found it!") but rather "hmm....that's
funny...”

Isaac Asimov

CONTENTS

Declaration

I declare that this thesis has been composed by myself the undersigned Erin G Worrall and that the work herein is entirely my own unless otherwise clearly acknowledged. This work has been submitted for the degree of Doctor of philosophy and has not been submitted for any other qualification, professional or otherwise.

Acknowledgements

I would like to thank my supervisor Ted Hupp for giving me this opportunity and for his great patience and enthusiasm in my work. Huge thanks goes to Jenny and Susy for proofreading my thesis. Thanks also goes to Bart 'The master of Dual-luciferase assays' for providing great assistance and expertise with performing the dual-luciferase assays, Liam Worrall, my brother, for helping with the structural modelling, and Anne-Sophie, Nicky and Jenny for her help with characterizing the phospho^{Ser17} MDM2 antibody. I would also like to thank everyone in the lab, both past and present for making my time in the lab very enjoyable even when things were not working and for putting up with my cheek!. Finally I would like to thank my parents, Christine and Gary Worrall, who have always provided me with the support I needed to complete this thesis.

Abstract

The tumour suppressor p53 has evolved a MDM2-dependent feedback loop that has a dual role as either a stimulator of p53 protein translation through mRNA binding or a stimulator of p53 protein degradation through the ubiquitin-proteasome system. A unique pseudo-substrate motif or "lid" in MDM2 is adjacent to its N-terminal hydrophobic drug-binding pocket and we have evaluated whether the lid of MDM2 is a physiological regulator of this dual function of MDM2. Deletion of this flexible pseudo-substrate motif inhibits MDM2 indicating that this peptide stretch can function as a positive regulatory motif. Phospho-mimetic mutation in the pseudo-substrate motif at codon 17 ($MDM2^{S17D}$) stabilizes the binding of MDM2 towards p53. Molecular modeling orientates the pseudo-substrate motif over a charged surface patch on the MDM2 surface at Arg97/Lys98 and mutation of these residues to the MDM4 equivalent reverses the activating effect of the phosphomimetic mutation. Transient or inducible low level expression of $MDM2^{WT}$ can promote an increase in p53 protein steady-state levels whilst the expression of $MDM2^{S17D}$ in cells results in p53 protein de-stabilization. Phospho-specific antibodies to the MDM2 lid demonstrate two physiological conditions that alter lid phosphorylation: (i) lid hypo-phosphorylation occurs after DNA damage where p53 protein is stabilized and (ii) lid hyper-phosphorylation occurs at high cell density under conditions where p53 protein is de-stabilized. Expression of $MDM2^{S17D}$ in cells also de-stabilizes hyperubiquitinated mutant p53 under conditions where $MDM2^{WT}$ has no effect on mutant p53 protein degradation. The lid functions as a flexible

regulatory motif whose phosphorylation switches MDM2 from a synthesis mode to a degradation mode with implications for defining the physiological signals that control the MDM2-p53 feedback regulatory loop.

Abbreviations

AD(Ac)	Acid domain
AH	Azaserine-Hypoxanthine
AI	Arabinose inducible
APBS	Adaptive Poisson-Boltzmann Solver (Calculating electrostatic properties)
ARF	Alternate reading frame
Arg (R)	Arginine
Asp (D)	Aspartic acid
ATM	Ataxia telangiectesia mutated protein
ATP	Adenosine tri-phosphate
ATR	ATM-Rad3-related protein
BALB/C	Albino strain of laboratory mouse
BAX	BCL2-associated X protein
BCR-ABL	An oncogene fusion protein consisting of BCR and ABL
BSA	Bovine serum albumin
$CaCl_2$	Calcium chloride
C-Abl	Nonreceptor tyrosine kinase
CD	Circular dichroism
CHIP	C-terminus of Hsc70-interacting protein (E3 ligase)
CHK1	Checkpoint kinase 1
CHK2	Checkpoint kinase 2
CK1	Casein kinase 1
COP-1	Constitutive photo-morphogenic 1 (E3 ligase)
CREB	cAMP response element binding
C-terminal	Carboxy-terminal
Cul1	E3 ligases cullin family

Cys (C)	Cysteine
dH_2O	distilled H_2O
DMEM	Dulbecco's modified eagle's medium
DMSO	Dimethyl sulfoxide
DNA	Deoxyribonucleic acid
DNA-PK	DNA-activated protein kinase
dNTP	Deoxynucleotide triphosphate
DOC	Deoxycholate
DP	E2F dimerisation partner
DTT	Dithiothreitol
E2	Ubiquitin-conjugating enzyme
E2F	A family of activating transcription factors
E3	A ligase which transfers ubiquitin from E2 to substrate
EDTA	Ethylenediaminetetraacetic acid
ESI-MS	Electrospray ionization mass spectrometry
FBS	Fetal Bovine Serum
FL	Full length
ELISA	Enzyme-linked ImmunoSorbent assay
GFAP	Glial fibrillary acidic protein
Gln (Q)	Glutamine
Glu (E)	Glutamic acid
Gly (G)	Glycine
GST	Glutathione-S-transferase
HATS	Histone acetyltransferases
HCl	Hydrochloric acid
HECT	Homologous to E6-associated protein (E6-AP) C-terminus (E3 ligase
His (H)	Histidine
HRP	Horseradish peroxidase

HSP90	Heat shock protein 90
Hy	Hydrophobic pocket
IB	Immunoblot
IC_{50}	Concentration of drug that is required for 50% inhibition *in vitro*
Ile (I)	Isoleucine
IPTG	Isopropyl-β-D-1-thiogalactopyranoside
IR	Ionising radiation
IRF-1	Interferon regulatory factor 1
IRF-2	Interferon regulatory factor 2
JNK	c-Jun N-terminal kinase
kDa	kilo-Dalton
KLH	Keyhole limpet hemocyanin
KOH	Potassium hydroxide
LB	Luria-Bertani
Leu (L)	Leucine
Lys (K)	Lysine
MCS	Multiple cloning site
MEF	Mouse embryonic fibroblast
MDM2	Murine double minute 2 protein (E3 ubiquitin ligase)
MDM4	Murine double minute 4 protein
MDM-ES	MDM2 binding domain encoding sequence
$MgCl_2$	Magnesium chloride
MOPS	3-(N-morpholino)propanesulfonic acid
N-terminal	Amino-terminal
NaCl	Sodium chloride
NaF	Sodium fluoride
NaOH	Sodium hydroxide
NEDD8	Neural precursor cell expressed, developmentally down-regulated 8 (UBL)

NLS	Nuclear localisation sequence
NMR	Nuclear magnetic resonance
Ni-NTA	Nickel-nitrilotriacetic acid
NoLS	Nucleolar localisation sequence
ORF	Open reading frame
p21	Cyclin-dependent kinase inhibitor
p53	Tumour suppressor p53
PARP1	Poly (ADP-ribose) polymerase family, member 1
PBS	Phosphate buffered saline
P/CAF	p300/CREB-binding protein associated factor
PCR	Polymerase chain reaction
PDB ID	Protein database identification
Phe (F)	Phenylalanine
PIAS1	Protein inhibitor of activated STAT-1
Pirh2	p53 induced protein with a RING-H2 domain (E3 ligase)
Pro (P)	Proline
PTM	Post translational modification
Pu	Purine
Py	Pyrimidine
PKB/Akt	Protein kinase B/RAC-serine/threonine protein kinase
RAM	Rabbit anti-mouse
Rb	Retinoblastoma protein
RbCl	Rubidium chloride
Rbx1	Ring box protein 1
RING	Really interesting new gene
RLU	Relative light units
RNA	Ribonucleic acid
RPMI 1640	Roswell park memorial institute
rpm	Revolutions per minute

SB	Sample buffer
SCF	Skp, Cullin, F-box containing complex
SCF^{Skp2}	Mammalian SCF complex, composed of Rbx1, Skp1, Cullin and Skp2
SDS	Sodium dodecyl sulfate
SDS-PAGE	Sodium dodecyl sulfate polyacrylamide gel electrophoresis
Ser (S)	Serine
siRNA	Small interference RNA
Skp1	S-phase kinase-associated protein 1A (p19A)
Skp2	S-phase kinase-associated protein 2 (p45)
SNP	Single nucleotide polymorphism
STAT-1	Signal transducer and activator of transcription-1
SUMO	Small Ubiquitin-like Modifier
Syc-7	Small molecule which binds the MDM2 hydrophobic pocket
TAE	Tris-Acetate-EDTA
TBE	Tris-Borate-EDTA
TCA	Trichloroacetic acid
Thr (T)	Threonine
Trp (W)	Tryptophan
Tyr (Y)	Tyrosine
Ub	Ubiquitination
UBC	Ubiquitin conjugating enzyme E2 domain
UBL	Ubiquitin-like molecule
UPS	Ubiquitin proteasome system
UV	Ultraviolet
WT	Wild type
WW	Protein-protein interaction site characterised by two conserved trypophans
YY1	Ying Yang 1

Zn	Zinc

Chapter 1

INTRODUCTION

1.1 Oncogenes and tumor suppressors in cancer

Cancer arises as a result of a change in the activity or expression of oncogenes or tumor suppressors. These changes generally occur at the somatic level but can also occur through germ-line mutations, leaving offspring predisposed to some cancers. Cancer arises from a series of mutations within both oncogenes and tumor suppressors. Oncogenes are a group of genes that, when mutated, are highly expressed or overactive and as a consequence act to initiate carcinogenesis. Genes encoding proteins that control cell proliferation, apoptosis or both are generally regarded as having the potential to become oncogenes. These genes encode proteins that can be categorized into 6 groups: transcription factors, chromatin remodelers, growth factors, growth factor receptors, signal transducers, and apoptosis regulators. They are generally activated by point mutations, which can alter protein activity, or by gene amplification. For example the RAS oncogene, when mutated at codon 12, 13 or 61, becomes constitutively active resulting in a constant signal transduction cascade which promotes cell survival.

Mutations in RAS are common in lung, colon and pancreatic carcinomas (Rodenhuis, 1992).

The discovery of oncogenes provided a simple and powerful explanation for how cell proliferation is driven and how mutation of these genes can result in uncontrolled cell growth. For any process that drives cell proliferation forward there needs to be a process which can slow it down or stall it. Such genes are termed tumor suppressors and they function as anti-growth genes. The p53 gene is a tumor suppressor gene, and, its activity stops the formation of tumors by activating the transcription of the cyclin dependent kinase inhibitor p21 and preventing cell division. If a person inherits only one functional copy of the p53 gene from their parents, they are predisposed to cancer and usually develop several independent tumors in a variety of tissues in early adulthood as a result of mutation of the remaining allele. This condition is rare, and is known as Li-Fraumeni syndrome.

1.2 Ubiquitination overview

Ubiquitin is a 76 amino acid protein which can be covalently attached to target lysines on proteins through the carboxyl group of its C-terminal residue (Gly76). Ubiquitin was the first protein shown to modify other proteins (Pickart, 2001). First thought to just be a way of ridding the cell of misfolded proteins it has become apparent that ubiquitination has a much larger role to play in cellular signalling mechanisms to a similar extent as other post-translational modifications (PTMs) such as phosphorylation (Pickart, 2001).

Ubiquitin can form poly-ubiquitin chains through attachment of other ubiquitin moieties at lysine 48 or lysine 63. Ubiquitin attached through lysine 48 generally marks a protein for degradation via the proteasome, while mono-ubiquitination or lysine 63 linked ubiquitin chains can have other effects such as influencing cellular localisation and protein function (Hicke 2001). Ubiquitin is attached onto the target protein through the sequential actions of activating (E1), conjugating (E2) and ligase (E3) enzymes. The C-terminal lysine residue of ubiquitin is activated in an ATP-dependent step via an E1 enzyme, of which there is only one in humans (Figure 1.1A). The activated ubiquitin is then transferred to a cysteine residue within the ubiquitin carrier protein, E2 (Figure 1.1B). The final step involves an E3 ligase which attaches the ubiquitin moiety via its C-terminus in an amide isopeptide linkage to the ε-amino group of a specific lysine within the target protein (Hershko and Ciechanover, 1998) (Figure 1.1C). In addition to the E1, E2, and E3 cascade there is also evidence of the involvement of an E4 enzyme which can help catalyze multi-ubiquitin chain formation along with E1, E2 and E3 enzymes (Koegl et al., 1999).

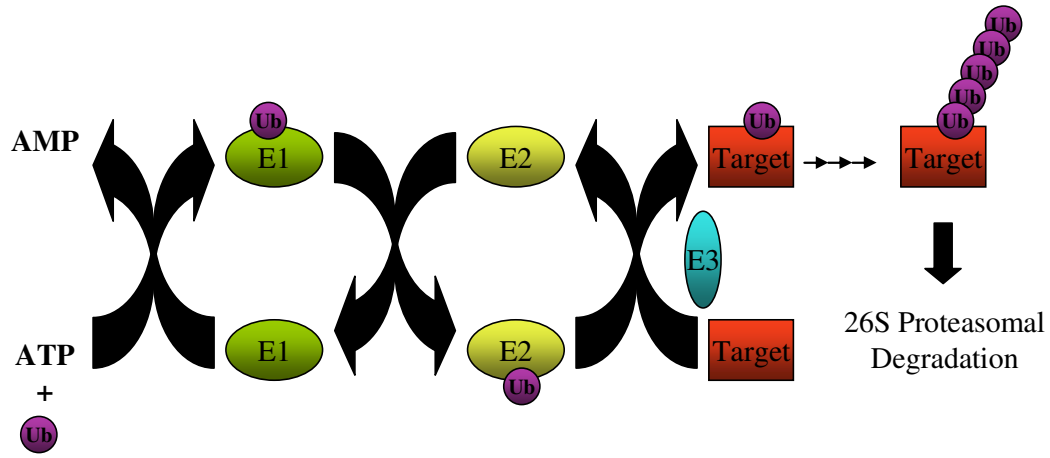

Figure 1.1 Ubiquitin transfer cascade. Ubiquitin (Ub) is activated by covalent attachment to E1 enzyme in an ATP-dependent reaction and is subsequently transferred to an E2 (ubiquitin-conjugating) enzyme. Ubiquitin is transferred from E2 to target substrate with or without the assistance of an E3 (ubiquitin ligase) enzyme. E3s control the specificity and timing of ubiquitination reactions. After several cycles of ubiquitination, the multiubiquitin chain-bearing substrate is recognized by the 26S proteasome and degraded.

1.2.1 E1 and E2 enzymes

There is only one E1 to begin the cascade off in mammals, yet there are around 60 mammalian genes encoding for E2's. This is the first step in substrate specificity in the ubiquitin proteasome system. Within the E2 enzyme is a 150 amino acid stretch which is highly conserved among E2's, called the ubiquitin conjugating enzyme E2 (UBC) domain and located within this the cysteine residue required for the E2's activity (Sullivan and Vierstra, 1991). E2's can range from being very small, consisting only of the core UBC domain, to very large with C or N terminus extensions, which can be

responsible for providing substrate specificity. E2's can either attach ubiquitin to the lysine on the target protein itself with the support of an E3, or it can attach the ubiquitin to the E3 before attachment to the target lysine (Mani and Gelmann, 2005).

1.2.2 E3 ligases

A second level of substrate specificity within the ubiquitin cascade is exerted by the E3 enzymes of which there are around 600 known enzymes. E3's work via many different mechanism, many of which are poorly understood, however they work either, through direct contact with ubiquitin or by helping the E2 transfer of ubiquitin to the substrate (Hershko et al., 1986) (Reiss et al., 1989). E3 ligases can be subcategorized into two classes, those which are: Homologous to E6-associated protein (E6-AP) C-Terminus (HECT) E3 ligase or: Really Interesting New Gene (RING) E3 ligases (Mani and Gelmann, 2005).

1.2.3 HECT E3 ligases

HECT E3 ligases work by covalently attaching the ubiquitin moiety from an E2 via thioester linkages before it is transferred to the substrate lysines. All HECT domain E3 ligases have a conserved 350 amino acid C-terminal HECT domain with a conserved cysteine residue. This cysteine is required for the conjugation of ubiquitin via a

transthiolation reaction which catalyzed by the E3 from the E2 (Scheffner et al., 1995). The N-terminal region of HECT E3 ligases provide the substrate specificity of the ligase and some forms contain a WW domain, characterised by two conserved tryptophan residues which form a pocket (Sudol et al., 1995b). This pocket can bind phospho-serine or phospho-threonine residues on the target protein suggesting that some kinds of phosphorylation may be a marker for ubiquitination by HECT E3 ligases. (Sudol et al., 1995a).

1.2.4 RING E3 ligases

RING E3 ligases are characterised by the presence of conserved cysteine and histidine residues orientated around two Zn^{+} ions (Joazeiro and Weissman, 2000). Rather than covalently binding ubiquitin before its transfer to the substrate, RING ligases provide a scaffold onto which the E2 and the substrate can bind, allowing transfer of ubiquitin directly from the E2 to the substrate. The RING E3 ligase's can be further sub-categorized into single or multi protein complexes. A good example of a single subunit E3 ligase is MDM2, which catalyzes the ubiquitination of the tumor suppressor p53 (Wallace et al., 2006), and CBL which is the E3 ligase for receptor tyrosine kinases (Joazeiro et al., 1999). The Skp1-cullin1-F-BOX (SCF) family represents the multi-subunit E3 ligase's (Deshaies, 1999). In the SCF enzyme complex, functions are divided between subunits with substrate recognition and E2 transfer being performed by different proteins within the complex. In the case of the mammalian SCF^{Skp2} complex,

the E2 is recruited through Rbx1 protein while cullin1 acts as a scaffold holding Rbx1 and Skp1, which recruits the F-BOX protein Skp2 for substrate recognition, in the correct positions (Jackson and Eldridge, 2002)

1.3 The Proteasome

Ubiquitination often leads to proteasomal degradation via the 26S proteasome. The 26S proteasome is a proteolytic multi-subunit complex whose main function is to unfold, breakdown and recycle proteins marked by ubiquitin chains (Kisselev and Goldberg, 2001). It consists of three main subunits, a 20S proteolytic core particle sandwiched between two 19S 'cap' regulatory complexes (Voges et al., 1999) (Figure 1.2). The 20S subunit is composed of four stacked rings with a core through the centre. Each outer ring is composed up of 7 α-subunits and each inner ring is composed of 7 β-subunits which posses the core proteolytic activity (Baumeister et al., 1998). The 19S subunits control substrate access into the proteolytic core through ubiquitin chain recognition. It is composed of a base and a lid and the lid is believed to be responsible for the recognition and cleavage of poly-ubiquitin chains. The base associates with the 20S subunit and contains 6 ATPases which are responsible for the ATP dependent opening of the α-ring of the 20S subunit allowing substrate access to the proteolytic region (Kohler et al., 2001).

The proteasome cleaves peptides multiple times before they are released, unlike conventional proteolytic enzymes which cleave peptides only once before they are released. This results in the release of peptides anywhere from 3-22 amino acids in length of approx 6 residues.

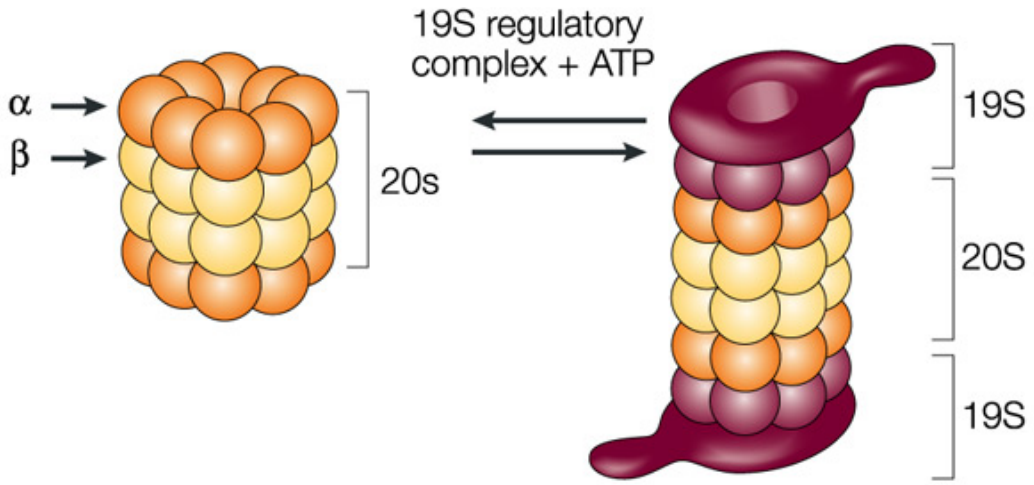

Figure 1.2 Proteasome Structure. Three dimensional image representing the 26S proteasome composed of a 20S complex consisting of two α and two β subunits and two 19S complexes at either end of the 20S complex, which act as lids. The 19S lids are responsible for ubiquitin recognition and catalyze entry into the 20S complex in an ATP dependent manner. (Adapted from (Adams, 2004).

1.3.1 Targeting the UPS

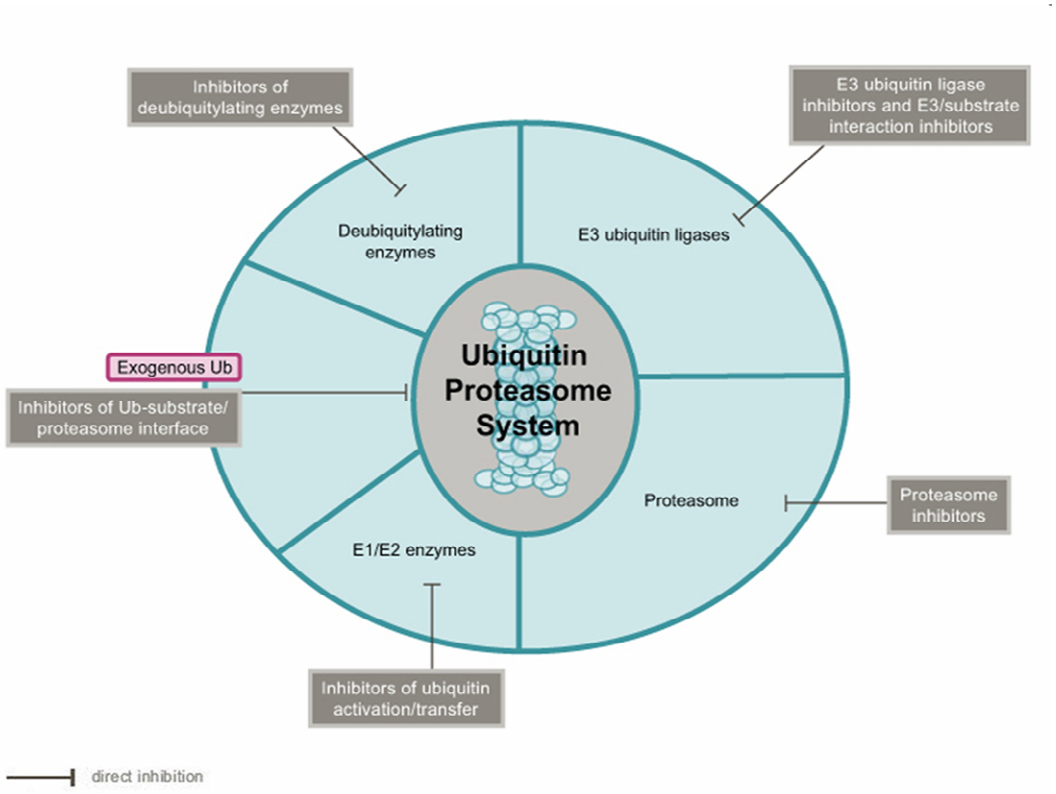

Figure 1.3 The UPS. Schematic representation of the ubiquitin proteasome system. The main UPS components and the types of inhibitors required for each stage are indicated (Adapted from (Guedat and Colland, 2007).

The growing understanding of the ubiquitin proteasome systems (UPS) involvement in human disease has led to the interest in developing small molecules that can inactivate specific components of the pathway (Figure 1.3). There are multiple steps within the UPS which can be targeted by such drugs; the earliest being the E1 enzyme and the latest being the proteasome. The ubiquitin activation step performed by the E1 is ATP dependent and provides a good starting point for drug design. The drug Gleevec,

developed by Novartis is a potent inhibitor of the oncogenic BCR-ABL fusion kinase by targeting its ATP pocket (Ren, 2005). Gleevec has since been shown to be less specific than originally thought and can bind a variety of ATP pockets with non-specific side effects.

The next step in the UPS is the transfer of ubiquitin from the E1 to the E2 enzyme. This step involves the E1 and E2 coming into contact with each other and thus providing the next possible druggable target. There is a growing realization that many protein-protein interactions occur through short linear peptide motifs and not through deep pocket interfaces. While these short linear peptide motifs may prove to be harder to inhibit, blocking these interactions may be a potential therapeutic target. The result of inhibiting the UPS at the E1, E2 stage is the global inhibition of the system.

1.3.2 Targeting E3 ligases

Targeting the E3 class of enzymes in the UPS provides a way of specifically controlling the activity of the E3's target protein. The targeting of one specific E3 ligase would allow the regulation of a distinct pathway, resulting in the stabilization of a subset of ubiquitinated proteins. For example, targeting and inhibiting the E3 ligase MDM2 would cause in the stabilization of its target p53, resulting in cell cycle arrest. The potential for such therapy could reduce any unwanted side effects of broad UPS inhibitors. There are three main classes of E3 ligases, RING, HECT and SCF complexes and the main difference between their mechanism of action is the mode of presenting the

E2 and ubiquitin moiety to the substrate. This difference obviously requires consideration when targeting E3 ligases.

For the RING class E3 ligases, there are two potential approaches for blocking their activity. Firstly it would be of benefit to disrupt the interaction between the RING finger and the E2 enzyme and secondly to disrupt the interaction of the E3 with the substrate. The latter strategy has yielded drugs such as Nutlin which inhibit the interaction between MDM2 and p53, but in this case it does not block p53 ubiquitination (Vassilev, 2004; Wallace et al., 2006). There are many potential druggable targets within the SCF ubiquitin ligases which due to their multi domain nature, possess numerous protein-protein interactions which could be targeted and disrupted. HECT domain E3 ligases bind the E2 as well as covalently binding ubiquitin. This provides three potential druggable interfaces, 1) blocking the interaction of the E2 with the E3, 1) blocking the attachment of ubiquitin to the E3 and, as with RING domain ligases, 3) blocking the E3-substrate interaction (Nalepa et al., 2006).

1.3.3 Targeting the proteasome directly

The final approach in targeting the UPS is to block the proteasome directly. The proteasome contains three types of active sites for proteolytic cleavage; chymotrypsin-like which cleaves after large hydrophobic residues, trypsin like which cleaves after basic residues and 'caspase-like' which cleaves after acidic residues (Kisselev and

Goldberg, 2001). The chymotrypsin-like sites were shown by genetic studies to be the main sites involved in protein degradation so these sites provided a target to develop inhibitors to. The proteasome inhibitor MG132 and the drug Velcade are such inhibitors. Velcade is an aldehyde derivative of three leucine residues with a blocked N-terminus. It had been predicted that inhibiting the proteasome would have a catastrophic effect on the cellular functions. However Velcade only inhibits the chymotrypsin like activity and as trypsin and caspase like activity is unaffected, Velcade can only reduce protein degradation by 40% at most. To inhibit peptide cleavage to a greater extent than this then more than one type of active sites need to be blocked within the proteasome and this can occur at higher concentrations of the drug Velcade (Goldberg, 2007; Kisselev et al., 2006). Targeting the ubiquitin proteasome pathway is an emerging concept in the fight against many human diseases including cancer and inflammatory diseases.

1.4 p53-structure/function

The human p53 gene has been mapped to the short arm of chromosome 17 (17q13), and spans approximately 20kb of DNA. The gene is composed of 11 exons, the first of which is non-coding and is localized 8-10kb away from exons 2-11 (Benchimol et al., 1985). Phylogenetic mapping elucidated five highly conserved regions within the p53

protein termed BOX-I (13-23), BOX-II (117-142), BOX-III (171-181), BOX-IV (234-250) and BOX-V (270-286) (Soussi and May, 1996).

The p53 protein consists of three functional domains; the N-terminal transactivation domain and proline rich region (amino acids 1-92); the central DNA binding domain (102-292); and the C-terminal negative regulatory domain and tetramerization domain (TD) (360-393) (May and May, 1999) (Figure 1.4).

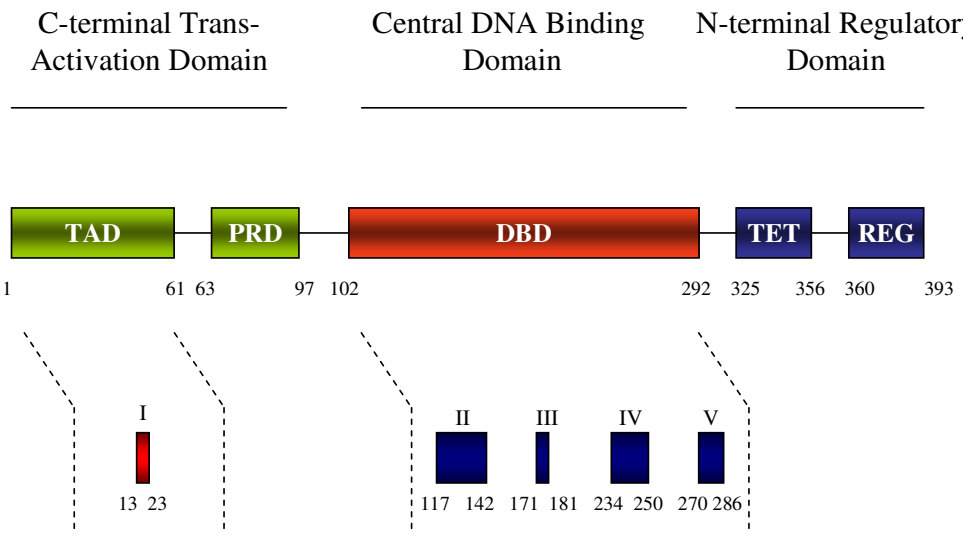

Figure 1.4 p53 Domain Structure. The N-terminus (green) contains the transactivation domain (TAD) and the proline-rich domain (PRD). The central region (red) contains the DNA-binding domain (DBD). The C-terminus (blue) contains the tetramerisation domain (TET) and the negative regulatory domain (REG). The corresponding amino acid residues are shown below each domain. The lower panel represents the highly conserved regions termed BOX-I, -II, -III, -IV, and -V with corresponding amino acids shown below each region.

1.4.1 The N-terminus of p53

The N-terminus of p53 is formed by two contiguous transcriptional activation subdomains (amino acids 1-42 and 43-63). Adjacent to these and completing the N-terminus is a proline rich domain (amino acids 62-91) with five repeats of the sequence PXXP which contribute to p53s apoptotic function. p53 interacts with components of the transcriptional machinery through the highly conserved BOX-I region within the transactivation domain. The N-terminus of p53 is also heavily phosphorylated in response to stress signals by a number of protein kinases. These include c-Jun N-terminal kinases (Oliner et al., 1993), the DNA activated protein kinase (DNA-PK) (Kamijo et al., 1998), casein kinase 1 (CK1) (Maclaine et al., 2008), ataxia-telangiectasia mutated kinase (ATM) and ataxia-telangiectasia related kinase (ATR) (Saito et al., 2002). C-terminal acetylation requires the binding of CBP/p300 to the N-terminus which can be stimulated by phosphorylation of p53 at ser15. Acetylation activates p53's function as a transcription factor. Phosphorylation within the N-terminus also leads to decreased interaction between p53 and its negative regulator MDM2 (Moll and Petrenko, 2003; Schon et al., 2002).

1.4.2 The Core-Domain of p53

The core region (102-292) forms a sequence specific DNA-binding domain consisting of the remaining four highly conserved regions BOX-II-BOX-V. p53 binds DNA through

a consensus DNA binding site which composed of two copies of the 10bp motif 5'-PuPuPuCWWWGPyPyPy-3' (Pu = purine base, Py = pyrimidine base, W = A/T) separated by up to 13 base pairs. (el-Deiry et al., 1992) The closer the sequence is to the consensus the higher the affinity for p53 binding. High affinity binding sites can be found in promoters of genes involved in cell cycle arrest whereas lower affinity sites are found in promoters of genes involved in apoptosis (Weinberg et al., 2005). With the advancement of crystallographic techniques came the structure of the core domain of p53. The structure revealed the presence of a large β-sandwich which forms a scaffold for DNA binding. The surface is formed by two large loops, L2 and L3, which are stabilized through a zinc ion and a loop-sheet-helix motif (Cho et al., 1994). The zinc ion is essential for p53 structure function as its removal drastically de-stabilizes the protein (Butler and Loh, 2003). The L3 is anchored to the minor groove of DNA via Arg248 while other conserved amino acids within the loop-sheet-helix motif make additional contacts with the major groove (Cho et al., 1994). Over 80% of p53 mutations are found within the core DNA binding domain highlighting the importance of the core domain in p53.

1.4.3 The C-terminus of p53

The C-terminus of p53 can also bind DNA, however this interaction is less sequence specific than the core region. The C-terminus can bind with high affinity to a variety of DNA structures including short single strands, X-irradiated DNA, and

insertion/deletions (Ahn and Prives, 2001). The C-terminus is thought to play a crucial role in determining the conformation of p53 and can switch p53 from latent to an active sequence specific DNA binding form. Allosteric regulation between the C-terminus and the core DNA binding domain is responsible for this interchange between the two states (Hupp and Lane, 1994a; Hupp et al., 1992). p53 can exist as a tetramer although under non stressed conditions it is usually present as a monomer (Sakaguchi et al., 1997). Upon binding to DNA consensus recognition elements, p53 forms tetramers through the tetramerization domain, and this is required for p53 to exert its activity as a transcription factor (Friedman et al., 1993; Kitayner et al., 2006). The tetramerization domain contains a β-strand linked to an α-helix by a single residue. Two monomers come together through their TDs to form a dimer. The p53 dimers then associate across a hydrophobic interface to form the tetramer (Jeffrey et al., 1995). Mutation within the TD decreases p53's ability to bind DNA. The formation of a tetramer is therefore integral to p53s activity as a sequence specific transcription factor (Lomax et al., 1998).

1.5 MDM2-structure/function

The murine double minute 2 (MDM2) gene was first identified in the 1980's and was found to be amplified in the spontaneously transformed 3T3-DM mouse cell line. Soon after this discovery, MDM2 was shown to be amplified in several human tumors and could bind to and inhibit p53 (Toledo and Wahl, 2007). A single nucleotide

polymorphism (SNP309) in the promoter of MDM2 can lead to its heightened expression by the increased binding of the transcriptional activator Sp1. This increase in MDM2 expression leads to the direct inhibition of p53, releasing the cell from p53 tumor suppression (Bond et al., 2004).

MDM2 is composed of a 'Lid' or pseudo-substrate domain, which at present has no known function, a hydrophobic pocket into which p53 binds, an acid domain which is involved in many protein interactions, a zinc finger which also has as yet no known function and a RING domain which is responsible for its ligase activity (Figure 1.5).

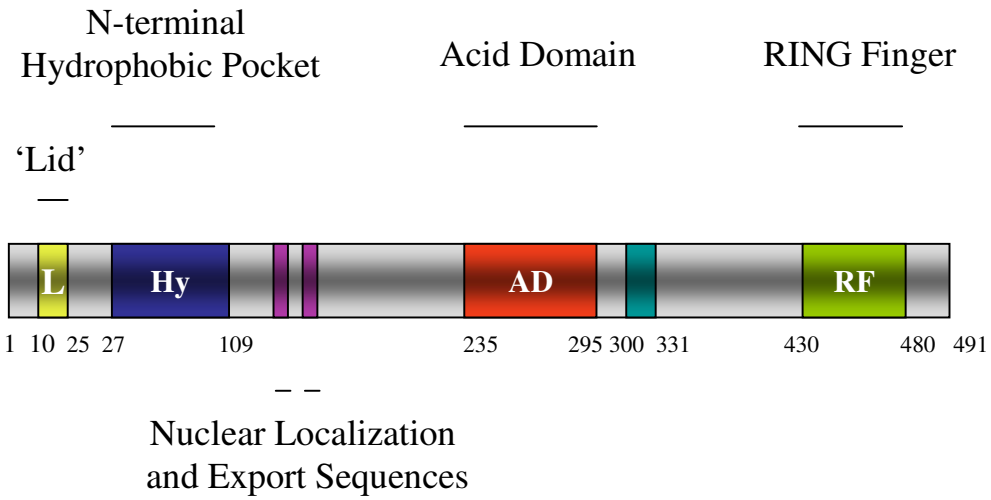

Figure 1.5 MDM2 Domain Structure. The N-terminus contains the Lid domain (yellow), the hydrophobic pocket responsible for binding p53 (blue) and the nuclear localization and export sequences (purple). The central region contains the acid domain (red) and the zinc finger (turquoise). The C-terminus consists of the RING finger (green) and embedded within the RING finger, an ATP binding site.

1.5.1 The MDM2 Lid

The N-terminus of MDM2 contains a flexible lid consisting of residues 10-25. This region is thought to compete with p53 for binding to the hydrophobic pocket of MDM2. The fact that the lid is not resolved in x-ray crystallography highlights its flexibility (McCoy et al., 2003). The lid peptide has a significant degree of homology to the p53-activation domain, suggesting that it might compete *in cis* for binding with p53 and act like a pseudo-substrate domain. Embedded within the lid sequence is a classic DNA-PK or ATM consensus (SQ-motif) whose phosphorylation is thought to disrupt the MDM2-p53 complex (Mayo et al., 1997).

1.5.2 The Hydrophobic Pocket of MDM2

MDM2 contains a hydrophobic pocket adjacent to the lid which consists of two globular repeats related by an approximate dyad axis of symmetry (Kussie et al., 1996). The two repeats come together via their hydrophobic faces and form the binding cleft for the p53 peptide (Uhrinova et al., 2005). This cleft or groove is 25 Å in length and begins as a very narrow and shallow cleft, then opens into a wider and deeper cleft. Crystal analysis shows the p53 peptide (18-26) adopts an amphipathic α-helical structure and binds into the wider deeper portion of the cleft. The remainder of the p53 peptide (27-29) is extended and associate with the shallow end of the cleft (Uhrinova et al., 2005). Three highly conserved amino acids, which are integral in p53s transactivation domain (Phe19,

Trp23 and Leu26), form a structure which fits tightly into the hydrophobic pocket of MDM2 (Lin et al., 1994; Picksley et al., 1994). The hydrophobic pocket has been shown to be highly flexible in terms of the peptides it can accommodate, in general the greater the helical structure of the peptide the higher its affinity for the pocket (Dastidar et al., 2008). Formation of a tight protein-protein interaction through a binding pocket makes this specific point of contact a very good site for drug development, with the aim of disrupting this interaction with small molecules.

1.5.3 The Acid Domain of MDM2

The acid domain of MDM2 is a site of many protein-protein interactions including p14ARF, L5, L11, L23, p300 and YY1 (Bothner et al., 2001; Dai and Lu, 2004; Marechal et al., 1994; Sui et al., 2004; Zhang et al., 2003). A second site for MDM2 to interact with p53 has also been discovered in the acid domain, and this interaction is essential for p53 ubiquitination (Wallace et al., 2006). This second site was first highlighted by the ability of peptides derived from the acid domain to interact with the core region of p53 (Yu et al., 2006b). Soon after this discovery, Wallace et al (2006) showed the direct interaction with MDM2 acid domain and the p53 BOX-V peptide (This study). It also showed that the acid domain of MDM2 and BOX-V region of p53 are essential for MDM2 catalyzed ubiquitination of p53. Structural data indicates that

the acid domain is mainly unstructured but can form β-strand structures upon ligand binding (Bothner et al., 2001).

p14/ARF activates p53 in response to mitogenic stimulus through binding to MDM2 via its acid domain, inhibiting its E3 ligase activity (Sherr, 1998; Zhang and Xiong, 2001), and sequestering it to the nucleolus (Weber et al., 1999). It has been proposed that binding of p14/ARF to MDM2 via the acid domain induces conformational changes within MDM2, exposing a cryptic nucleolar localization sequence (NoLS) in its C-terminus (Lohrum et al., 2001; Weber et al., 2000). ARF is also reported to stimulate MDM2 mediated p53 sumoylation through an unknown mechanism (Xirodimas et al., 2002). What is known is that the level of p53 sumoylation is regulated by MDM2 and ARF through a mechanism which requires the formation of a p53-MDM2-ARF complex (Chen and Chen, 2003).

In a mechanism similar to ARFs, several ribosomal proteins, L5, L11 and L23 have been shown to inhibit MDM2s E3 ligase function through binding to the acid domain (Bhat et al., 2004; Dai and Lu, 2004; Dai et al., 2004; Jin et al., 2004).

YY1 is a transcription factor that plays a crucial role in development however its full role and actions remain to be elucidated. YY1 knockdown by siRNA was shown to result in the accumulation of p53 in DT40 cells as a result of reduced ubiquitination. Conversely over expression of YY1 in DT40 cells resulted in increased p53 ubiquitination. It is thought that YY1 promotes the interaction between p53 and MDM2 which is essential for ubiquitination (Sui et al., 2004).

1.5.4 The RING finger domain of MDM2

The MDM2 RING finger is essential for its function as an E3 ligase and mutation of any of the Zn^{+} co-ordinating residues renders the protein inactive (Fang et al., 2000). The MDM2 RING domain is atypical when compared to conventional RING motifs with respect to the Zn+ coordinating cysteines and its multi-functions in the body (Poyurovsky et al., 2007). The C-terminal RING co-ordinates the dual activity of MDM2 in E2-mediated ubiquitin transfer (Linke et al., 2008) and in promotion of the MDM2-dependent stimulation of p53 protein synthesis (Candeias et al., 2008). Imbedded within the RING domain is an ATP-binding motif that regulates the chaperone functions of MDM2 (Stevens et al., 2008; Wawrzynow et al., 2007). At the extreme C-terminal is a peptide tail that also helps maintain RING domain conformation (Poyurovsky et al., 2007) (Uldrijan et al., 2007).

1.6 The MDM2:p53 interaction as a therapeutic target

The biological importance of p53 has been apparent for some time now. The myriad of roles MDM2 and p53 play within the cell and the elucidation of the structure of the MDM2:p53 interface has led to the realization that the MDM2:p53 interaction is a "druggable" target (Kussie et al., 1996). As previously discussed p53 is a transcription factor which controls the cellular response to stress through the induction of the cyclin dependent kinase inhibitor p21 (Xiong et al., 1993). MDM2 down regulates p53 activity

via a negative feedback loop through binding to the a-helical transactivation domain of p53 (Wu et al., 1993). In addition to inhibiting transactivation function of p53, MDM2 also exports p53 from the nucleus and targets it for proteasomal degradation via ubiquitination (Roth Levine 1998), (Pickart, 2001; Tao and Levine, 1999).

p53 is phosphorylated on specific serine residues in its transactivation domain in response to stress. This abrogates p53's interaction with MDM2 and activates its function as a transcription factor (Jimenez et al., 1999). Overexpression of MDM2 leads to inhibition of the p53 pathway and uncontrolled cell proliferation due to expression of the cyclin dependent kinase (CDK) inhibitor p21, and release from the inhibitory effects of the cell cycle. Amplification of the Mdm2 gene is observed in around 7% of human tumors and is most commonly found in soft tissue tumors (20%), osteosarcomas (16%) and oesophageal carcinomas (13%) (Momand et al., 1998). As a result of this amplification and suppression of p53 signalling, tumors become less susceptible to chemotherapeutic agents and do not undergo programmed cell death, or apoptosis. Treating cells that overproduce MDM2 with inhibitors which block the MDM2:p53 interaction should therefore result in the stabilization and accumulation of p53, increase MDM2 levels, and the activation of p53 target genes such as p21 and BAX. This in turn would cause cell cycle arrest in G1 and G2 phases and/or apoptosis (Vassilev, 2005). These factors put the disruption of the MDM2:p53 interaction at the forefront of therapeutic targeting for the treatment of cancer (Chene, 2003). A series of MDM2:p53 antagonists have been developed with varying success which includes antibodies and RNAi as proof of principle. Three other classes of inhibitors have been developed so

far, and they are peptide aptamers, naturally occurring compounds and small molecule inhibitors.

1.6.1 Antibodies and RNAi

Antibodies and RNAi targeting of the p53 pathway showed that by inhibiting MDM2 it is possible to stabilize and activate p53 signaling. Injecting the MDM2 N-terminal antibody 3G5 into cells resulted in the accumulation and stabilization of p53 (Blaydes and Wynford-Thomas, 1998). To date, antibodies are by far the most successful class of protein-protein interaction inhibitors available to target and disrupt the MDM2/p53 pathway but the difficulty in their administration (injection) and production has favoured the use of small molecules which can be administered orally ((Puppo et al., 2005). RNAi has also show that targeted knock down of MDM2 leads to the accumulation and activation of p53 (Tortora et al., 2000). Despite vast alteration of the oligonucleotide backbone of RNA to improve its stability *in vivo*, the problem still exists as to delivery of antibodies and RNAi across both cellular and nuclear membranes (Elmen et al., 2005).

1.6.2 Peptide Aptamers

MDM2 can bind with high affinity to 15 amino acid peptides derived from the transactivation domain of p53 (Fig 1.6). Further studies have developed more potent versions of this p53 peptide which inhibit the interaction between MDM2 and p53 to a higher degree (Bottger et al., 1997). When these peptides are directly applied to cells or expressed as peptide fusion proteins, p53 accumulation and activation can be observed. Crystal analysis of the structure of the MDM2 hydrophobic pocket in complex with the p53 peptide showed that only three amino acid side chains from the p53 peptide were buried within the deep pocket (Chene et al., 2000).

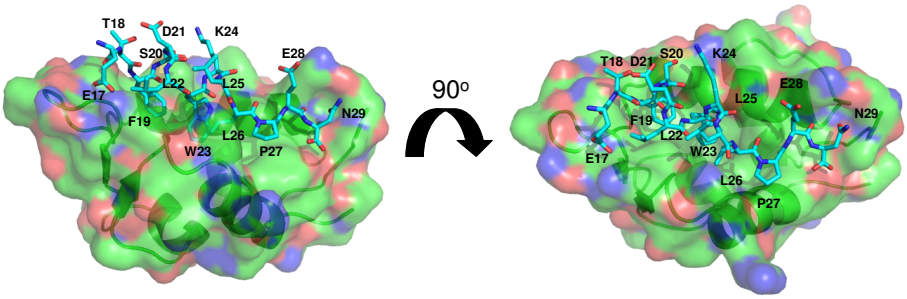

Figure 1.6. The MDM2 N-terminus with the BOX-I peptide of p53 bound within the hydrophobic pocket. F19, W23 and L26 are buried deep in the hydrophobic pocket of MDM2. Figures made using Pymol.

1.6.3 Natural inhibitors of the MDM2:p53 interaction

Of the drugs available for cancer treatment today, around 60% have arisen from natural products such as plant extracts. However, only three natural products have been found

to be effective in inhibiting MDM2:p53 interactions (Newman et al., 2003), these are chalcone based inhibitors, chlorofusin, and hexylitaconic acid.

Chalcones were proposed to bind to MDM2 within its canonical p53 binding pocket and inhibit MDM2:p53 interaction (Stoll et al., 2001). Although p53 levels accumulate after treatment with chalcones free p53 cannot bind to DNA and so is inactive (Murray and Gellman, 2007). This observation led a reduction into research on the chalcones so there mode of action still remains elusive.

Chlorofusin was identified as a MDM2:p53 inhibitor by screening 54,000 products generated from the fermentations of a wide range of microorganisms. Chlorofusin is a cyclic peptide and was shown to bind to the N-terminus of MDM2 with the ability to inhibit the MDM2:p53 interaction (Duncan et al., 2003). Chlorofusin is being used today to model potential analogues to elucidate the structure/activity relationship of this class of inhibitors so as to better understand there role and mechanism of action.

Hexylitaconic acid is a recently discovered inhibitor of the MDM2:p53 interaction, and is derived from a marine fungus (Tsukamoto et al., 2006). This inhibitor is structurally distinct from other inhibitors and more work is needed to characterize its mechanism of action.

1.6.4 Small molecule inhibitors of MDM2:p53 interaction

Small molecule inhibitors of the MDM2:p53 binding interface have also been developed. Drugs such as Syc-7, Nutlins and Benzodiazepinediones have been modeled to fit within the MDM2 hydrophobic pocket.

Syc-7 was the first non-peptidic small molecule inhibitor of the MDM2:p53 interaction (Zhao et al., 2002). It was designed *in silico* using knowledge of co-crystalised MDM2 and p53 peptide to mimic the orientation of Phe19 and Trp23 of the p53 BOX-I peptide which bind tightly into the binding cleft. Although the potency of syc-7 is very low, it provides a platform for the development of other drugs using a similar approach.

Nutlins were discovered through a high throughput screen of potential lead structures generated by Roche. They were the first small molecules shown to have high potency both *in vivo* and *in vitro*. Crystal structures of Nutlin bound to MDM2 revealed that Nutlin binding mimics the interactions of the p53 peptide, with a bromophenyl ring sitting deep in the tryptophan binding pocket of MDM2 and another bromophenyl ring occupying the leucine site while an ethyl ether side chain is directed towards the phenylalanine binding pocket. The imidazoline scaffold of Nutlin substitutes for the α-helical backbone and directs the side chains into their respective pockets (Figure 1.7). Nutlin was shown to activate p53 *in vivo* and arrest cells in G1 and G2 phases, preventing mitosis. Oral Nutlin treatment of nude mice, with established tumor xenografts resulted in a 90% reduction in tumor growth (Vassilev et al., 2004). Due to its potential Nutlin is already being screened for treatment of acute myeloid leukemia and multiple myeloma (Kojima et al., 2005; Stuhmer et al., 2005). Nutlin can only

activate p53 in tumors with wild type (WT) p53, however, as 50% of tumors are reported to have mutant p53, Roche devised a way to still use Nutlin in the treatment of these cancers. The process works as follows; pre-treatment with Nutlin induces cell cycle arrest in normal proliferating cells but does not affect cells with mutant p53. Subsequent treatment with a mitotic inhibitor, such as paclitaxel, causes mitotic arrest and apoptosis in cancer cells, but does not cause cytotoxic effects in normal cells (Carvajal et al., 2005).

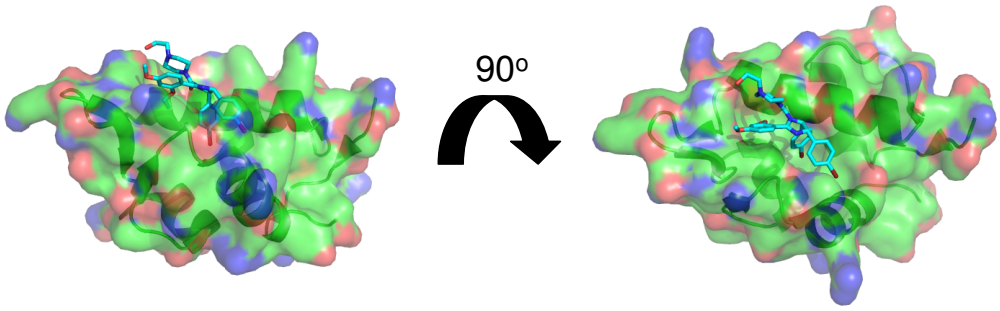

Figure 1.7. The MDM2 N-terminus with the drug Nutlin occupying the hydrophobic pocket. Nutlin fits within the binding pockets for F19, W23 and L26 of the p53 peptide. Figures made using Pymol.

Benzodiazepinediones were developed using high throughput screens to identify MDM2:p53 inhibitors by Johnson and Johnson Pharmaceuticals. Once again the compound was found to occupy the Trp23, Leu26 and Phe19 pockets of MDM2 (Grasberger et al., 2005). The drug was 375 times less potent in cells than *in vitro* and so was optimized to make it more permeable to cells and applied as a sensitizing agent

in conjunction with doxorubicin (Koblish et al., 2006). It was found that when used in conjunction with doxorubicin the level of doxorubicin required was vastly reduced in order to have the same effect. This synergism results in a reduction in side affects seen with doxorubicin alone (Koblish et al., 2006).

1.7 MDM2 models

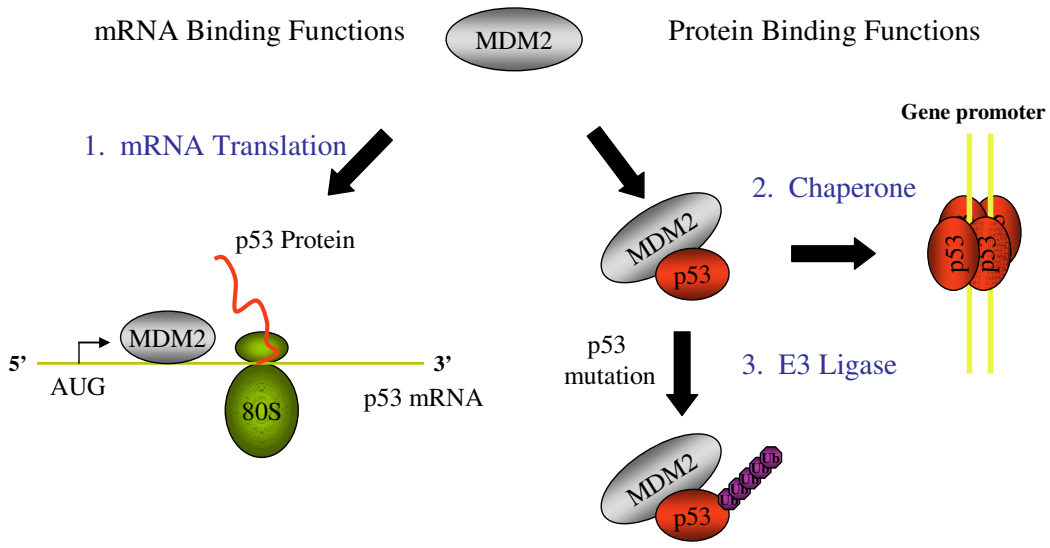

Figure 1.8 MDM2 Functions. MDM2 has three potential roles in regulating the activity of p53. Firstly it can promote p53 translation via binding to its mRNA, secondly it can chaperone p53 onto its transcriptional target promoters and thirdly, it functions as an E3 ligase to ubiquitinate p53. Mutations within p53 favour the ubiquitination route.

1.7.1 Ubiquitination and transrepression

Perhaps MDM2's most famous role is as a negative regulator of p53. This is achieved in two ways, either by MDM2 binding via its N-terminus to the p53 BOX-I domain, thus preventing p53 interactions with the basal transcription machinery such as p300 (Arva et al., 2005), or by targeting p53 for degradation via the proteasome (Figure 1.8) (Michael and Oren, 2003; Toledo and Wahl, 2007). The importance of MDM2 in p53 regulation is highlighted by the rescue of embryonic lethal MDM2 knockout mice by knockout of p53 (Jones et al., 1995). After cellular stress, such as exposure to UV or ionizing radiation (IR), both of which cause DNA damage, p53 becomes phosphorylated at specific serine and threonine residues in its transactivation domain. These phosphorylations impair the ability of MDM2 to bind to p53 through the TAD and as such MDM2 is unable to inhibit or degrade p53. This results in the accumulation and stabilization of p53 as a result of MDM2 not being able to inhibit or degrade it. Together with p53 modifications, MDM2 can also be modified by phosphorylation and this can result in reduced ubiquitination of p53. Following ionizing radiation, ATM rapidly phosphorylates MDM2 at serine 395 and this lowers its E3 ligase potential towards p53 (Maya et al., 2001). MDM2 can also interact with TAFII250, which promotes the phosphorylation of the acid domain of MDM2 by CK2. This results in increased p53 turnover. In contrast, phosphorylation of MDM2 at tyrosine 276 by c-Abl promotes its interaction with ARF, thus increasing its localisation to the nucleolus and decreasing p53 turnover (Allende-Vega et al., 2008; Dias et al., 2006). Multiple

phosphorylation sites are present within the acid domain of MDM2 and these been shown to be phosphorylated by a wide range of kinases (Hay and Meek, 2000). This region could provide an important role in regulating MDM2s function as an E3 ligase towards p53.

1.7.1.1 MDM4

MDM4 is a close relation and paralogue of MDM2. MDM4 shares much structural similarity to MDM2, including the presence of a RING but with one important difference in that it lacks its E3 ligase activity (Shvarts et al., 1996). From knockout studies in mice, it was discovered that MDM4 knockout mice die in the uterus, from p53 dependent cell proliferation arrest (Jackson and Berberich, 2000). It was hypothesised that MDM2 and MDM4 work closely together, with MDM4 stabilizing MDM2 and MDM2 facilitating nuclear import of MDM4 (Jackson and Berberich, 2000). One important feature of MDM4 is that its expression is not stimulated by p53 and its promoter does not contain p53 recognition elements (Marine and Jochemsen, 2005). A model incorporating the roles of MDM2 and MDM4 exists which suggested that under normal non-stressed conditions, p53 is ubiquitinated by MDM2 and kept inactive by MDM4 binding to its transactivation domain. Following cellular stress, MDM2 degrades MDM4, and perhaps to some extent itself, leading to the accumulation and activation of p53. As p53 transactivates the MDM2, increased MDM2 leads to elevated levels of MDM4 degradation and consequently further activated p53. After the cellular

stress has passed, MDM2 targets p53 for degradation and thus lowering p53 levels and as MDM4 levels increase, p53 activity returns to pre stress levels (Toledo et al., 2006).

1.7.1.2 Ubiquitination mechanism

While much is known about MDM2s function as an E3 ligase and how its activity is regulated, be it via post translational modifications, or protein-protein interactions, very little is known about the mechanism behind MDM2 catalyzed ubiquitination of p53. The E3 ligase catalyzed reaction involves at least two distinct steps, firstly the recognition of the substrates 'ubiquitination signal' and secondly the covalent attachment of one or more ubiquitin moieties to the substrate (Pickart, 2001). The accepted view, based upon evidence at that time, was that MDM2 mediated ubiquitination of p53 proceeded through the binding of the MDM2 N-terminus to the BOX-I site within the transactivation domain of p53. This was supported by evidence that mutation of single residue (Phe19) within the BOX-I domain of p53 prevented MDM2 catalyzed ubiquitination and that BOX-I mimetics could inhibit stable MDM2-p53 complex formation (Bottger et al., 1997; Lin et al., 1994; Liu et al., 2001). Previous studies have highlighted that MDM2 can still bind to p53 lacking the conventional N-terminal binding domain in the presence of RNA and that this site has the ability to regulate p53 ubiquitination in cells (Burch et al., 2000; Shimizu et al., 2002). Evidence was therefore beginning to emerge that suggested that ubiquitination of p53 was not solely controlled by the N-terminal interactions. Before the emergence of a second

possible binding site in p53, it was shown that the acid domain of MDM2 was essential for p53 ubiquitination (Meulmeester et al., 2003).

1.7.2 MDM2 as a chaperone

As well as its ubiquitination function, MDM2 has also been shown to be an effective chaperone of p53 and E2F1 (Stevens et al., 2008; Wawrzynow et al., 2007). It has previously been reported that the transient interaction of HSP90 with p53 is required for the correct assembly of the p53 tetramer on DNA, and that this occurs in an ATP dependent manner (Walerych et al., 2004). HSP90 can cooperate with MDM2 and CHIP (C-terminus of HSP70 Interacting Protein) to stimulate the unfolding of the native p53 tetramer (Burch et al., 2004). MDM2 can substitute for HSP90 in the ATP dependent folding of p53 onto the p21 promoter sequence (Figure 1.8) (Wawrzynow et al., 2007). This leads to the proposed model whereby MDM2 can bind p53 and partially unfold it acting as a molecular chaperone. Following cellular stress and activation of p53, MDM2 dissociates from the p53 protein resulting in spontaneous refolding of the p53 tetramer. This repeated binding, dissociation and refolding event could lead to p53 being in the correct conformation to bind DNA (Wawrzynow et al., 2007). MDM2 localises with latent p53 at the promoter sequences before but not after stress such as UV, supporting the idea of dissociation of MDM2 from p53 following cellular stress (White et al., 2006). This dual function of MDM2 is thought to regulate the equilibrium

of whether p53 should be folded correctly onto its promoter elements in cooperation with HSP90 or whether MDM2 should function as an E3 ligase and degrade p53. There is also evidence of additional E3 ligases functioning as molecular chaperones, such as CHIP, which can specifically recognise unfolded proteins after stress such as heat shock (Rosser et al., 2007).

Unlike p53, MDM2 appears to have the opposite effect on E2F1 with regards to its chaperone functions. E2F1 is misfolded in an ATP dependent manner and prevented from binding to its promoter elements. Thus the ATP binding motif within the MDM2 RING domain has clearly evolved to manipulate MDM2 protein-protein interactions in a substrate specific manner.

1.7.3 MDM2 in p53 mRNA binding

MDM2 has been shown to bind to p53 mRNA and stimulate p53 and its isoform lacking the N-terminus TAD, p53/47, translation in a manner which is independent of MDM2-p53 protein interactions. MDM2 can bind p53 mRNA through p53s MDM2 binding domain encoding sequence (MDM-ES) via the MDM2 RING domain, and this regulates the rate of p53 mRNA translation. Silent mutations introduced within the MDM-ES of p53 reduce the binding of MDM2 to p53 mRNA presumably by disrupting the RNA structure. Mutation of codon 446 in the MDM2 RING domain, which has previously been shown to be responsible for MDM2 binding to RNA, reduces the p53 mRNA

binding ability of MDM2 (Elenbaas et al., 1996). Experimental data also confirms that MDM2 is present at the polysomes in situations where MDM2 has high binding affinity for p53 mRNA, and that this allows increased p53 translation and reduced p53 ubiquitination (Candeias et al., 2008). The physiological factors that regulate the ability of MDM2 to promote the synthesis of p53 on one hand or its degradation on the other are not clear; indeed p53 synthesis, elevated specific activity, and enhanced rates degradation might even be coupled (Liu et al., 2001)

1.8 Post translational modifications of MDM2

As previously described, MDM2 contains several conserved functional regions, a flexible lid, an N-terminal hydrophobic pocket, an acid domain and a RING domain, all of which are required for MDM2 to function correctly as an E3 ligase, a chaperone or in mRNA binding. MDM2s activity is regulated by multiple post translational modifications (PTMs) depending on the cellular signals. Such PTM's include self ubiquitination, sumoylation, neddylation, acetylation and phosphorylation.

1.8.1 MDM2 auto-ubiquitination

MDM2's activity as an E3 ligase can mediate auto-ubiquitination as well as substrate ubiquitination (Fang et al., 2000). However this finding has recently been challenged

by *in vivo* mouse models whereby mutant MDM2 lacking its E3 ligase function is degraded in the same way as MDM2 WT. This study came to this conclusion by a number of observations; first MDM2 wild type and RING mutant constructs have the same half life, both are stabilised by the addition of the proteasome inhibitor MG132 and both yield identical ubiquitin modified bands following MG132 treatment. They felt it was unlikely that another E3 ligase would be able to target and ubiquitinate the MDM2 RING mutant with exactly the same kinetics as wild type MDM2 autoubiquitinates itself (Clegg et al., 2008). As such they proposed that both wild-type and mutant MDM2 are ubiquitinated by an as yet unknown E3 ligase. In support of this it has recently been reported that the histone acetyl transferase, PCAF, can both ubiquitinate and degrade MDM2 (Linares et al., 2007). The observation that MDM2 can autoubiquitinated is thought to come about by over expression of the protein within the cell via transfection. When MDM2 WT or MDM2 RING mutant are over expressed in cells, the MDM2 WT can be autoubiquitinated whereas the RING mutant tends to accumulate. It is thought that the endogenous E3 ligase cannot keep up with ubiquitination of exogenous MDM2 and that at these high levels, MDM2 gains the ability to auto-ubiquitinate, thus MDM2 WT can degrade itself and the RING mutant which lacks the ability to ubiquitinate isn't degraded and therefore accumulates (Clegg et al., 2008).

1.8.2 MDM2 can be Neddylated

Ubiquitin is the founding member of the ubiquitin like family of proteins (UBL). Like ubiquitin, ubiquitin like proteins are small proteins that are covalently ligated to target protein via an iso-peptide linkage between the C-terminal carboxyl group of ubiquitin like proteins and the ε-amino group of a lysine residue in the target protein (Ciechanover, 1998). Two of these ubiquitin like proteins include SUMO and NEDD8, and their effects on protein regulatory functions differ to that of ubiquitination (Weissman, 2001).

Amongst the myriad of UBL family members, NEDD8 is the most homologous to ubiquitin. The mechanism of NEDD8 conjugation to its target protein is analogous to that of ubiquitination. E1 and E2 enzymes are required for NEDD8 activation and conjugation to target proteins. A role for NEDD8 conjugation has been highlighted in plant, fungal and animal systems and is thought to be involved with cell proliferation, viability and development (Cernac et al., 1997; Osaka et al., 2000; Tateishi et al., 2001).

MDM2 has been shown to neddylate p53 both *in vivo* and *in vitro* and this neddylation inhibits p53's transcriptional activity but does not target it for degradation. MDM2 is also a target for neddylation and a functional RING finger is required to achieve this. MDM2 controls neddylation of bothp53 and itself, thus the NEDD8 conjugation pathway inhibits both the transcriptional activity of p53 and the suppressive effect of MDM2 on p53 function (Xirodimas et al., 2004).

1.8.3 MDM2 can be Sumoylated

The reversible modification of proteins involved in gene expression by the small ubiquitin like modifier (SUMO) can regulate protein stability, localization, protein-protein interactions and DNA binding. Like that of NEDD8 and ubiquitin conjugation, sumoylation is mechanistically similar, with the activation and transfer achieved by E1 and E2 enzymes. Sumoylation is thought to play a major role in proteins involved with gene expression (Gill, 2003).

MDM2 can be sumoylated *in vivo* and *in vitro* by the E2 enzyme Ubc9, and the E3 ligases PIAS1 and PIASxβ (Buschmann et al., 2001; Miyauchi et al., 2002). Sumoylation is thought to regulate MDM2s localization within the cell, facilitating SUMO-mediated nuclear entry which can be regulated by ARF (Miyauchi et al., 2002). ARF inhibits MDM2 catalyzed p53 ubiquitination but promotes MDM2 sumoylation (Xirodimas et al., 2002). This supports the idea that SUMO and ubiquitin modifications can be mutually exclusive and/or antagonistic (Meek and Knippschild, 2003). Using a mutant Ubc9 to act as a dominant negative and down regulate sumoylation in cells it was found that sumoylation of MDM2 was reduced and this was accompanied by an increase in ubiquitination of MDM2 and the concomitant decrease in p53 ubiquitination (Buschmann et al., 2001). Thus sumoylation provides a mechanism in which to regulate the activity of MDM2's ligase function.

1.8.4 MDM2 can be Acetylated

Sequence specific transcription factors can be activated by the cofactors histone acetyl-transferases (HATS) such as p300, CREB binding protein (CBP) or p300/CPB-associated factor (P/CAF). HAT-mediated facilitation of gene expression usually involves acetylation by HATS of core histones at the target gene promoters, generating a more accessible chromatin conformation for the transcriptional machinery to access (Jenuwein and Allis, 2001). As well as acetylating histones, transcription factors can also be acetylated directly (Kouzarides, 2000). p53 is such a transcription factor which is targeted for acetylation by p300, and thus activates transcriptional activity. MDM2 can negatively regulate this acetylation by binding to p53 transactivating domain masking the p300 binding site (Gu et al., 1997).

MDM2 can interact with p300 and CBP and can lead to an increase in p53 ubiquitination (Grossman et al., 2003; Grossman et al., 1998). Further studies identified MDM2 a target for acetylation by CBP and p300 (Wang et al., 2004). Although the interaction between p300 and CBP can lead to an increase in p53 ubiquitination, the acetylation of MDM2 reduces its activity as an E3 ligase towards p53 and can increase its own degradation (Wang et al., 2004). Thus p300/CBP may play a dual role in activating p53 transcriptional activity and inactivating MDM2's negative regulation of p53.

1.8.5 MDM2 can be Phosphorylated

As briefly eluded to earlier MDM2 is subject to control by phosphorylation at multiple residues. Nearly 20% of the amino acid sequence of MDM2 is serine or threonine residues, many of which have been shown to be phosphorylated *in vivo* (Meek and Knippschild, 2003). The N-terminus and the acid domain contain the two main clusters of phosphorylation residues within the MDM2 protein (Hay and Meek, 2000).

MDM2 is phosphorylated by ATM at ser395 in response to genotoxic stress and this modification can be observed via western blot by the loss of the 2A10 epitope via epitope masking. Direct phosphorylation of MDM2 by ATM inhibits MDM2's ability to turnover p53 (Maya et al., 2001). Tyr394 of MDM2 can be phosphorylated by the protein-tyrosine kinase c-Abl in a DNA damage-dependent manner, blocking the ability of MDM2 to down regulate p53 activity (Sionov et al., 2001). C-Abl is also a target of ATM, which raises the question of a two hit phosphorylation mechanism with ATM phosphorylating a kinase which in turn can phosphorylate MDM2 but also phosphorylating MDM2 itself at residues adjacent to each other (Meek and Knippschild, 2003).

Akt is thought to regulate MDM2's translocation to the nucleus via phosphorylation of residues 166 and 186 which lie in close proximity to the nuclear export and nuclear localization sequences of MDM2 (Mayo and Donner, 2001). This phosphorylation stimulates p53 ubiquitination and reduces MDM2's interaction with ARF (Ogawara et al., 2002; Zhou and Elledge, 2000)..

A cluster of amino acids in the acid domain of MDM2 have been shown to be phosphorylated (Blattner et al., 2002; Hay and Meek, 2000). This cluster of amino acids are thought to be phosphorylated under normal cellular conditions and play a role in MDM2 catalyzed p53 degradation, so as to maintain low p53 levels in the absence of stress (Blattner et al., 2002).

There are many more phosphorylation sites in the MDM2 protein, and very little is known about some of these. Like many other PTM's, phosphorylation can regulate MDM2's sub-cellular localization, its stability and its activity as an E3 ligase towards p53. Figure 1.9 summarizes MDM2 phosphorylations.

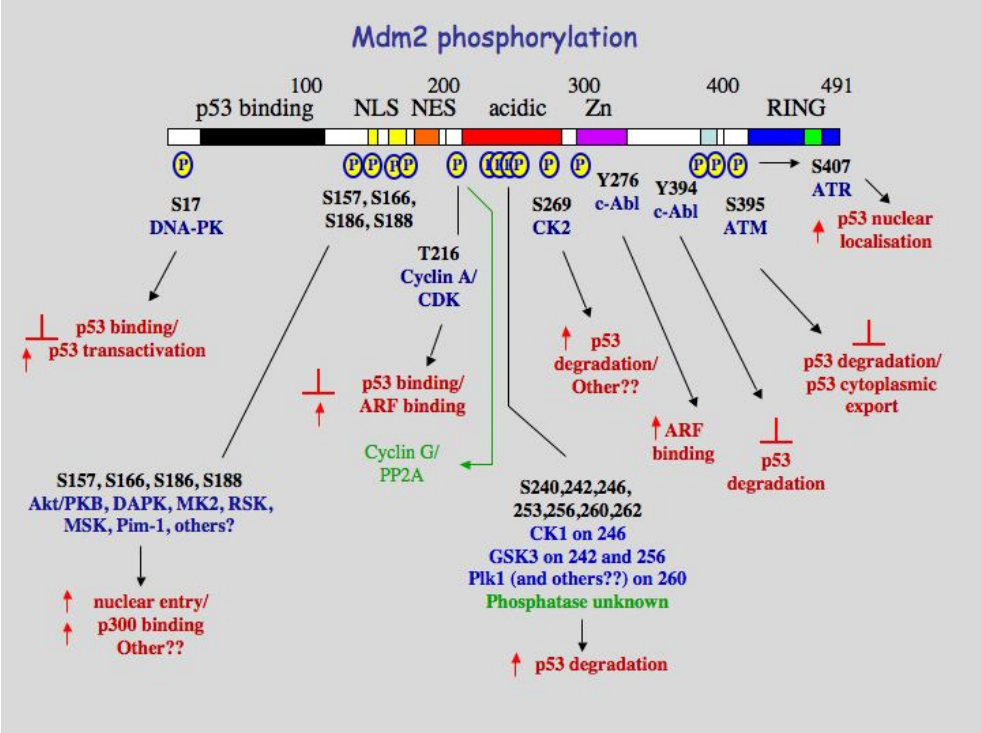

Figure 1.9 Schematic diagram showing the sites of phosphorylation within the MDM2 protein. Where possible potential kinases are indicated. The effects of phosphorylation on p53s activity are also shown. (Adapted from (Meek and Knippschild, 2003)

1.9 p53 post translational modifications

As with MDM2, p53 is targeted for a multiple array of PTMs including ubiquitination, neddylation, sumoylation, acetylation and phosphorylation. Many of these PTM's can act in concert to elicit a desired effect, highlighting the deep complexity of p53 function and regulation (Figure 1.10).

1.9.1 Ubiquitination, Neddylation and Sumoylation of p53

p53 is targeted for degradation by MDM2 via ubiquitination of specific lysine residues contained within its C-terminus. These lysine's are also subject to modification by the ubiquitin like proteins, NEDD8, and SUMO which regulates the MDM2:p53 interaction and protein stability.

As well as being modified by ubiquitin, which targets p53 for degradation, p53 can be modified by NEDD8 and SUMO however these modifications do not target p53 for degradation but instead effect p53 activity. Lysines 370, 372 and 373 of p53 have been implicated in NEDD8 conjugation (Xirodimas et al., 2004). It is interesting to note that these residues are also targeted for ubiquitination. Neddylation results in reduced p53 transcriptional activity (Xirodimas et al., 2004).

p53 can be sumoylated at lysine 386 which results in the activation of p53's transcriptional activity independent of p53 ubiquitination (Gostissa et al., 1999).

1.9.2 Acetylation of p53

p300/CBP serves as a co-activator for p53 by mediating histone acetylation as well as targeting p53 for acetylation within its C-terminus. Acetylation also occurs on residues used for ubiquitination thus acetylation results in p53 stabilization as a consequence of blocking MDM2 catalyzed ubiquitination (Gu and Roeder, 1997). Not only is p53 activated by blocking MDM2 ubiquitination, but acetylation causes conformational changes within p53 which enhances its specific DNA binding activity (Friedler et al., 2005; Gu and Roeder, 1997).

1.9.3 Phosphorylation of p53

In response to stress, phosphorylation of p53 occurs on numerous sites within its N-terminal transactivation domain, the core DNA binding domain and the C-terminal domain. These phosphorylation events are mediated by many different protein kinases that respond to different stresses including, ATM, ATR, CHK1, CHK2, JNK and p38. Significant redundancies are observed in that the same p53 site is often phosphorylated by different protein kinases (Appella and Anderson, 2001; Bode and Dong, 2004)

Generally, phosphorylation of p53 is associated with protein stabilisation and transcriptional activation (Craig et al., 1999; Hupp and Lane, 1994b). Due to the magnitude of p53 post-translational modifications, it has been proposed that a distinctive combination of phosphorylated residues may be required for additional modifications,

leading to maximal activation of p53 (Bode and Dong, 2004). For example, phosphorylation of p53 at Ser15 occurs rapidly in response to DNA damage and prepares the protein for subsequent modifications, including phosphorylation at threonine-18 and serine-20 by additional kinases (Saito et al., 2003). Phosphorylation at serine-15, threonine-18 and serine-20 stimulate the recruitment of transcriptional co-activators such as p300/CBP, while blocking the interaction with MDM2, and enhance p53 transcriptional activity (Craig et al., 1999; Saito et al., 2003). Similarly, phosphorylation of p53 at serine-33, threonine-81, and serine-315 promotes its interaction with the propyl isomerase, PIN1. PIN1 mediates a conformational change in p53 and augments p53 activity (Zacchi et al., 2002; Zheng et al., 2002). Figure 1.10 summarizes p53 phosphorylation sites.

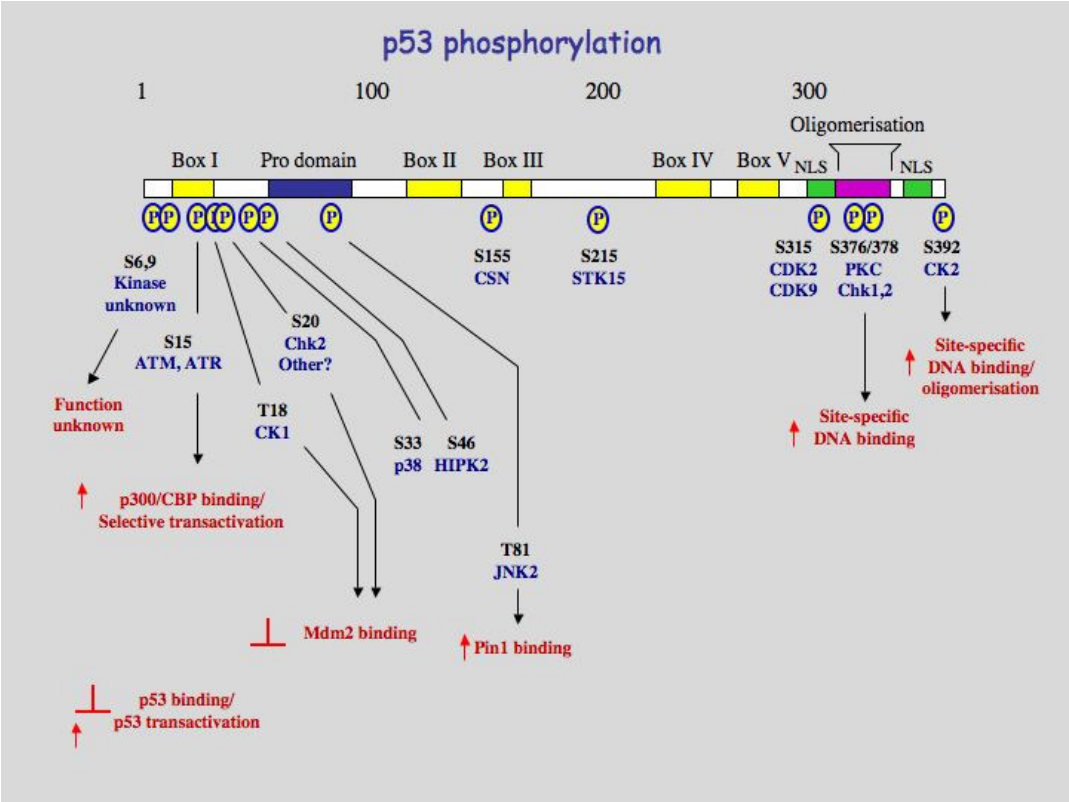

Figure 1.10 p53 Phosphorylation. Schematic diagram indicating the potential phosphorylation sites within p53 and where possible the kinase responsible. The effect on p53 function is indicated. Adapted from http://www.dundee.ac.uk/biomedres/meek.htm.

1.10 The aim of this thesis

As discussed the ubiquitin proteasome system (UPS) is an attractive target for cancer therapy, thus new ways need to be developed to target it. The components of the UPS are now well known, starting from the E1 through to the proteasome itself. With much specificity brought about by the different E2s and even more E3s the ability to switch off

one particular ubiquitination pathway is of great interest. If it was possible to protect one protein from degradation then many unwanted side effects caused by general UBS inhibition would be a thing of the past. One such protein is p53. Stabilizing p53 would result in cell cycle arrest followed by DNA repair and/or apoptosis. p53 is targeted for degradation by the E3 ligase MDM2. MDM2 is overexpressed in up to 7% of human cancers resulting in the inactivation of p53. There have been many attempts to target the MDM2:p53 interaction in the hope of stabilizing and blocking p53 ubiquitination with varying degrees of success. However before drugs can be successfully modelled a better understanding of the mechanism of MDM2 catalyzed p53 ubiquitination is needed. Given the time MDM2 and p53 have been known and the extensive research into them, it is surprising that very little is know about how MDM2 transfers the ubiquitin moiety form the E2 to p53. The aim of this thesis was to use biochemical and cellular analysis to further our understanding of this mechanism.

Chapter 2

MATERIALS AND METHODS

2.1 General Reagents

Chemicals and reagents were supplied by Sigma unless otherwise stated. Tissue culture reagents including Dulbecco's modified eagle's medium (DMEM), RPMI 1640, penicillin/streptomycin solution, trypsin-EDTA solution and Lipofectamine™2000 were supplied by Invitrogen unless otherwise stated, while fetal bovine serum (FBS) was supplied by Autogen Bioclear.

2.2 Equipment

Faxitron® cabinet X-ray system, 43855D (Faxitron X-ray Corporation) was used to carry out X-irradiation treatment. A Fluroskan (Ascent FL), PowerwaveXS™ microplate reader (Bio-Tek), and an Envision fluorescence detector (Perkin Elmer) were used to read 96-well plates. DNA concentrations were measured using a NanoDrop® spectrophotometer. SDS PAGE was carried out using Biorad Protean II mini-gel system.

X-ray films were developed using a Mediphot 937 developer. Sorvall RC-5C plus and Eppendorf 5415R were used for all centrifugations.

2.3 Cell Culture

2.3.1 ell lines and Media

All cells were kept in a humidified incubator at 37^{o}C. Media were supplemented with 10 % (v/v) fetal bovine serum (FBS). DMEM and RPMI-1640 were further supplemented with 1 % (v/v) penicillin/streptomycin.

Cell Line	**Source**	**Medium**	**% CO_2**
A375	Human skin, malignant melanoma	DMEM	10
MEFs (p53-/-mdm2-/-)	Mouse embryonic fibroblasts	DMEM	10
H1299	Human, non-small cell lung carcinoma	RPMI-1640	5

Table 2.1 List of cell lines used in this study.

2.3.2 Subculturing, storage and recovery of cells

Freezing media

50 % (v/v) Fetal bovine serum

10 % (v/v) DMSO

40 % (v/v) Tissue culture media (depending on cell line)

Cells were subcultured 2-3 times per week in 10 cm diameter culture dishes in sterile conditions and split to a maximal dilution of 1/10. The media was discarded and the cells were washed with sterile phosphate buffered saline (PBS). 1x Trypsin-EDTA solution (0.5 ml/ 10 cm diameter culture dishes) was added and the cells were placed in the incubator until the cells started to detach from the culture dish. The cells were taken up into media (9.5 ml/ 10 cm diameter culture dishes) and then split 1:10 into new culture dishes with fresh media (10 ml/ 10 cm diameter culture dishes).

Cells were kept in liquid nitrogen for long-term storage. To prepare cells for storage a 10 cm diameter culture dish with confluent cells was trypsinised and the cells collected by centrifugation (1000 rpm, 5 min, 4 ºC). The cell pellet was gently resuspended in 4 ml freezing media and transferred to cryotubes (Nunc) at 1 ml/ tube. The cells were frozen down slowly in Nalgene™ Cryo 1 ºC freezing containers and then transferred to liquid nitrogen.

To recover the cells the tubes were thawed quickly at 37 ºC and the cells transferred to a culture dish containing fresh media. The media was changed the following day and the cells were left to grow until they were confluent before being subcultured for the first time

2.3.3 Transient transfections

Cells were seeded out onto 6-, 24well plates or 10 cm^2 plates 24 h prior to transfection without antibiotics and grown to 80-90 % confluency. The cells were transfected with plasmid DNA (pcDNA3.1; pDEST vectors, Invitrogen) using Lipofectmine™ 2000 (Invitrogen) according to manufacturer's handbook. DNA was transfected at a ration of 1:1 using Lipofectamine™ 2000. Cells were then incubated at 37°C overnight before they were harvested or subjected to chemical treatment or stress.

2.4 Microbiological Techniques

All microbiological techniques were carried out under aseptic conditions.

2.4.1 Growing bacterial cultures

Luria-Bertani (LB) broth

1 % (w/v) Tryptone
0.5 % (w/v) Yeast extract
1 % (w/v) NaCl
Sterilised by autoclaving at 121 °C for 20 min

Selective antibiotics used

Ampicillin (Sigma) at 50 µg/ml

Kanamycin at 100mg/ml

5 ml LB media (containing a selective antibiotic if required) was inoculated with a colony of bacteria from a stock plate or from a glycerol stock and incubated for several hours overnight at 37 °C (225 rpm). This starter culture was then transferred to 200 ml LB media (containing antibiotics if appropriate) and incubated under the same conditions overnight. Culture flask capacities were at least 5x the volume of the culture being grown to allow for aeration.

2.4.2 Glycerol stocks

Glycerol stocks of bacterial cells were prepared by adding 0.15 ml of sterile glycerol to 0.85 ml of liquid bacterial culture in a cryovial (Nunc) and snap frozen. The cells were stored at –70 °C.

2.4.3 Agar bacterial culture dishes

LB agar

1 % (w/v) Tryptone
0.5 % (w/v) Yeast extract
1 % (w/v) NaCl
1.5 % (w/v) Agar, granulated
Sterilised by autoclaving at 121 °C for 20 min.

LB agar was liquefied by heating in a microwave oven. When the agar was hand warm it was poured into 90 mm diameter Petri dishes (Sterilin) and left to cool. If antibiotic selection was required, the antibiotic was added to the agar immediately before pouring. The culture dishes were stored at 4 °C for no longer than one month. Prior to use the plates were dried at 37 °C for 1 h.

2.4.4 Preparation of competent cells

Heat shock method

Transforming buffer 1 (TFBI)
30 mM Potassium acetate
100 mM RbCl
10 mM $CaCl_2$
50 mM $MnCl_2$
15 % (v/v) Glycerol
Adjust to pH 5.8 with acetic acid and sterilise by filtration.

Transforming buffer 2 (TFBII)
10 mM MOPS
75 mM $CaCl_2$
10 mM $RbCl_2$
15 % (v/v) Glycerol
Adjust to pH 6.5 with KOH and sterilise by filtration.

A starter culture of DH5α cells was set up by transferring a colony of bacteria from a stockplate to 2 ml of LB in a 15 ml sterile tube. The culture was incubated overnight at 37 °C and with agitation at 225 rpm. This culture was diluted 1/100 in 200 ml of LB and incubated at 37 °C at 225 rpm until the OD_{600nm} lay within 0.3-0.5. The cells were collected by centrifugation (10 min, 8000 rpm, 4 °C) and resuspended in ice-cold 80 ml of TFBI buffer at 2/5 of the original 200 ml culture volume. After 10 min of incubation on ice the cells were again centrifuged (5 min, 2500 rpm, 4 °C) and gently resuspended

in 8 ml of TFBII buffer at 1/25 of the original 200 ml culture volume. The cells were incubated on ice for 15 min and 200 µl aliquots were added to pre-chilled microcentrifuge tubes. The aliquots were snap frozen on dry ice and stored at –70 °C.

2.4.5 Transformation of bacteria

2.4.5.1 Heat shock method

100 µl of DH5α competent cells were defrosted on ice and mixed with 0.1-0.5 µg of plasmid DNA. The cells were incubated on ice for 45 min and heat-shocked at 42°C for 2 min. Following another 2 min incubation on ice, 1 ml LB media was added and the culture was incubated at 37 °C at 225 rpm for 30 min in a 15 ml sterile tube. Cells were then plated onto LB agar bacterial culture dishes containing selective antibiotic where appropriate and incubated overnight at 37 °C.

2.5 Molecular Biology Methods

2.5.1 Plasmid DNA

Amplification of plasmid DNA – A single colony of bacteria containing the plasmid required was used to inoculate a starter culture of 5 ml of LB containing selective antibiotic and incubated at 37 °C at 225 rpm for 4-8 h in a 50 ml sterile tube. The starter culture was then transferred to a larger 100 ml liquid bacterial culture and incubated overnight at 37 °C at 225 rpm in a 500 ml flask.

Purification of plasmid DNA – Cells from the culture grown for amplification of plasmid DNA were collected by centrifugation at 6000 rpm for 20 min at 4 °C. Plasmid DNA was isolated using Qiagen Maxi™ and Mini™ prep kits according to manufacturer's instructions. The DNA was resuspended in nuclease-free dH_2O and stored at -20 °C.

Quantification of plasmid *DNA* – The concentration of plasmid DNA was determined by spectrophotometry at 260 nm using the PowerwaveXS™ Microplate Spectrophotometer (Bio-Tek). Plasmid DNA was diluted 1/100 and 100 µl volumes were added to wells of a 96-well UV-Star™ Plate (Greiner), using 100 µl dH_2O as a blank control. 50 µg/ml DNA gives an OD_{260nm} of 1 A thus DNA concentrations could be calculated. The plate reader software (KCJunior™) adjusted for a 1 cm light pathlength.

2.5.2 SDS-PAGE

2.5.2.1 Preparation of cell lysates

Cell lysis

0.1 % or 1 % Triton X-100 lysis buffer
50 mM HEPES pH 7.6
0.1 mM EDTA
150 mM NaCl
1x protease inhibitor mix*
0.1 % or 1 % (v/v) Triton X-100
10 mM NaF
Stored at -20 ºC in aliquots.
2 mM DTT (add prior to use)

Urea lysis (Denaturing) buffer
7 M Urea
0.1 M DTT
0.05 % (v/v) Triton X-100
25 mM NaCl
25 mM HEPES pH 7.6
Buffer prepared just prior to use.

***10x Protease inhibitor mix**
10 µg/ml Leupeptin
4 µg/ml Aprotinin
2 µg/ml Pepstatin
1.2 mM Benzamidine
10 µg/ml Soya bean trypsin inhibitor
400 µg/ml Pefabloc
1 mM EDTA
Stored at -20 ºC in aliquots.

SDS sample buffer (SB)
5 % (w/v) SDS
25 % (v/v) Glycerol
125 mM Tris pH 6.8
0.02 % (w/v) Bromophenol blue
DTT (1 M) added to buffer (1 DTT : 4 SB) prior to use

Cells were washed with cold PBS, scraped with 150 µl of PBS into microcentrifuge tubes and then centrifuged at 5000 rpm for 5 min at 4 ºC. The supernatant was removed and cell lysis buffer was added in excess of the cell pellet (50-100 µl per well in a 6-well plate). The cells were resuspended by pipeting the cell lysis buffer up and down several times. Samples were then incubated on ice for 20 min. The cell lysate was centrifuged at 13000 rpm for 2 min and the supernatant was recovered. The cell pellet was recovered and lysed further by resuspending it in 200 µl of SDS sample buffer and heated at 70 ºC for 10 min. Samples were then sonicated (Soniprep150^{TM}, MSE) twice for 10 sec (Level 2-3). Samples were snap-frozen in liquid nitrogen and stored at -70 ºC.

2.5.2.2 Protein precipitation

Trichloroacetic acid (TCA) was used to precipitant protein and concentrate protein samples using the following method. 2 % deoxycholate (DOC) was added to the samples to a final concentration of 0.02 % and incubated at room temperature for 15 min. 24 % TCA was added to a final concentration of 8 % and incubated on ice for 1 hr. The precipitated proteins were pelleted by centrifugation at 13,000 *g* for 10 min at 4 ^{o}C. The supernatant was removed and the pellet washed with 200 µl ice cold acetone to remove residual TCA. The protein pellet was air dried for 1 – 2 min before resuspending in either urea lysis buffer or 4 x SDS sample buffer (4 % SDS, 250 mM Tris-HCl pH 6.8, 10 mM EDTA, 0.2 M DTT, 1% Bromophenol blue).

2.5.2.3 Protein quantification

Protein concentrations were determined using the BCA^{TM} Assay kit (Pierce, Perbio Science) in a 96-well plate measuring absorbance at 562 nm with the PowerwaveXS^{TM} Microplate Spectrophotometer (Bio-Tek). Read-outs were converted to concentrations using the standard curve generated from the BSA standards and adjusted by the dilution factor.

Biorad protein assay dye reagent concentrate was diluted 1 in 5 in distilled water. 1 µl diluted protein sample was added to 200 µl of this solution in a clear 96-well plate

and mixed. The absorbance at 595 nm was measured and the protein concentration was determined from a standard curve generated from known concentrations of BSA.

2.5.3 Preparation of gels and separation of proteins by SDS-PAGE

Running buffer
192 mM Glycine
25 mM Tris
0.1 % (w/v) SDS

Separating gel – 10% (per 5 ml)
30 % Acrylamide mix* 1.7 ml
1.5 M Tris (pH 8.8) 1.3 ml
10 % SDS 0.05 ml
10 % Ammonium peroxidisulphate 0.05 ml
TEMED (Sigma) 0.002 ml
dH_2O 1.9 ml

Separating gel – 15 % (per 5 ml)
30 % Acrylamide mix* 2.5 ml
1.5 M Tris (pH 8.8) 1.3 ml
10 % SDS 0.05 ml
10 % Ammonium peroxidisulphate 0.05 ml
TEMED (Sigma) 0.002 ml
dH_2O 1.1 ml

Stacking gel – 5 % (per 1 ml)
30 % Acrylamide mix* 0.17 ml
1.5 M Tris (pH 6.8) 0.13 ml
10 % SDS 0.01 ml
10 % Ammonium peroxidisulphate 0.01 ml
TEMED (Sigma) 0.001 ml
dH_2O 0.68 ml

* Acrylamide mix (National Diagnostics; Ultrapure Protogel) consists of 30 % (w/v) acrylamide and 0.8 % (w/v) bis-acrylamide.

SDS-polyacrylamide gels at polyacrylamide concentrations of 10 % or 15 % were prepared [described by Laemlli *et al* (1970)] using a MiniProtean3^{TM} (Bio-Rad) blot. The separating gel was left to polymerise and overlaid with water to straighten the top of the gel. The water was then removed and the stacking gel with a polyacrylamide concentration of 5 % was added together with a 10- or 15-well comb, which was also

left to polymerise. The combs were removed and the wells were washed out with Running buffer.

SDS sample buffer was added to the cell lysates containing between 25-50 µg of protein in a ratio of 1:1 (v/v) and samples were heated at 95 ºC for 5 min prior to loading. 5 µl of pre-stained protein standards (Bio-Rad) were loaded in the first well as size markers. Proteins were separated by electrophoresis in Running buffer at 100-170 V until the Bromophenol blue dye front reached the bottom of the gel.

2.5.4 Detection of fractionated protein

Gels were removed from the glass plates and the stacking gel was discarded.

Coomassie brilliant blue staining

Destain 1
50 % (v/v) Methanol
10 % (v/v) Acetic acid

Destain 2
7.5 % (v/v) Methanol
10 % (v/v) Acetic acid

Coomassie brilliant blue stain
50 % (v/v) Methanol
10 % (v/v) Acetic acid
0.2 % (w/v) Coomassie Blue R-250

Gels were transferred to a dish containing Destain 1 for >5 min and then placed into another dish containing Coomassie Blue Stain. The duration of the staining procedure depended on the strength of the staining required (5 min to 12 h) and in some cases the stain was preheated to 45 ºC to increase staining even further. Gels were then placed in a dish containing Destain 2. A folded tissue was used to absorb excess dye and Destain 2

was renewed as needed. Destaining was performed until the bands became visible and the background staining was removed. Gels were air-dried in between DryEase MiniCellophane™ sheets (Invitrogen) in a DryEase GelDrying™ system (Invitrogen).

2.5.5 Immunoblotting

10x PBS (Phosphate-Buffered Saline)
1.37 M NaCl
0.1 M Na_2HPO4
0.027 M KCl
0.018 M KH_2PO_4
Adjust pH to 7.4 with HCl

PBS+Tween (PBST)
1x PBS + 0.1 % (v/v) Tween 20

Transfer buffer
192 mM Glycine
25 mM Tris
20 % (v/v) Methanol

ECL Solution 1
100 mM Tris pH 8.5
2.5 mM Luminol stock
0.4 mM p-Coumaric acid

ECL Solution 2
100 mM Tris pH 8.5
0.02 % (v/v) H_2O_2
Solutions stored at 4 ºC in the dark.

The separated proteins were transferred electrophoretically to PROTRAN™ nitrocellulose transfer membranes (Schleicher & Schuell Biosciences) in tanks with agitated Transfer buffer and an ice block to control the temperature. Electroblotting was carried out at 100 V for 1 h or at 20 mA overnight. After transfer of proteins the membranes were washed in PBST and stained with black ink (Pelikan) diluted in PBST (1/100) for 10-15 min. Membranes were washed again in PBST to remove the excess stain and non-specific antibody binding was blocked by a 1 h incubation in PBST + 5 %

(w/v) dried skimmed milk (PBST5M; Marvel). The membranes were then incubated with the primary antibody in PBST5M for 1 h at RT (or overnight at 4 ºC). Following three 5x 5 min washes in PBST, the appropriate secondary antibody (conjugated to horse radish peroxidase; DAKO) diluted 1/1000 – 1/2000 in PBST5M was added to the membrane and incubated for 1 h at RT. Membranes were again washed for 5x 5 min with PBST and specific bands were detected by enhanced chemiluminescence (ECL). Membranes were overlaid with ECL solution 1 and 2 (mixed 1:1) for 1 min, blotted dry and exposed to Hyperfilm^{TM} ECL (Amersham Biosciences), which was then developed.

2.5.6 Antibodies

2.5.6.1 Primary antibodies

Table 2.2 List of primary antibodies used in this study.

Target	kDa	Clonality	Supplier	Dilution
β - actin	42	Mouse Monoclonal	Abcam	1:5000
E2F-1	60	Rabbit Polyclonal	Santa Cruz	1:1000
IRF-1 (C-20)	48	Mouse Monoclonal	BD	1:1000
MDM2 (2A9)	90	Mouse Monoclonal	Moravian Biotechnology	1:1000
MDM2 (2A10)	90	Mouse Monoclonal	Moravian Biotechnology	1:2000
MDM2 (4B2)	90	Mouse Monoclonal	Moravian Biotechnology	1:1000
p21 (Ab-1)	21	Mouse Monoclonal	Oncogene	1:1000
p53 (DO1)	53	Mouse Monoclonal	Moravian Biotechnology	1:5000
p53 (DO12)	53	Mouse Monoclonal	Moravian Biotechnology	1:1000
p53 (CM-1)	53	Rabbit Polyclonal	Moravian Biotechnology	1:1000
Phospho^{Ser17} MDM2 (9G11)	90	Mouse Monoclonal	Moravian Biotechnology	1:200

2.5.6.2 Secondary antibodies

Secondary antibodies were sourced from Dako and HRP-conjugated forms of Rabbit α-Mouse IgG; Swine α-Rabbit IgG; Rabbit α-goat IgG; Rabbit α-sheep IgG were used.

2.5.7 Stripping Membranes

Stripping buffer

50 mM Tris pH 6.8
2 % (w/v) SDS
100 mM β-mercaptoethanol

Antibodies bound to membranes were removed by stripping when the blots needed to be re-probed. The stripping buffer was heated to 50 ºC in a water bath and added to the membrane. The blot was kept at 50 ºC in the water bath for 15-30 min with occasional agitation. The membrane was rinsed multiple times with PBS and was then immunoblotted as described above.

2.6 Cloning and Site Directed Mutagenesis (SDM)

2.6.1 Polymerases

Hot-start Taq polymerase amplification

PCR Master mix/reaction	**Cycling conditions**
1xPCR buffer (Qiagen) 1mM dNTPs (Promega) 0.1µM forward and reverse primers 1µg DNA template HotstarTaqTM DNA polymerase 5units/reaction (Qiagen) ddH2O up to a final volume of 50 µl	Taq activation:95°C for 15min, Denaturation:95°C for 30sec, Annealing: 53.6°C for 30sec, Elongation:72°C for 1min Cycle to step 2 x30 times, 72°C x 5min. 4 °C for t∞

In order to ensure maximum yield of amplification for each product, different annealing times, varying from 50-70°C, along with elongation times between 30sec-3min, were tried. 100ng of DNA template were used as initial concentration.

PFU polymerase reaction

PFU® Turbo amplification was used instead of Taq polymerase for site directed mutagenesis because of it is a highly thermostable *Pfu* DNA polymerase and possesses 3' to 5' exonuclease proof-reading activity that enables the polymerase to correct nucleotide-misincorporation errors. This means that *Pfu* DNA polymerase-generated

PCR fragments will have fewer errors than *Taq*-generated PCR inserts. All reactions performed in a DNA Engine DyadTM machine.

PCR Master mix/reaction

1x cloned PFU® buffer (Stratagene)
1mM dNTPs (Promega)
0.5mM MgCl2 (Qiagen)
0.1µM forward and reverse primers
5% (v/v) DMSO
1µg DNA template
PFU® Turbo DNA polymerase 2.5 units/reaction (Stratagene)
ddH2O up to a final volume of 50 µl

Cycling conditions

Taq activation:95°C for 15min,
Denaturation:95°C for 30sec,
Annealing: 53.6°C for 30sec,
Elongation:72°C for 1min
Cycle to step 2 x30 times,
72°C x 5min.
4 °C for t∞

2.6.2 Agarose gel electrophoresis

50x TAE (Tris-Acetate EDTA)

2M Tris pH 6.8,
0.1M Na2EDTA.2H2O
4% Acetic acid (v/v)
Adjust pH to 8.5

6x DNA loading buffer

0.25% Bromophenol blue (w/v)
0.25% Xylene cyanol (w/v)
15% Ficoll 400 (w/v)

TAE buffer was diluted (50x) to 1x and 1% (w/v) ultrapure agarose was added. The solution was heated in a microwave oven until the agarose is completely dissolved and left to cool down to handwarm under the hood. Ethidium Bromide EtBr was added to a

final concentration of 5% (w/v). The solution was then poured into a horizontal electrophoresis gel tray with a 10-well or bigger comb inserter and left to solidify. When solid, the agarose gel was submerged in a horizontal electrophoresis tank filled in 1xTAE buffer. DNA loading buffer (6x) was added to the samples (3µl of site-directed mutagenesis DNA or 10µl of PCR amplified DNA) to 1x and then loaded onto the gel. 1kb DNA ladder was also loaded at 5µl volume. Electrophoresis at 100V at room temperature followed till adequate separation was achieved and then the bands were visualized by UV light using a CHEMI Genius2 BioImaging SystemTM (Syngene) and the GenesnapTM tool with an ethidium bromide filter and transilluminator. The images were captured with a Sony UP-D895MD.

For cloning the DNA was extracted from the gel using a DNA gel purification kit from Qiagen.

2.6.3 Restriction enzyme digestion and Ligation of DNA in the appropriate vector

Restriction enzyme digestion of the vector and the DNA-insert is required after PCR amplification. The restriction endonucleases recognize specific sequences to digest. As far as the insert is concerned the adequate restriction enzymes were chosen according to the Multiple Cloning Site (MCS) of the vector to be inserted in. Restriction digests were performed to manufacturers protocol (New England Bio-labs).

Ligation reaction	**Formula for the vector:insert ratio**
1x Ligation Buffer (10x Promega) 10-100ng vector DNA xng insert 10units of T_4 ligase (10u/ µl , Promega) ddH_2O up to 10µ	µg of vector x size of insert (Kb) x ratio insert size pf vector (Kb) vector

After digestion the vector plasmid and the DNA-insert were ready to be ligated. The above reaction was incubated at 4 °C in Eppendorf tubes, overnight. For each ligation different ratios insert:vector were applied each time, varying between 1:1 and 5:1, according to the size of the insert when compared to the vector.

2.6.4 Site-directed mutagenesis and Cloning

2.6.4.1 Primer design

Cloning primers were designed with a length of around 20-30 bp spaced over the beginning or end of the MDM2 open reading frame with restriction sites or a homologous recombination site incorporated into them.

Oligonucleotides were purchased from Sigma-Aldrich, de-salt purified for cloning and were reconstituted in nuclease-free ddH_2O.

Table 2.3: Cloning Primers

Name	Restriction Site and vector	Primer Sequence
Full length MDM2 Forward	Nco1 pENTR11	5'GACCATGTGCAATACCAACATGTC3'
Full length MDM2 Reverse	Xho1 pENTR11	5'GCCTCGAGCTAGGGGAAATAAGTTAG3'
N-terminal tagged MDM2 Forward	BamH1 pENTR11	5'GCGGATCCGGTGCAATACCAACATGTCTG3'
N-terminal tagged Acid Domain Forward	BamH1 pENTR11	5'GTGGATCCGGGAACATTCAGGTGATTG3'
N-terminal tagged Acid Domain Reverse	Xho1 pENTR11	5'GCCTCGAGCTACTCATCATCTTCATCTG3'
N-terminal tagged ΔN MDM2 Forward	Homologous recombination pENTR221	5'GGGGACAAGTTTGTACAAAAAAGCAGGCTTAATGATCTACAGGAACTTGGTAGTAGTCAAT3'
N-terminal tagged ΔN MDM2 Reverse	Homologous recombination pENTR221	5'GGGGACCACTTTGTACAAGAAAGCTGGGTCCTAGGGGAAATAAGTTAGCACAATCAT3'
His-tagged Acid Domain Forward	Nde1 pET-15b	5'GGCATATGGAACATTCAGGTGATTGGTTG3'
His-tagged Acid Domain Reverse	Xho1 pET-15b	5'GCCTCGAGCTCATCATCTTCATCTGAGAG3'

2.6.4.2 Site-directed mutagenesis

Primers containing the desired mutations were designed according to the guidelines in the QuikChange™ Site-Directed Mutagenesis Kit Manual (Stratagene). Oligonucleotides were purchased from Sigma-Aldrich de-salt purified and were

reconstituted in nuclease-free ddH_2O. Site-directed mutagenesis was carried using the QuikChange™ Site-Directed Mutagenesis Kit (Stratagene) according to manufacturer's instructions. After mutant strand synthesis reaction, 1 µl of *DpnI* restriction enzyme (10U/µl) was added to the amplification reaction and mixed. The reaction mixture was microcentrifuged for 1 minutes and incubated at 37°C for up to 4 hours to digest the parental (nonmutated) dsDNA. After incubation, 2 µl of *DpnI*-treated DNA was used to transform 25 µl of DH5α competent cells using heat-shock method.

Table 2.4: Site Directed Mutagenesis Primers

Name	Amino acid mutation	Primer sequence
R97S/K98P Forward	Arginine 97 to Serine Lysine 98 to Proline	5'CTGTGAAAGAGCACAGCCCCAT ATATACCATGATC3'
R97S/K98P Reverse	Arginine 97 to Serine Lysine 98 to Proline	5'GATCATGGTATATATGGGGCTGT GCTCTTTCACAG3'
S17A Forward	Serine 17 to Alanine	5'TGATGGTGCTGTAACCACCGCCC AGATTCCAGCTTCG3'
S17A Reverse	Serine 17 to Alanine	5'CGAAGCTGGAATCTGGGCGGTG GTTACAGCACCATCA3'
S17E Forward	Serine 17 to Glutamate	5'TGATGGTGCTGTAACCACCGAGC AGATTCCAGCTTCG3'
S17E Reverse	Serine 17 to Glutamate	5'CGAAGCTGGAATCTGCTCGGTGG TTACAGCACCATCA3'
S17N Forward	Serine 17 to Asparagine	5'TGATGGTGCTGTAACCACCAACC AGATTCCAGCTTCG3'

S17N Reverse	Serine 17 to Asparagine	5'CGAAGCTGGAATCTGGTTGGTGG TTACAGCACCATCA3'
S17D Forward	Serine 17 to Aspartate	5'GGTGCTGTAACCACCGACCAGAT TCCAGCTTCG3'
S17D Reverse	Serine 17 to Aspartate	5'CGAAGCTGGAATCTGGTCGGTG GTTACAGCACC3'
D17S reverse Forward	Aspartate 17 to Serine	5'GGTGCTGTAACCACCTCACAGAT TCCAGCTTCG3'
D17S reverse Reverse	Aspartate 17 to Serine	5'CGAAGCTGGAATCTGTGAGGTG GTTACAGCACC3'
S237F Forward	Serine 237 to Phenylalanine	5'CAGTTTCAGATCAGTTTTTGTA GAATTTG3'
S237F Reverse	Serine 237 to Phenylalanine	5'CAAATTCTACAAAAAACTGATCT GAAACTG3'
F240K Forward	Phenylalanine 240 to Lysine	5'GTTTAGTGTAGAAAAAGAAGTT GAATCTC3'
F240K Reverse	Phenylalanine 240 to Lysine	5'GAGATTCAACTTCTTTTTCTACA CTAAAC3'

2.6.5 Sequence analysis of plasmid DNA

All sequence analysis was performed by the Sequencing Unit at the MRC Human Genetics Unit, Edinburgh. Ten µl of sequencing reaction containing 2 µl of BigDye® Terminator 3.1 (Applied Biosystems), 3.2 pmol of primer, 1x BigDye Sequencing buffer (Applied Biosystems), 250 ng of DNA template and nuclease-free ddH_2O was

assembled. The sequencing reaction was thermal-cycled using cycling parameters according to the manufacturer's instructions.

The sequenced DNA was then precipitated by mixing the reaction with 2.5 µl of 125 mM EDTA and 30 µl of 100 % (v/v) ethanol. After vortexing, the reaction was incubated at room temperature for 15 minutes. After centrifuging at 13000 rpm for 20 minutes, the solution was removed and precipitated DNA was microcentrifuged for 20 seconds. Residual ethanol was removed before 30 µl of 70 % (v/v) ethanol was added to the precipitated DNA and centrifuged at 13000 rpm for 5 minutes. The ethanol was removed before the precipitated DNA was microcentrifuged for 20 seconds. Residual ethanol was removed and the precipitated DNA was left to air-dry before sequence-analysed.

2.7 Protein Purification

2.7.1 GST-Purification

BL21 cells were transformed with pDEST-15 full length MDM2 or acid domain MDM2 for GST-tagged expression and a single colony was picked to make a starter culture. The starter culture was diluted to 1:100 in half a litre of LB and grown at 37^{o}C until OD_{600nm} was about 0.6-0.9. The culture was then induced with 0.2% arabinose 4 hours

at room temperature with shaking (225 rpm). Following induction cells were pelleted and resuspended in 10ml of 50mM Tris-ph8 and snap frozen.

The suspension was slowly allowed to defrost before adding 0.3M KCl, 10X protease inhibitor mix and 0.5% NP40. Cells were then sonicated twice for 10 seconds and left on ice for 20 minutes. Cells were again pelleted and supernatant was incubated with 0.25ml GST-beads (Qiagen) for 3 hours. Beads were then washed 3 times in 50mM Tris-pH8 before 500µl elution buffer (0.1M HEPES, 10xprotease inhibitor mix, 50mM Glutathione, pH 7.5 with NaOH) was added and left overnight at 4^{o}C rotating. Elutions were then loaded onto a 10% SDS-PAGE gel and coomassie stained.

2.7.2 His-purification

Cultures were grown and induced as for GST-purification. After induction the cells were pelleted and resuspended in 10ml of lysis buffer (20mM Tris pH8, 150mM NaCl, 0.1% NP-40, 10% glycerol, 10mM $MgCl_2$) and sonicated as before and spun down. The supernatant was added to 250ul of Ni-NTA agarose beads (Qiagen) washed in PBS, and incubated for 1 hour at 4^{o}C. Supernatant was removed, leaving enough to transfer beads to a small column and washed 6x with lysis buffer + 40mM imidazole. Protein was then eluted in 14 fractions of 0.5 ml using lysis buffer plus 250mM imidazole. All fractions were run out on an 18% gel. Peak fractions were then pooled and loaded onto an

equilibrated fast flow Q-column (GE Healthcare) and eluted off with a high salt concentration.

2.7.3 Native protein Purification

pDEST14-MDM2 constructs were overexpressed in BL21 arabinose inducible (AI) *E.coli* for 3 hours at room temperature. Cells were harvested by centrifugation at 6 000g for 10 minutes and frozen in liquid nitrogen. Bacterial pellet was lysed in 10% sucrose, 50mM Tris-HCl (pH8), 150mM NaCl and 150ug/ml lysozyme and left on ice for 45 minutes before sonication. After sonication 2mM Pefabloc, 5mM DTT and 1mM benzamidine was added to lysate before centrifugation at 30 000g for 20 minutes. Lysate was loaded onto a fast flow SP column (GE Healthcare) equilibrated with buffer A (25mM Hepes, pH7.5, 10% glycerol, 1mM benzamidine, 5mM DTT, 50mM KCl and 2mM Pefabloc). Bound protein was eluted with increasing salt concentration using buffer B (same as buffer A but 1M KCl).

Lysis Buffer	**Wash Buffer**	**Elution Buffer**
20mM Tris pH 8, 150mM NaCl 0.1% NP40 10mM $MgCl_2$	+ 40mM Imidazole	+ 250mM Imidazole

2.8 Assays

2.8.1 ELISA

A 96-well microtiter plate (Corning Inc.) was coated with purified p53 (50ng per well) diluted in 0.1 M Na_2HCO_3, pH 7.6, and incubated overnight at 4 °C. Each well was washed 6x with PBS containing 0.1% Tween 20 (PBS-T) followed by incubation for 1 h at room temperature with gentle agitation in PBS-T supplemented with 3% bovine serum albumin. The wells were washed 6x with PBS-T prior to incubation with appropriate amounts of purified $MDM2^{WT}$, $MDM2^{\Delta lid}$, or $MDM2^{S17D}$ mutants diluted in PBS-T 3% bovine serum albumin for 1 h at room temperature. For competition ELISA's a fixed concentration of 25ng MDM2 was used with a titration of appropriate inhibitor added at the same time. After 1 h incubation the plate was washed again 6x with PBS-T and incubated with MDM2 specific antibody 2A10 (1:1000 in PBS-T 3% BSA) for 1 h at room temperature. For peptide ELISA's plate was coated with streptavidin overnight, washed 6x with PBS-T and biotinylated peptides were added for 1 hour followed by addition of MDM2. Following a further 6x washes with PBS-T wells were incubated with secondary rabbit anti mouse horseradish peroxidase antibodies followed by further washing and ECL. The results were quantified using Fluoroskan Ascent FL equipment (Labsystems) and analyzed with Ascent Software version 2.4.1 (Labsystems).

Peptides BOXIa, BOXIb, BOXVa, and BOXVb were from Chiron Mimetopes and Nutlin3a from Alexis Biochemicals

BOXIa	Biotin-SGSGPPLSQETFSDLWKLLP
BOXIb (12.1)	Biotin-SGSGMPRFMDYWEGLN
BOXVa	Biotin-SGSGRNSFEVRVCACPGRD
BOXVb (Rb1)	Biotin-SGSGDQIMMCSMYGICKVKNIDLK

2.8.2 *In Vitro* Ubiquitination Assay

Reactions contained 25 mM HEPES (pH 8.0); 10 mM $MgCl_2$; 4 mM ATP; 0.5 mM DTT; 0.05% (v/v) Triton X-100; 0.25 mM benzamidine; 10 mM creatine phosphate; 3.5 units/ml creatine kinase; ubiquitin (2 μg); E1 (100 nM), E2 (1 μM), and pure p53(0.5 μg). Reactions were started with purified $MDM2^{WT}$, $MDM2^{\Delta lid}$ or $MDM2^{S17D}$ at various concentrations (50-200ng), incubated for 15 min at 30°C, and analyzed with 4%–12% NuPAGE gels in a MOPS buffer system (Invitrogen) followed by immunoblot. For temperature gradient MDM2 was subjected to heat shock for 5 minutes prior to addition to ubiquitination reaction.

Master Mix:

366μl H_2O
10μl 1M HEPES (pH8)
2.4μl 1M $MgCl_2$
2μl 10% Triton X-100

0.2µl 1M DTT
6µl 0.2M ATP
0.4µl 1M Benzamidine
3.2µl 10mg/ml Ubiquitin

2.8.3 In vivo ubiquitination assay

The H1299 cells were transfected with 0.5 µg p53 and 0.5 µg His-Ubiquitin (His-Ub) , in a 6-well plate. 4 hours prior to harvesting, the cells were treated with the proteasome inhibitor MG132 (50 µM; Sigma). 24 hours post transfection, the cells were harvested in 1 ml ice-cold PBS. Prior to centrifuging, this 1 ml was divided into two parts: 800 µl for analysis by His-pulldown, and 200 µl for analysis by direct lysis. Both parts were then centrifuged at 5,000 rpm for 5 min at 4ºC, the supernatant was discarded, and the cell pellets were snap-frozen in liquid nitrogen.

His-Pulldown

Buffer A: 6 M Guanidium-HCl, 95 mM Na_2HPO_4, 5.3 mM NaH_2PO_4, 10 mM Tris-HCl (pH 8.0), 0.01 M β-mercaptoethanol
Adjust pH to 8.0

Buffer B: 8 M Urea, 95 mM Na_2HPO_4, 5.3 mM NaH_2PO_4, 10 mM Tris-HCl (pH 8.0),
0.01 M β-mercaptoethanol
Adjust pH to 8.0

Buffer C: 8 M Urea, 22.5 mM Na_2HPO_4, 77.5 mM NaH_2PO_4, 10 mM Tris-HCl (pH 8.0),
0.01 M β-mercaptoethanol
Adjust pH to 6.3

Buffer D: Buffer C + 0.2% Triton X-100

Buffer E: Buffer C + 0.1% Triton X-100

Lysis Buffer: Buffer A + 5 mM Imidazole

Elution Buffer: 0.2 M Imidazole, 5% SDS, 0.15 M Tris-HCl (pH 6.7), 10% glycerol, 0.72 M β-mercaptoethanol

The thawed pellet (800 µl) was lysed in 1 ml freshly prepared ubiquitination lysis buffer by pipetting up and down using a liquipette (Elkay). The lysate was transferred to a 15 ml falcon tube containing a further 4 ml of lysis buffer. 75 µl of Ni^{2+}-NTA Agarose beads (GeHealthcare) was added to each tube, following which the tube was placed on a rotating table overnight at 4ºC.

The beads were collected by centrifugation at 2000 rpm for 3 min at 4ºC and the supernatant was carefully removed. The beads were washed in 750 µl Buffer A, and transferred to microfuge tubes. The tubes were then placed on a rotating table for 15 min at RT, following which the beads were collected by centrifugation at 2000 rpm for 4 min. The supernatant was discarded. In a similar manner, the beads were washed with buffers B-E.

Following the wash with buffer E, 75 µl of elution buffer was added to the beads, and the tubes were incubated on a rotating table for 30 min at RT. The beads were collected by centrifugation at 13,200 rpm for 5 min at 4ºC. The supernatant was mixed with an equal volume of sample buffer.

50 µl of each sample was loaded on a pre-cat Novex 4012% gel (Invitrogen), which was subsequently run in 1X MOPS buffer (Invitrogen) at 200 V for about 1 hour. The separated proteins were then transferred to a nitrocellulose membrane and analysed by immunoblotting using anti-p53 antibody.

2.8.4 AlphaScreen

AlphaScreen (amplified luminescent proximity homogeneous assay), the donor bead is streptavidin labeled and linked to the relevant biotin linked peptide. The acceptor bead contains protein A, an appropriate antibody and its target protein. The AlphaScreen relies on the conjugation of proteins to the functional groups of hydrogel coated donor and acceptor beads. Excitation (680 nm) of photosensitizers present on the donor bead results in the production of singlet oxygen. If the acceptor bead is brought into close proximity (within ~ 200 nm) to the donor by the formation of a protein-peptide complex the singlet oxygen will react with thioxene derivatives on the acceptor bead generating chemiluminescence at 370 nm. Energy transfer to fluorescent acceptors in the same bead shifts the emission to 520-620 nm.

5µl of protein A beads were added to 0.6ml of envision buffer + 1.25ml of GST-mAb and wrapped in foil. In another Eppendorf 5ml of streptavidin coated beads were added to 0.6ml of envision buffer and foil wrapped. A 96 well plate (Cornstar) was blocked with 3% BSA.

Peptides were prepared in 10µl of envision buffer as such that when diluted to 50µl they will be at desired concentration. 20µl of streptavidin coated beads prepared as described were added to each tube and left to incubate for 1 hr in the dark. 20µl of protein A coated beads + GST-Ab was added to tubes and transferred to the 96 well plate (which was washed 3x in PBST). The plate was covered and allowed to incubate for 1 hr with gentle agitation in the dark. The plate was then read on an Envision fluorescence detector (Perkin Elmer).

2.8.5 Dual Luciferase Reporter Assay

Human Lung Carcinoma H1299 cell line was seeded onto 24 well plates. Upon reaching 80-90% confluency the cells were transfected by means of lipofectamine™ 2000 (Invitrogen) reagent with the total amount of DNA for all wells kept constant at 0.8 µg. In all experiments focusing on transcriptional potential of desired proteins an optimised ratio between the 'experimental' reporter and the 'control' reporter has been set up in order to minimize unspecific *in trans* effects between promoters of cotransfected plasmids. Thus (30ng) pGL4.10[*luc2*] bearing a 44base stretch of the *p21* promoter ('experimental' reporter) was mixed with 70ng of the phRL-CMV ('control' reporter). To this mixture 150ng of the pcDNA3.1 p53wt or pcDNA3.1 p53F19A, 7.5-550ng pDEST-3.2 $MDM2^{S17D}$ or $MDM2^{D17S}$, $MDM2^{S17N}$, $MDM2^{S17A}$, $MDM2^{S17N}$, $MDM2^{R97S:K98P}$, $MDM2^{S237F}$, or $MDM2^{F240K}$ were added. The DNA mixtures, with

appropriate controls were made up accordingly for each well to be transfected with the addition of pcDNA3.1 empty vector the make up the 0.8µg total DNA were necessary.

Twenty four hours post transfection, the cells were washed once in ice-cold PBS and passively lysed with 1x Passive Lysis Buffer (supplied with the Dual-Luciferase® Reporter Assay System from Promega) Afterwards the Dual-Luciferase® Reporter Assay System supplied by Promega, was performed in accordance to the technical manual supplied with the kit. The assay was carried out on 96 well black polypropylene plates and the luminescent signals were measured with the Thermo Scientific Fluoroskan Ascent Multimode Reader.

2.8.6 Immunoprecipitation protocol

Lysis Buffer

50mM HEPES pH 7.2
150mM NaCl
0.5%Tween20
Protease Inhibitor mix (10x)

Cell pellets were resuspended in 200ml of ice cold lysis buffer mixed well and incubated on ice for 15 minutes. Cell debris was spun down at 10000 rpm for 20 minutes at 4^{o}C. Lysate was pre-cleared with 100µl of sephadex CL-4B beads (Sigma-Aldrich). Beads were washed 3x in cold lysis buffer. The beads were added to the cell lysate in a 1.7ml Eppendorf and incubated for 40 minutes at 4^{o}C with rotation. The beads were spun down

at 5000 rpm and supernatant transferred to a new Eppendorf and protein concentration was calculated by bradford.

2µg of 2A10 antibody was added to lysate (200-800 µg) and incubated for 2 hrs at 4°C with rotation. 15µl of protein G beads (GE healthcare) were added to Eppendorf and left to incubate for an hour. The beads were spun down at 5000rpm at 4°C for 2 minutes. Beads were washed 4x with ice cold PBS.

The antibody-antigen complex was removed by the addition of 50µl of sample buffer followed by incubation at 95°C for 5 minutes. Beads were spun at 10000 rpm for 5 minutes and sample buffer removed. 10µl of elution was resolved on a 10% gel.

2.8.7 ProtoArray®

ProtoArrays® were performed to manufacturers guidelines. Briefly, 500 nM of MDM2 was diluted in probing buffer (PBS, 5mM MgCl2, 0.5mM DTT, 0.05%Triton X-100, 5% glycerol, 1% BSA) for 2 hrs. The array was washed 3x 10 mins in probing buffer before adding the primary antibody 2A10 for 1 hr. Array was then washed a further 3x in probing buffer followed by AlexaFluor-rabbit anti-mouse secondary antibody was added for 1 hr. Array was washed 3x with probing buffer followed by analysis.

Imaging of the protoarrays are carried out using Scan Array Express from Perkin Elmer. Scan array settings for imaging Alexa647 arrays: Laser 633nm, Alexa647 filter sets, Laser power 75%, PMT 45, Resolution 10 µm. The pmt gain and laser power is

specific to each fluorophore. Data processing was carried out using BlueFuse software. The Bluefuse software (originally developed for 2 channel or two colour DNA arrays) is adapted for data processing of protoarrays.

Data processing on the bluefuse involves grid alignment of array to the GAL file (to locate each protein position to its subsequent reference number. Quantitation is then carried out, with each spot being assigned a FLAG confidence score. The flag score is a measure of confidence in interaction depending on the spot intensity, shape and integrity. Bluefuse uses an "advanced statistical modelling technology". Bluefuse then generates an output file with each spot matched to its reference number. Next, simple perl script written by Dr. Karl Burgess (Strathclyde University) is then used to for data sorting. The perl script matches the protein reference number to its full protein name to allow easy identification of protein spots with its corresponding score to the protein ID.

2.9 Antibody Production

2.9.1 Immunisation protocol

Four BALB/C mice were used for immunization. On day one an intraperitoneal injection of 10-50 μg of phospho peptide coupled to KLH in complete Freunds adjuvant was carried out. This is repeated on day 21 but this time in incomplete Freunds adjuvant. At this point tail bleeds are collected and screened against the peptide in a

dot-blot. Another intraperitoneal injection is carried out at day 42 also in incomplete Freunds adjuvant. Tail bleeds were once again collected and screened against the peptide in a dot-blot. On days 45 and 46 two intraperitoneal injections of KLH coupled peptide are performed in PBS. On day 47 the mice are sacrificed prior to fusion.

2.9.2 Fusion

Culture Media		
DEM Media 1000mg/ L glucose		400 mL
Penicillin & Streptomycin	→ 1%	5 mL
FBS	→ 10%	50 mL
200nM Glutamine	→ 1%	5 mL
Fusion Media (w/o FBS)		
DEM Media 1000mg/ L glucose		450 mL
Penicillin & Streptomycin	→ 1%	5.5 mL
AH Media (SIGMA A9666)		
DEM Media 1000mg/ L glucose		400 mL
Penicillin & Streptomycin	→ 1%	5 mL
FBS	→ 20%	100 mL
200nM Glutamine	→ 1%	5 mL
Lyophilized AH (Azaserine-Hypoxanthine, 50x, γ-irradiated, Sigma A9666)	→ 1x	1 vial

The spleens were remove from the mice into a sterile petri dish and cleaned of all fats. The spleen was then washed with fusion media outside then fusion media was injected into the spleen multiple times to wash out the splenocytes. The splenocytes were then transferred to a 50ml falcon and left to settle to the bottom. The Petri dish was washed

with more fusion media and transferred to a 50ml falcon tube. Six dishes of 60% confluent myeloma cells were then resuspended in 4 falcon tubes each containing 40ml of media. The splenocytes were spun down for 10min at 1000rpm at room temperature. The media was then removed leaving a small volume to loosen the pellet. 35ml of fresh fusion media was added to one tube and the splenocytes were resuspended before pooling it with the second tube of splenocytes. These were spun down as before and the media removed leaving a small volume to resuspend the cells in. The myeloma cells and splenocytes were mixed in ratio 5 splenocytes : 1 myeloma SP2 cells in 40 ml of Fusion media in falcon tubes. The cells were then spun down for 7 minutes at room temperature and each falcon tube was resuspended in 50ml of AH media. 50µl of fusion cells was added to each well in 15 96 well plates. After three days 50 ml fresh AH media was added to the wells and after seven days 200ml of AH media was added. Screening begun after day 11, hybridomas that were growing well were picked for screening. Hybridomas were check and screened daily for two weeks.

2.9.3 Dot Blot

20 µg of either rabbit anti mouse Ig (RAM) or phospho peptide (coupled to BSA) in PBS were bound to nitrocellulose membrane for 2 hrs at 37^{o}C. The membranes are blocked with 10% fetal calf serum (FBS) in DMEM for 2 hrs at room temperature. For screening 2ml of supernatant from each tested hybridoma or tail bleed was added onto a

labeled spot on the both membranes, Ig and peptide, followed by a 2 hr incubation. Membranes were washed 3x in PBS for 5 minutes and incubated with rabbit anti mouse secondary antibody diluted 1:100 in DMEM plus 10% FBS. The membranes were then washed 3x in PBS for 5 minutes before developing with 1, 4-chloronapthol (Sigma-Aldrich) until dots begin to appear.

Chapter 3

THE ROLE OF THE ACID DOMAIN IN MDM2 CATALYZED UBIQUITINATION OF P53

3.1 Introduction

p53 is a sequence specific DNA binding protein that functions as a transcription factor activating target genes involved in DNA repair or apoptosis after cellular stress or insult (Harris and Levine, 2005). Four distinct E3-ligases negatively regulate p53 activity: MDM2, Pirh2, COP-1, and CHIP (Brooks and Gu, 2006), by ubiquitination and degradation via the proteasome. p53 can also be positively regulated via the transcriptional co-activator p300, thus the p53 pathway is controlled by the fine balance between p300-stimulated acetylation and E3-ligase catalyzed ubiquitination (Shimizu and Hupp, 2003).

MDM2 exerts its negative effect on p53 in two distinct ways, firstly by competing with p300 for binding to the N-terminal transactivating domain and secondly by repressing p53-dependent gene transcription (Arva et al., 2005). Mutations within the p53 transactivation domain can lead to p53 mutants which can escape MDM2 mediated transrepression (Lin et al., 1994). Alternatively MDM2 acts as an E3-ubiquitin

ligase and facilitates the ubiquitination and subsequent degradation of p53 (Michael and Oren, 2003). Nuclear magnetic resonance (NMR) studies have highlighted the flexibility of the MDM2 hydrophobic pocket and substantial conformational changes are observed upon ligand binding (Schon et al., 2004). The drug Nutlin, which was designed to mimic the p53 activation domain, can disrupt MDM2-p53 interactions in cells leaving large pools of active p53 (Vassilev et al., 2004).

The mechanism of MDM2-catalyzed ubiquitination of p53 is largely undefined, but there is an intrinsic conformational restraint to ubiquitination of the native p53 tetramer which is relieved when the tetrameric structure is distorted upon MDM2 binding. The binding site on protein targets required for ubiquitination is often referred to as the 'ubiquitination signal' and can be composed of a simple linear stretch of amino acids or a more complex signal comprising a conformational sensitive motif (Laney and Hochstrasser, 1999). In many cases, the ubiquitination signal for a given E3-ligase is poorly or incompletely defined as is the case with p53.

The conventional point of contact between MDM2 and p53 is through the transactivation domain in p53 and the hydrophobic pocket of MDM2. This chapter looks at a second contact site within MDM2 and p53 and its role in the ubiquitination of p53. The results presented are focused on the role of the MDM2 acid domain and p53-BOX-V interactions and were studied using AlphaScreen, circular dichroism and mass spectroscopy. They form part of a larger piece of research that identified the mechanism whereby MDM2 catalyzes the ubiquitination of p53 and this will eluded to further in the discussion.

3.2 Results

3.2.1 Cloning and purification of GST-tagged full length MDM2 and acid domain MDM2

In order to investigate the importance of the acid domain in MDM2 mediated ubiquitination of p53, we generated mutant forms of MDM2 to study the biochemistry it. These included full length (FL) MDM2, delta N-terminus (ΔN) MDM2, delta acid domain (ΔAD) MDM2 and acid domain only MDM2 (AD).

Full length GST-MDM2 and GST-Acid Domain were cloned into pDEST15 as described in materials and methods. PCR of full length MDM2 generated a product with an approx size of 1500 bp which corresponds to the actual size of the MDM2 open reading frame (ORF) (1473 bp) (Fig 3.1 lanes 2 and 3). PCR amplification of the acid domain of MDM2 generated a product of around 200 bp in size which corresponds to size of acidic domain (Fig 3.1 lanes 5 and 6). PCR Fragments were ligated into pENTR11 as described in materials and methods, then using homologous recombination were inserted into the pDEST15 vector for GST-tagged expression of protein in *Esherichia coli*.

GST-tagged AD, FL, ΔAD (gift from Aart Jochebson) and ΔN were cloned as described in materials and methods. MDM2 constructs were all expressed in BL21 AI

cells, and purified using glutathione sepharose 4B beads. Analysis of purified GST-MDM2 AD by coomassie staining showed a strong band with an approx molecular mass of 31 KDa and immunoblot of the same fraction using an MDM2 specific antibody (2A10) confirmed this band to be MDM2 AD (Fig 3.2A lanes 1-4). Full length MDM2 purified to a lesser extent as shown in figure 3.2B lanes 1 and 2 by a faint band at 125 kDa by coomassie stain but more evident when imunoblotted with 2A10 (Fig 3.2B lanes 3 and 4). Purification of ΔAD resulted in a band around 90 kDa which was confirmed as ΔAD (Fig 3.2C, lanes 1-4). Finally ΔN MDM2 was purified giving just one band around 97 KDa in size (Fig 3.2D, lanes 1 and 2).

3.2.2 Classic MDM2 binding ligands do not block ubiquitination of p53

Many proteins targeted for ubiquitination contain a ubiquitination signal which promotes the target proteins ubiquitination through contact with the E3 ligase. In p53 it was thought to involve the N-terminus. In order to study the interactions we used peptides from the N-terminus and the BOX-V region of p53. These peptides were added to a ubiquitination reaction containing p53, MDM2, E1, E2, and ATP and the ability of MDM2 to ubiquitinate p53 was analysed by western blot. Ubiquitination of p53 is observed as a ladder of high molecular weight forms of p53.

Peptide aptamers targeting the N-terminal hydrophobic pocket of MDM2 such as BOX-I, 12.1 (an optimized BOX-I) and the drug Nutlin are incapable of inhibiting

MDM2 mediated p53 ubiquitination (Figure 3.3 A,B lanes 1-12, and C, lanes 1-7). Titrations of increasing concentrations of BOX-I, 12.1 and Nutlin (3-50μM) showed little change in MDM2 ubiquitination towards p53 Figure 3.3 A, B lanes 1-12, and C, lanes 1-7). The results presented above suggest that the BOX-I domain of p53 alone is not sufficient to form the ubiquitination signal for p53 as blocking this interaction with peptide aptamers or drugs is insufficient to inhibit p53 ubiquitination by MDM2. Thus, alternative interaction sites out with the N-terminal activation domain of p53 most likely comprise the ubiquitination signal for MDM2 targeting. It is surprising that Nutlin failed to inhibit MDM2 E3-ligase activity *in vitro* as it has previously been shown that Nutlin-treated cells accumulate transcriptionally active p53 protein (Vassilev et al., 2004). We also show an increase in p53 ubiquitination after treatment of A375 with Nutlin, highlighting that blocking the N-terminal interactions between MDM2 and p53 is insufficient to inhibit p53 ubiquitination, and actually stimulates p53 ubiquitination (Fig 3.3D).

Peptides from the core domain of p53, which are contiguous with the S9-S10 linker motif previously shown to control p53-MDM2 binding (Shimizu et al., 2002), capable of inhibiting the ubiquitination of p53 were identified by a chemical genetics screen (Wallace et al., 2006). These peptides mapped to the BOX-V region which is within the core DNA binding domain of p53. A separate study identified a peptide from the RB-MDM2 interface, Rb1, which showed homology to the S9-S10linker/BOX-V region of p53. Further investigation showed both peptides were able to inhibit ubiquitination of p53 yet with very different potencies. The BOX-V peptide inhibits

MDM2 E3-ligase activity with an $I_{0.5}$ in the range of 20–30 μM (Fig 3.4, lanes 9-13) whilst Rb1 titrations showed that it had a 100-fold lower $I_{0.5}$ than the BOX-V peptide (Fig 3.4, lanes 4-8). Ubiquitination assays were performed at three different time points in order to elucidate any subtle differences in ability of peptides to interfere with ubiquitination which might indicate differences in binding properties (Fig 3.3A, B, and C). At 7 minutes incubation, both peptides were able to inhibit p53 ubiquitination to the same extent (Fig 3.4A Rb1: lanes 4-8, BOX-V: lanes 9-13 compared to lane 3). However after 10 minutes, the BOX-V peptide can be seen to have reduced inhibitory effect at 10 and 20 μM concentrations against equivalent 0.25 and 0.5 μM of Rb1 (Fig 3.4B, Rb1: lanes 4-8, BOX-V: lanes 9-13 compared to lane 3). Finally, after 15 minutes incubation, strong ubiquitinated forms of p53 are observed in the presence of the BOX-V peptide whereas the Rb1 peptide still maintains a substantial inhibition of p53 ubiquitination as observed by the lack of high molecular weight ladder. (Fig 3.4C Rb1: lanes 4-8, BOX-V: lanes 9-13 compared to lane 3).

This data provides evidence for two interesting aspects. Firstly that the Rb1 peptide is a more potent inhibitor of MDM2 mediated p53 ubiquitination than the BOX-V peptide and secondly that the BOX-V seems to bind with a lower affinity to MDM2 or has a higher rate of dissociation from MDM2 than Rb1 and as such is less potent and so permits the ubiquitination of p53.

3.2.3 Rb1 and BOXV peptides bind the acidic domain of MDM2 by AlphaScreen

The interaction between Rb1 and MDM2 was mapped using multiple mutant protein forms by ELISA and AlphaScreen (Wallace et al 2006). This data identified the acid domain as a possible site of contact within MDM2 as only recombinant protein containing the acid domain showed any binding to the peptide. Given that Rb1 was identified by showing homology to S9-S10linker/BOX-V region it was hypothesized that the BOX-V peptide may also bind to the acid domain of MDM2.

To complement the above experiments, an MDM2 acid domain deletion mutant protein (ΔAD) was expressed and purified from *E. coli* (Fig 3.2C). When binding of the ΔAD to Rb1, BOX-V or BOX-I was compared with binding of the isolated acid domain, the results were complementary. BOX-V and Rb1 bound to the acid domain of MDM2 with high affinity but not to the ΔAD protein where binding was no greater than the control peptide (Fig 3.5A and C), whereas BOX-I did not bind to the acid domain but bound to the ΔAD protein (Fig 3.5B)

This data highlights the acid domain as being the site of contact for the BOX-V peptide of p53 as well as confirming that the Rb1 peptide bound the acid domain. Although previous studies had identified a second interaction within MDM2 and p53 this was the first direct evidence that the BOX-V region in p53 bound the acid domain of MDM2.

3.2.4 Purification of cleavable 6xHis tagged acid domain for biophysical studies

Untagged acid domain MDM2 was required to perform circular dichroism and mass spectroscopy. GST is known to form dimers so in order to draw any conclusions from CD and Mass spectroscopy the tag needed to be removed from MDM2. To achieve this, the acid domain of MDM2 was cloned into the pET-15b vector to express it as a His-fusion protein. This vector contains a thrombin cleavage site between the tag and the protein which permits the cleavage of the tag from the recombinant protein following expression and purification.

To begin with the construct was expressed in *E.coli* and purified using Nickel agarose affinity chromatography (Fig 3.6A). A high degree of protein purity is needed for biophysical studies so the purified His tagged MDM2 was further purified using Ion exchange chromatography to achieve this high degree of purity. The peak fractions from nickel agarose purification (4-9) were loaded onto a HiTrap FF-monoQ column and bound proteins were eluted using a salt gradient from 0-1M. Samples were collected and resolved by SDS PAGE and analysed by coomassie staining (Fig 3.6B). His-AD showed a long elution profile from fractions 6-21. Peak fractions (15-22) were pooled and concentrated using Centricon centrifugal filter devices with a molecular weight cut off of 3 KDa. The His tag was then cleaved from the concentrated AD using RECOMT Sigma Thrombin CleanCleave^{TM} kit (Fig 3.6C). Comparing cleaved and uncleaved his-AD shows cleavage was 100% successful (Fig 3.6C, lanes 1 and 2). The free His tag was then removed from the prep by passing the mix over nickel agarose

beads to bind the His tag. The flow through contained pure untagged AD and this was used in further biophysical studies (Fig 3.6C lane 3).

3.2.5 Far-UV circular dichroism (CD) analysis of human MDM2 acidic domain interaction with BOX-V peptide

The BOX-V peptide has been previously shown to bind to the acidic domain of MDM2 using AlphaScreen, but this technique can not be used to examine effects of peptide binding on induced structural changes. Circular dichroism (CD) in the far-UV range however, can be used to estimate the secondary structure content of a sample of MDM2. Far-UV CD was used to investigate the hypothesis that changes within the secondary structure of MDM2 accompany peptide binding to the acidic domain of human MDM2. CD spectra in the far UV range (190 - 250 nm) of recombinant AD protein only, BOX-V peptide only and AD plus BOX-V were measured.

CD spectra are additive, so changes in secondary structure caused by protein interaction can be by assessed by calculating a difference spectra [(Protein + peptide) - peptide] and comparing it to protein alone. AD alone has a spectra characteristic of a random-coil (disordered) conformation, dominated by large negative band at 200 nm (Fig 3.7 Yellow). Analysis of the data with CDSSTR, an algorithm for deconvoluting the CD spectra into its contributing secondary structures, predicts a protein with approximately 10 % helix, 30 % sheet, 25 % turn and 35 % disordered.

The BOX-V and BOX-V + AD spectra also are characteristic of a random-coil. The difference spectra [(AD + BOX-V) – BOX-V] and protein spectra are super-imposable suggesting no coupled binding-folding event (Fig 3.7 Green).

3.2.6 Mass-Spectrometry confirms BOX-V and Rb1 bind the acidic domain

To further characterize the interactions between the AD and BOX-V and Rb1 peptides, MDM2 acid domain – peptide mass spectrometry was performed to determine whether stable protein/peptide complexes could be detected. Direct infusion electrospray ionization mass spectrometry (ESI-MS) was performed to analyse the native AD. Ionization conditions were optimized to retain any solution formed complexes. MDM2 acid domain showed a small peak which indicated the acid domain could form a dimer (Fig 3.8A). When acid domain was analyzed in presence of the BOX-V peptide the overall charge state of the acid domain shifted from 5^+ to 4^+ states with complex formation between a dimer of peptide and monomer of acid domain being observed (Fig 3.8B-upper spectra compared to lower spectra).

Analysis of the ESI-MS spectra of AD in the presence of Rb1 peptide showed similar binding characteristics to AD/BOX-V, with a reduction in charge state of predominantly 5^+ to 4^+ (Fig 3.8C-upper spectra compared to lower spectra) and a small complex formation between a dimer of Rb1 and monomer of MDM2 acid domain (Fig 3.8D).

During the course of the ESI-MS analysis it was found that BOX-V or Rb1 multimers were present in solution (data not shown) and so the resulting peptide dimer-MDM2 complexes are not thought to result from non-specific binding or binding formed during the desolvation process. The fact that peptide-MDM2 complexes are still observed in the presence of such dimers suggests the peptide dimerization does not affect the protein interface but binding it is weak so little is retained.

3.2.7 The N-terminus and acidic domain of MDM2 are required for ubiquitination of p53

After verifying that the BOX-I peptide bound to the N-terminus of MDM2 and the inhibitory peptides, Rb1 and BOX-V bound to the acid domain of MDM2 we went on to examine whether these two domains within MDM2 are essential for ubiquitination of its substrates. GST-MDM2 is fully functional in catalyzing the ubiquitination of p53 *in vitro* (Fig 3.9A, lanes 1-5). When the first 120 amino acids of MDM2 encompassing the hydrophobic pocket, are removed its ability to target and ubiquitinate p53 is lost (Fig 3.9A, lanes 6-10). The acid domain also proved crucial to MDM2s' E3-ligase properties as ΔAD could no longer catalyze p53 ubiquitination (Fig 3.9B lanes 5-7 compared to lanes 2-4).

These studies show that the N-terminus and the acid domain are crucial components of MDM2 for it to function as an E3 ligase.

3.2.8 The BOX-V region of p53 is required for ubiquitination

Having identified the BOX-V region of p53 as a second contact site for the MDM2 acid domain, the requirement of the BOX-V site was analyzed. A naturally occurring isoform of p53 which lacks the BOX-V region, called ΔBOX-Vp53, was expressed and purified as a GST fusion protein in insect cells and was purified using GST affinity chromatography (Fig 3.10A lanes 6-10). As a control for ubiquitination experiments, GST-wtp53 was also expressed and purified in the same way (Fig 3.10 lanes 1-5). The concentration of p53 protein forms were normalized by western and Bradford and equivalent concentrations of p53 were mixed with purified MDM2 in an *in vitro* ubiquitination reaction. While MDM2 can still catalyze ubiquitination of GST-wtp53, it was unable to ubiquitinate the p53 form lacking the BOX-V region, highlighting the requirement of this site for efficient ubiquitination of p53 by MDM2. This isoform is still transcriptionally active, suggesting it may have evolved to avoid proteasomal degradation by MDM2 (Rohaly et al., 2005).

3.3 Discussion

The oncoprotein MDM2 is a key negative regulator of the p53 tumor-suppressor protein and can regulate the activity of p53 by two distinct mechanisms. First, MDM2 can

function as a transcriptional repressor of p53 that inhibits p53's activity by preventing recruitment of transcriptional co-factors (Arva et al., 2005). However, it is the second function of MDM2 as a regulator of p53 protein degradation that has excited the most interest in recent years. MDM2 acts as an E3-ubiquitin ligase for p53, promoting its nuclear export and proteasome-dependent degradation (Brooks and Gu, 2006).

In contrast to the mechanism of ubiquitin transfer, defined by the classic E1-E2 conjugation reactions, the mechanism of MDM2-catalyzed ubiquitination of p53 and the mechanism of action of RING E3-ligases in general is largely undefined. The E3-ligase-catalyzed reaction involves at least two distinct steps: E3 recognition of the substrates' "ubiquitination signal" and covalent ligation of one or more ubiquitin moieties to the substrate (Pickart, 2001). The accepted view, based on available evidence, was that MDM2-mediated ubiquitination of p53 proceeded through binding of the MDM2 N-terminal domain to a BOX-I ubiquitination signal in p53. This view was supported by the finding that mutation of a single phenylalanine residue in the BOX-I domain of p53 prevented MDM2-mediated stabilization of p53 and that a BOX-I mimetic could inhibit formation of a stable p53-MDM2 complex (Bottger et al., 1997; Lin et al., 1994; Liu et al., 2001; Vassilev et al., 2004). However, this finding is complicated by the observation that BOX-I mimetics, including Nutlin, do not inhibit MDM2 E3-ligase activity and efficient ubiquitination of p53 still occurs in their presence (Fig 3.3A, B and C). If, as previously assumed, the BOX-I domain of p53 contained the primary ubiquitination signal for MDM2 targeting, molecules like Nutlin and the 12.1 peptide would be expected to block its ubiquitination by MDM2. Nutlin was identified in a screen for

MDM2 agonists that fit into MDM2s hydrophobic pocket (Vassilev et al., 2004) and therefore competes with the p53-BOX-I domain for binding to MDM2. During this work it was shown that although Nutlin is able to disrupt the interaction between the N-terminal domain of MDM2 and the BOX-I transactivation domain of p53 (Wallace et al., 2006), it does not inhibit MDM2-dependent ubiquitination of p53 (Fig 3.3C). In addition, when the status of endogenous p53 was examined in A375 cells treated with Nutlin, we found that the accumulation of transcriptionally active p53 protein was associated with an increase in modified forms of the p53 protein (Fig3.3D).

The concept that an MDM2 docking site other than the BOX-I motif of p53 could be involved in p53 ubiquitination was originally suggested by studies showing that ribonucleic acid can induce binding of MDM2 to p53 lacking the BOX-I domain (Burch et al., 2000). A motif within the BOX-V domain is a candidate for this p53 ubiquitination signal, as a peptide from this region can inhibit ubiquitination with an $I_{0.5}$ of between 20 and 30 μM (Fig 3.4A, B and C). These data are consistent with a previous report identifying the BOX-V region as a conformationally flexible docking site for MDM2 that could control p53 ubiquitination in cells (Shimizu et al., 2002). The data presented here goes further and highlights a secondary contact site between the acid domain of MDM2 and the BOX-V peptide of p53 (Fig 3.5A, B and C). Furthermore, deletion of the N-terminus or the acid domain of MDM2 abolishes its ability to function as an E3-ligase, demonstrating that both of these contact sites are required for MDM2 to catalyze ubiquitination of p53 (Fig 3.8A and B). In support of this conclusion, removal

of the BOX-V region of p53 results in a p53 protein refractory to ubiquitination by MDM2 (Fig 3.9A and B).

Biophysical techniques, such as circular dichroism (CD), failed to detect any ligand binding induced changes in the structure to the acid domain of MDM2. In fact binding between the acid domain and the BOX-V peptide was not detected. One conclusion that can be drawn from the spectra is that the MDM2 acid domain shows a random-coil (disordered) conformation. This data supports previous work which suggests that the acid domain is unstructured (Bothner et al., 2001). In fact this same work showed structural changes in the acidic domain occur upon ligand binding, focusing in particular on the interaction between MDM2 acid domain and ARF. Using ARF peptides they demonstrated induced structural changes within MDM2 upon ligand binding, from disordered, random conformations to β-strand secondary structures (Bothner et al., 2001). These β-strand structures have been predicted to occur within the acid domain using secondary structure prediction programmes.

One possible explanation for our lack of observed change in MDM2 structure in the presence of BOX-V may be due to the poor solubility of the BOX-V peptide in water, required for CD analysis. Further detailed investigations using peptides with higher affinity for MDM2 may reveal certain induced conformational changes within the E3 ligase, but as this was not the main focus of my project, this work was put to one side.

Mass spectrometry analysis of MDM2 acid domain/ BOX-V and Rb1 interactions supported the findings obtained from AlphaScreen and confirmed the

interaction between the BOX-V and Rb1 peptides with MDM2 acid domain. The observation that the acid domain dimers diminish in the presence of peptide could have some relevance to acid domain function. It is widely believed that MDM2 functions as a homodimer, or heterodimer with MDM4, dimerizing through their ring finger domains (Linke et al., 2008; Tanimura et al., 1999; Uldrijan et al., 2007). This dimerization could bring the acid domains into contact which each other, and this contact could become distorted upon ligand binding.

The discovery that the BOX-V domain of p53 forms part of the ubiquitination signal within p53 and its regulation by the acid domain of MDM2 formed a major part of a piece of research published in Molecular Cell in 2006 entitled Dual-Site regulation of MDM2 E3-ubiquitin ligase activity (Wallace et al., 2006). This paper proposed a model where by the binding of the N-terminus of p53 to the hydrophobic pocket of MDM2 induces a conformational change within MDM2 allowing binding to occur between the acid domain of MDM2 and the ubiquitination signal (BOX-V) of p53, thus facilitating the MDM2 catalyzed ubiquitination of p53 (Fig 3.11). This model was tested by the use of a mutant form of p53 called $p53^{F19A}$ that is normally refractory to ubiquitination by MDM2 due to the fact that it can no longer bind the N-terminus of MDM2. If this model were true, addition of peptides or drugs that occupy the hydrophobic pocket should 'prime' MDM2, allowing the acid domain to form a contact with the BOX-V region of p53 and facilitate its ubiquitination. This proved to be the case as adding in trans BOX-I, 12.1 or Nutlin *in trans* induces the ubiquitination of this mutant p53 (Wallace et al., 2006).

At least one ubiquitination signal is therefore located within the DNA binding domain of p53, and access to this signal sequence is regulated through p53-BOX-I interactions with MDM2. NMR analysis has also shown that the acid domain of MDM2 can bind directly to the DNA binding domain of p53 (Yu et al., 2006b). The acid-domain fragment of MDM2 induced significant chemical shifts within DNA-contact residues within the p53 BOX-V region. Together, these data suggest that MDM2 has an allosteric pocket in the N terminus that requires to be occupied in order to dock onto the ubiquitination signal in the BOX-V domain of p53. This docking may then distort the overall conformation of the DNA binding domain of the p53 tetramer and permit E2-catalyzed ubiquitin transfer.

A vast majority of drugs designed to stabilize p53 in cells are modeled to fit within the MDM2 hydrophobic pocket. It may be that drugs targeting this second interaction may prove to be better, anti-cancer agents by inhibiting the cellular degradation of p53, thus maintaining control over cell proliferation and cell cycle.

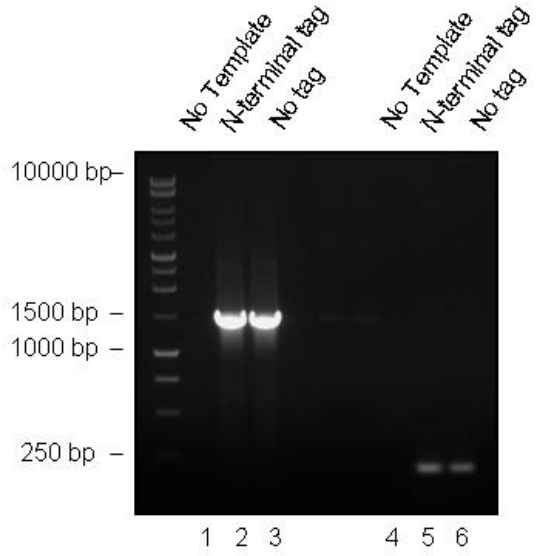

Figure 3.1 PCR cloning of MDM2 full length and MDM2 acid domain. PCR was performed as described in the materials and methods and reaction products were resolved on a 1% agarose gel containing ethidium bromide. Lane 1: no template control, lane 2 and 3: duplicate PCR with MDM2 ORF template. Lane 4: no template control, lane 5 and 6: duplicate PCR with MDM2 ORF template.

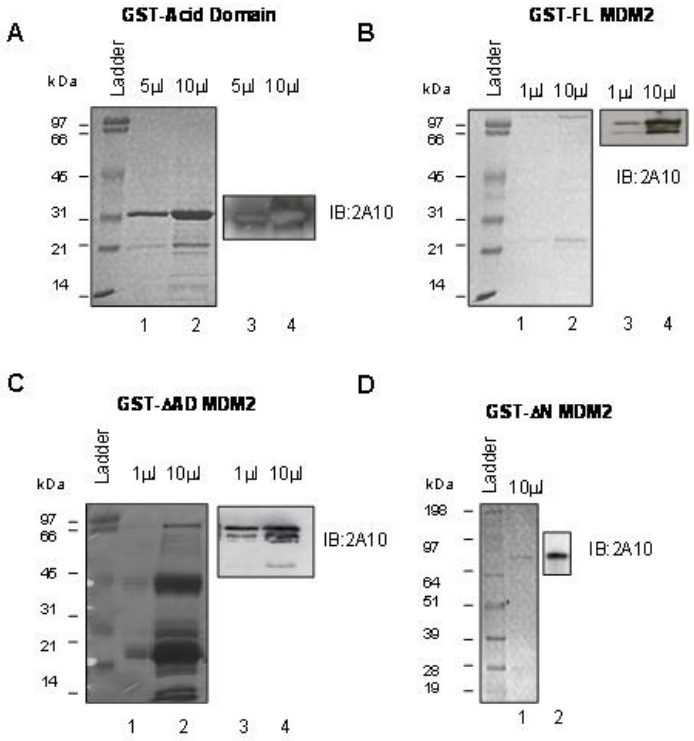

Figure 3.2 Purification of GST-tagged full length, acid domain, Δacid domain and ΔN MDM2. GST-AD, FL, ΔAD and ΔN MDM2 were purified by GST affinity chromatography and portions of purified protein fractions wew resolved by 12% SDS-PAGE unless otherwise stated. Proteins were either visulaised by coomassie staining or by immuno blotting (IB) using the MDM2 specific monoclonal antibody 2A10. **(A)** Purified GST-AD. Lanes 1 and 2: 5 and 10 µl portions of purified GST-AD visualised by coomassie. Lanes 3 and 4: IB of same fractions with 2A10. (B) Purified GST-FL. Lanes 1 and 2: 1 and 10 µl portions of purified GST-FL visualised by coomassie. Lanes 3 and 4: IB of same fractions with 2A10. (C) Purified GST-ΔAD. Lanes 1 and 2: 5 and 10 µl portions of purified GST-ΔAD visulaised by coomassie. Lanes 3 and 4: IB of same fractions with 2A10. (D) Purified GST-ΔN. Lane 1: 10 µl portion of purified GST-ΔN visulaised by coomassie. Lanes 2: IB of same fraction with 2A10.

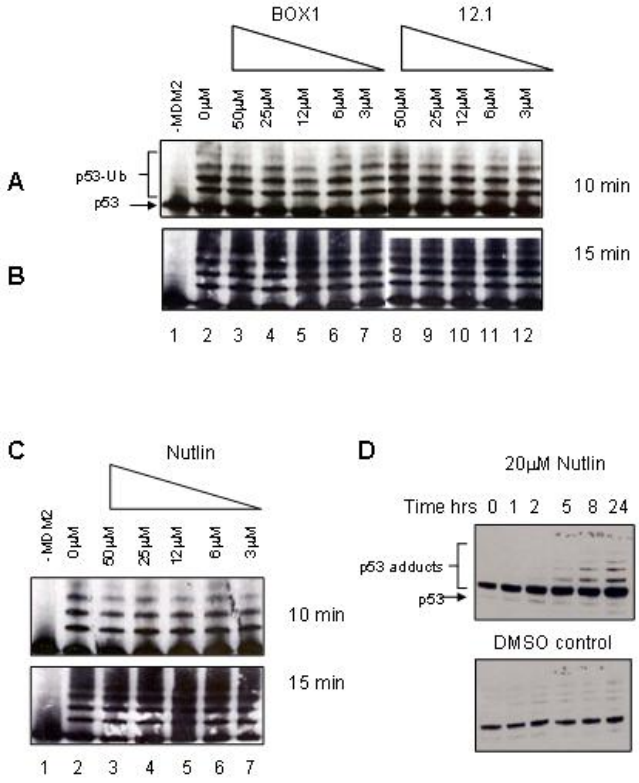

Figure 3.3 BOX-I, 12.1 and Nutlin do not inhibit MDM2 catalyzed p53 ubiquitination. (A) *In vitro* ubiquitination assays containing p53, MDM2, E1, E2 and ATP were incubated at 30°C for 10 minutes in the presence of a titration of either BOX-I (Lanes 3-7 compared to lane 2) or 12.1 (Lanes 8-12 compared to lane 2). **(B)** Ubiquitination assay created as in **(A)** but incubated at 30°C for 15 minutes. **(C)** Ubiquitination assay created as in **(A)** but contained increasing concentrations of the drug Nutlin. **(D)** A375 cells treated with 20mM of Nutlin for indicated time points. Cells were harvested, lysed and analysed by IB with DO1.

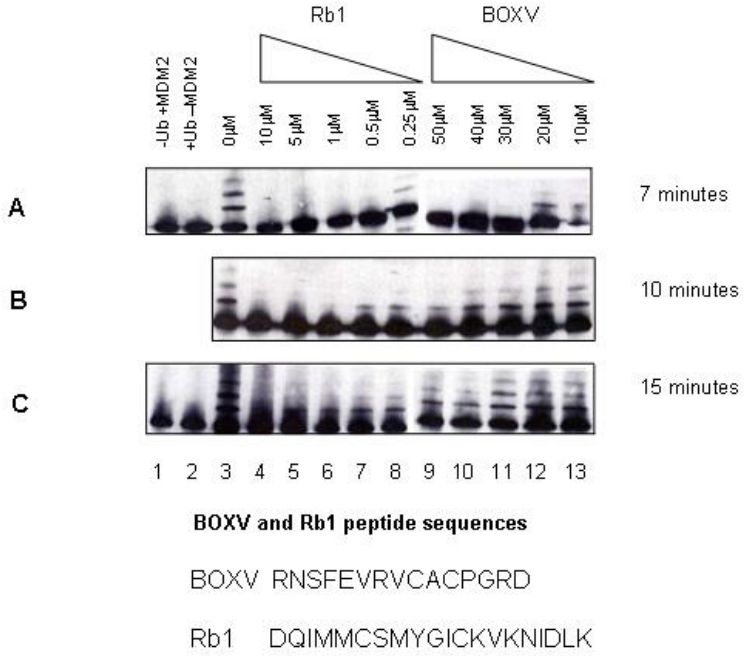

Figure 3.4 BOX-V and Rb1 inhibit MDM2 catalyzed p53 ubiquitination. **(A)** *In vitro* ubiquitination assays containing p53, MDM2, E1, E2 and ATP were incubated at 30°C for 7 minutes. Lane 3: positive control, lanes 4-8: in the presence of increasing concentrations of the Rb1 peptide, lanes 9-13: in the presence of increasing concentrations of BOX-V peptide. show a titratable inhibition of ubiquitination by Rb1 compared to lane 3. **(B)** and **(C)** As in **(A)** but incubated for 10 and 15 minutes respectively.

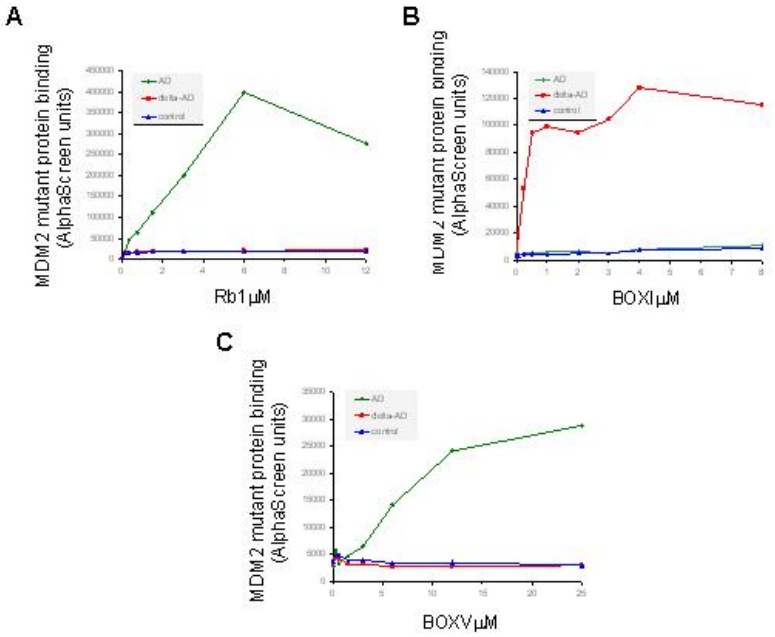

Figure 3.5 BOX-V and Rb1 peptides bind to the Acid Domain of MDM2. Analysis of mutant MDM2 binding activity to Rb1 (A) BOX-I (B) or BOX-V (C). Peptides were incubated with GST-ΔAD-MDM2 (70ng) or GST-AD (50ng), and binding was measured with an AlphaScreen IgG (protein A) detection kit with anti-GST antibody.

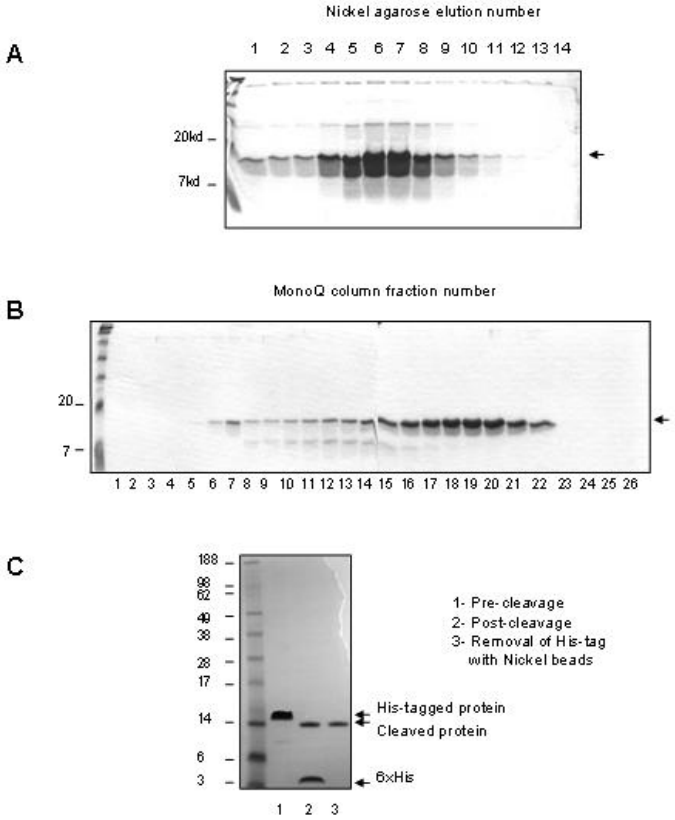

Figure 3.6 Purification of 6xHis-tagged acid domain for biophysical studies. Proteins were resolved by SDS-PAGE on an 18% gel unless otherwise stated. **(A)** Elution profile of his-AD from Ni^{+}beads. **(B)** To further purify the protein the peak fractions 4-9 from Ni^{+} elution were subjected to ion-exchange chromatography using a HiTrap-FF mono-Q column (*Amersham* Biosciences). Protein was eluted in 1ml fractions using an increasing salt gradient from 0M-1M KCl. **(C)** Cleavage of 6xhis tag using RECOMT Sigma Thrombin CleanCleave™ Kit. Proteins resolved on a NOVEX 4-12% pre-cast gel. Lane 1: uncleaved MDM2, Lane 2: cleaved MDM2 and lane 3: flow through from Ni^{+} agarose to remove cleaved histidine tag.

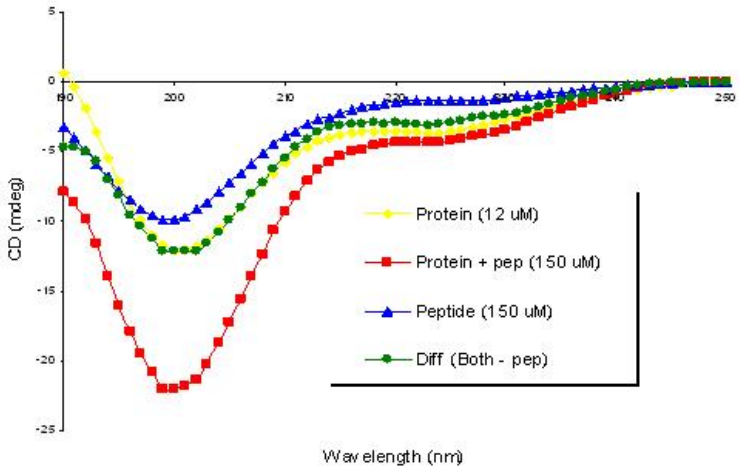

Figure 3.7 Far-UV circular dichroism as a method to identify structural changes in the MDM2 acid domain upon ligand binding. (A) Yellow: Acid domain (12μM) alone. Red: Acid domain (12μM) plus BOX-V peptide (150μM). Blue: BOX-V (150μM) only. Green: The difference spectra [(AD + BOX-V) – BOX-V] and acid domain spectra are superimposable suggesting no coupled binding-folding event.

A. Acid Domain only

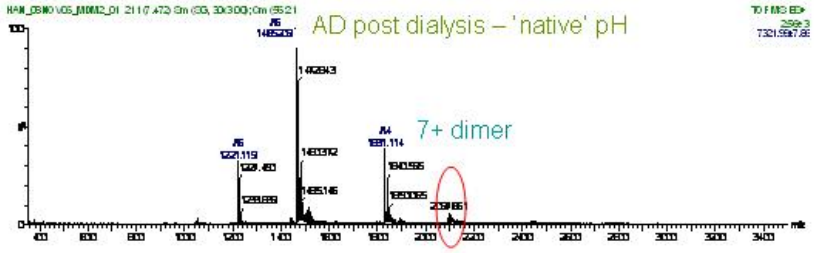

B. AD plus BOX-V

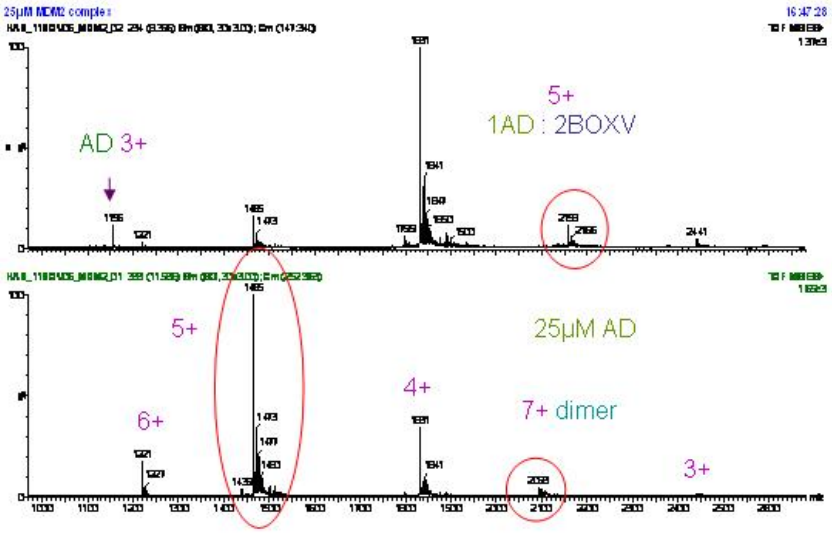

C. AD plus Rb1

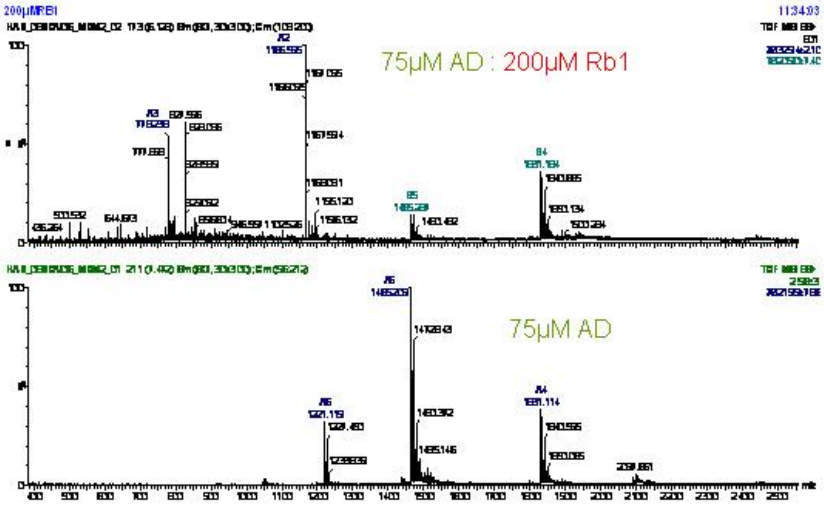

D AD plus Rb1

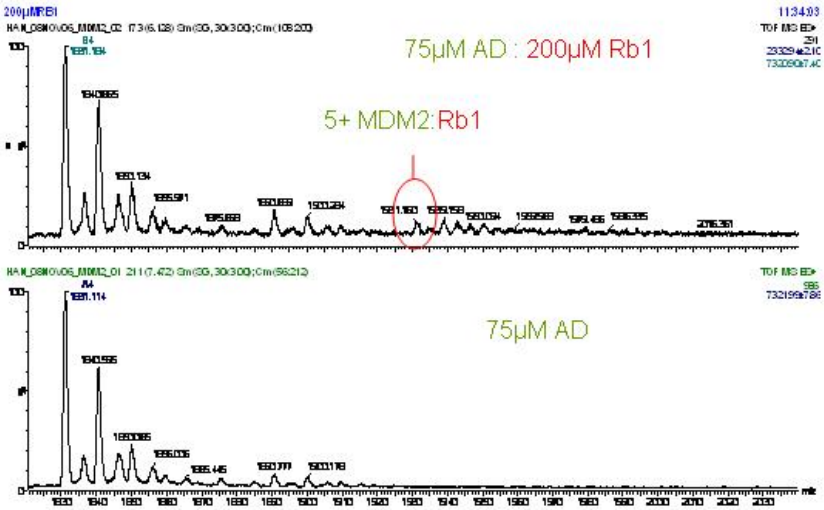

Figure 3.8 Mass-spectroscopy reveals acid domain-peptide interactions. **(A)** Mass spectra of acid domain alone shows presence of a 7^+ dimer (25μM). **(B)** BOX-V acid domain interactions were observed between a dimer of BOX-V (50μM) and monomer of acid domain (25μM) (upper spectra). Charge state of acid domain shifts from 5^+ to 4^+ in the presence of BOX-V (lower spectra compared to upper spectra). **(C)** Acid domain (75μM) charge state shifts from 5^+ to 4^+ in presence of Rb1 (200μM) (lower spectra compared to upper spectra). **(D)** A more detailed analysis of Rb1-acid domain spectra reveals complex formation with 5^+ charge between a dimer of Rb1 and a monomer of acid domain (upper spectra). This peak is absent from protein only spectra (lower spectra).

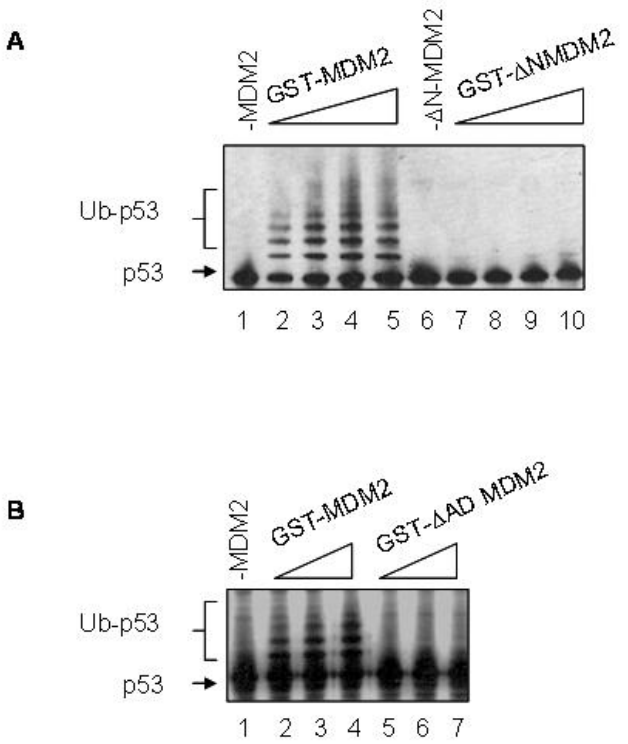

Figure 3.9 The N-terminus and acid domain of MDM2 are required for its E3-ligase activity. Proteins were resolve by SDS-PAGE on NOVEX4-12% pre-cast gels. *In vitro* p53 ubiquitination assay using GST-tagged MDM2 constructs. **(A)** Lanes 2-5: control. GST-ΔN MDM2 (lanes 7-10, 50-200ng). **(B)** Wild type GST-MDM2 (lanes 2-4, 50-150ng). GST-ΔAD MDM2 (lanes 5-7, 50-150ng).

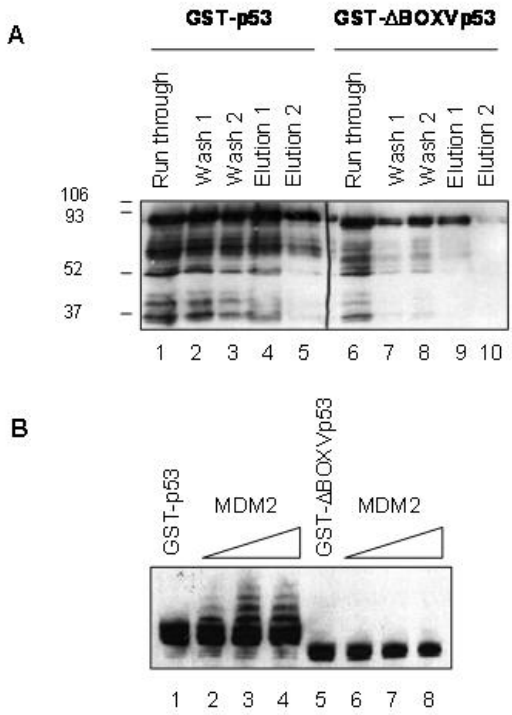

Figure 3.10 The BOX-V region of p53 is essential for its MDM2 catalyzed ubiquitination. **(A)** Purification of GST-wtp53 and GST-Δp53 from SF9 cell lysates. Lanes 1-5 show the purification of GST-wtp53, from run through (lane 1), wash 1 and 2 (lanes 2 and 3), and elutions (lanes 4 and 5). Lanes 6-10 show the same purification procedure but with GST-Δp53. **(B)** A titration of MDM2 (50-150ng) is capable of ubiquitinating GST-wtp53 (lanes 2-4) but not GST-Δp53 (lanes 6-8).

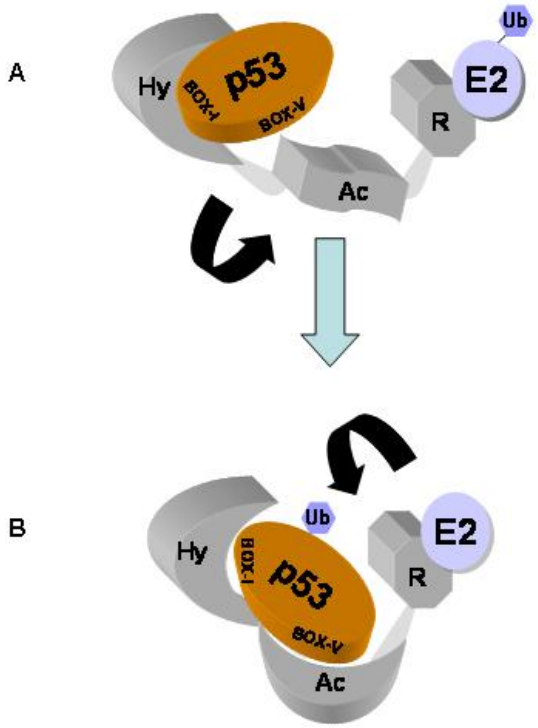

Figure 3.11 Model illustrating the dual-site mechanism where by MDM2 facilitates the ubiquitin of p53. **(A)** MDM2 binds p53 BOX-I site through its hydrophobic pocket which induces conformational changes in MDM2, allowing the acid domain to dock to the BOX-V ubiquitination signal in the core of p53. **(B)** This secondary interaction signals for the E2 mediated ubiquitin transfer to specific lysines within the p53 protein.

Chapter 4

PHOSPHO-MIMETIC MUTATION IN THE MDM2 LID ACTIVATES MDM2 E3-LIGASE FUNCTION

4.1 Introduction

MDM2 has been dissected into multiple mini-domains with specific biochemical functions: an N-terminal allosteric hydrophobic pocket which interacts with specific linear peptide motifs in proteins such as p53 (Kussie et al., 1996); an internal acidic domain that binds a range of substrates (Yu et al., 2006a), a C-terminal RING domain that co-ordinates E2 functions in ubiquitin transfer (Linke et al., 2008) and promotes MDM2-dependent stimulation of p53 protein synthesis (Candeias et al., 2008), an ATP-binding motif imbedded within the RING domain that regulates chaperonin functions of MDM2 (Wawrzynow et al., 2007), and a C-terminal peptide tail that maintains RING domain conformation (Poyurovsky et al., 2007) (Uldrijan et al., 2007). Reconstitution of the ubiquitin ligase function of MDM2 using purified proteins has demonstrated a two-site docking model for ubiquitination of p53 (Wallace et al., 2006). This involves occupation of the N-terminal hydrophobic pocket by a priming ligand (natural sequences in proteins like p53 or drug leads like Nutlin) that induces a docking event between the

acidic domain of MDM2 and a ubiquitin-signal in the DNA-binding domain of p53 (Yu et al., 2006a) (Wallace et al., 2006). It is known that this dual-site docking catalyzes the ubiquitination of p53, however the details of the conformational changes that mediate this reaction have yet to be defined.

One of the intriguing features of the dual-site model for MDM2 function is that its N-terminal hydrophobic pocket requires a ligand to prime and stimulate the E3 ligase function of MDM2 (Wallace et al., 2006). Prior to these studies, it was thought that ligands that bind to this pocket in MDM2 would block its ubiquitination function; indeed such ligands do block MDM2 activity in relation to its transrepression of p53 (Vassilev, 2004). This dual-site model for MDM2 function is also compatible with the allosteric nature of MDM2 as further evidenced by the flexibility of the N-terminal hydrophobic domain in the presence of distinct peptide-ligands (Schon et al., 2004; Uhrinova et al., 2005). In order to test the dual-site model of MDM2 docking to p53, the contribution of a flexible N-terminal peptide motif adjacent to the hydrophobic pocket of MDM2 was examined. This peptide lid (aa12-25) has a significant degree of homology to the p53-activation domain fragment (aa10-26), suggesting that it might be able to compete *in cis* for binding with p53 and act like a pseudo-substrate domain (Fig 4.1A). However, as ligands like Nutlin that fill the hydrophobic pocket can stimulate MDM2 E3 ubiquitin ligase function (Wallace et al., 2006), the role of the pseudo-substrate motif is not necessarily evident - would it function as a positive or negative cofactor in regulating the stability of the MDM2:p53 complex?

Multiple sequence alignment of MDM2 and MDM4 reveals the evolutionary divergence between MDM2 homologues and the paralogue MDM4 at the pseudo-substrate motif (aa 16-23). (Fig 4.1B) MDM4 has evolved without the presence of a lid highlighting its specific roles within MDM2.

In this chapter, I show that the phospho-mimetic lid surprisingly stabilizes the MDM2:p53 complex through an allosteric model which is consistent with the pseudo-substrate motif functioning as a positive regulatory motif. This model is consistent with: (i) the dual site docking function of MDM2 (Wallace et al., 2006), (ii) the intrinsic flexibility of the N-terminal domain of MDM2 (Schon et al., 2004; Uhrinova et al., 2005), and (iii) the ability of the phospho-mimetic pseudo-substrate motif to change the conformation of MDM2 (McCoy et al., 2003). The gain-of-function effect on MDM2 induced by pseudo-substrate motif mutation has implications for how the MDM2:p53 axis can be regulated post-translationally in cells and for strategies aimed at inhibiting the E3 ubiquitin ligase function of MDM2.

4.2 Results

4.2.1 MDM2 lid forms a positive regulatory motif

In order to further evaluate the dual-site docking model of MDM2 function, the effects of the pseudo-substrate motif or 'lid' on the E3 Ubiquitin ligase function of MDM2 were

evaluated. Complimenting the model where a phospho-mimetic pseudo-substrate motif occupies the hydrophobic binding pocket of MDM2 (McCoy et al., 2003), an NMR study of the unliganded *apo*-form of the N-terminal domain of MDM2 revealed the pseudo-substrate motif to be largely unstructured (Uhrinova et al., 2005). To clarify the role of this flexible motif, purified untagged wild-type MDM2 and MDM2 mutants were generated, including a mutant with an N-terminal flexible pseudo-substrate motif deletion ($MDM2^{\Delta lid}$). Proteins were purified from *E.coli* using HiTrapFF SP affinity chromatography (Fig 4.2A, B and C). $MDM2^{WT}$, $MDM2^{\Delta lid}$ and $MDM2^{S17D}$ eluted over a wide peak around fractions 1-31 with residual elution seen throughout the remaining fractions (Fig 4.2A, B and C). Ubiquitination reactions were set up with p53, E1, E2, ATP and MDM2 to assay the proteins activity. A titration of $MDM2^{WT}$ (Fig 4.3A, lanes 1-5) or $MDM2^{\Delta Lid}$ (Fig 4.3A, lanes 6-10) in ubiquitination reactions demonstrated that $MDM2^{\Delta lid}$ has a lower specific activity, although it can still catalyze ubiquitination. Surprisingly, the phospho-mimetic mutation did not inhibit the ubiquitination function of MDM2 as expected; rather the Asp^{17} mutation increased the specific activity of MDM2 as an E3-ubiquitin ligase (Fig 4.3B, lanes 5-7 vs 2-4).

The lowered specific activity of $MDM2^{\Delta Lid}$ suggests the pseudo-substrate motif normally has an intrinsic positive regulatory effect on MDM2 function. Regulatory domains often alter the thermostability of an enzyme or protein (Dyson and Wright, 2002) so we evaluated whether the pseudo-substrate motif deletion alters the thermostability of MDM2. Ubiquitination reactions were set up as before but the MDM2 was pre-incubated at certain temperatures for 5 minutes before addition to the

reaction. MDM2WT was completely unaffected by pre-incubation, even at 50^{o}C (Fig 4.3C, lanes 2-6 vs 1). The pre-incubation of MDM2$^{\Delta Lid}$ at any temperature completely inactivated the E3 ubiquitin ligase function of the protein as seen by the reduction in ubiquitinated p53 bands (Fig 4.3C, lanes 8-12 vs 7). By contrast, MDM2^{S17D} behaved more like MDM2^{WT} and did not show signs of thermosensitivity (Fig 4.3C lanes 13-18 vs lanes 7-12). These data indicate that the phospho-mimetic substitution at Ser17 has an opposite and stimulatory effect on MDM2 stability compared to the pseudo-substrate motif-deletion mutant of MDM2.

In order to test whether the loss of the lid influenced the in vivo activity/stability of MDM2 we transfected MDM2$^{\Delta lid}$ in to H1299 cells. MDM2$^{\Delta lid}$ was less stable in cells as seen by decreased expression compared to MDM2^{WT} and MDM2^{S17D} in H1299 cells and this is correlated with its decreased ability to act as an E3 ligase (Fig 4.3D).

These data suggest that the pseudo-substrate motif contributes positively to maintaining the thermostability of MDM2 protein.

4.2.2 Higher specific activity of MDM2^{S17D} towards p53 can be attributed to increased binding to p53

Next, we analyzed whether the enhanced specific activity of MDM2^{S17D} could be attributed to enhanced binding affinity for p53 protein. A titration of MDM2^{S17D}, MDM2^{WT}, or MDM2$^{\Delta Lid}$ provided a correlation between specific activity of an E3-

ubiquitin ligase and enhanced affinity for p53 (Fig 4.4A). Although $MDM2^{\Delta Lid}$ was essentially unable to form a stable contact with p53 as a result of pseudo-substrate motif-deletion, $MDM2^{S17D}$ exhibited a striking increase in its binding affinity for p53 compared to $MDM2^{WT}$ (Fig 4.4A). The pre-incubation of $MDM2^{S17D}$, $MDM2^{WT}$, or $MDM2^{\Delta Lid}$ at distinct temperatures had no effect on $MDM2^{WT}$ protein affinity or $MDM2^{S17D}$ affinity for p53 (Fig 4.4B). This elevated affinity of MDM2 for p53 as a result of the Asp^{17} mutation contrasts with the expected ability of this substitution to de-stabilize the MDM2:p53 complex (McCoy et al., 2003).

4.2.3 Effect of phospho-mimetic mutation is only seen in low expression vectors

Sets of cellular studies were carried out to determine whether the $MDM2^{S17D}$ protein exhibited increased specific activity in cells. Using MDM2 overproduced in pcDNA3.1-based expression vectors, surprisingly we did not observe any difference in the specific activity of $MDM2^{S17D}$ compared to $MDM2^{WT}$. The promoters within vector constructs that drive the overproduction of genes in tissue culture cells are designed to maximally produce a target protein. It is possible that such excessive over production of protein may not represent physiological expression levels and may swamp the normal regulatory machinery and this intern could mask any subtle effects caused by a phospho-mimetic substitute. (Clegg et al., 2008). As a result, expression vectors that produce lower and possibly more physiological levels of MDM2 protein (Fig 4.5A, lanes 1-3) than standard

expression vectors (Figure 4.5A, lanes 4-6) were used. Dual-luciferase assays to analyse MDM2 function revealed the difference between these two constructs with high expression MDM2 transrepressing p53 much better than pDEST3.2 MDM2 which produced only slight transrepression and even sometimes stimulation (Fig 4.5B). Under these conditions of more physiological levels of intracellular MDM2 protein, a striking effect of the S17D substitution on MDM2 function as a p53 inhibitor was observed compared to pcDNA 3.1 $MDM2^{WT}$ and pDEST 3.2 $MDM2^{\Delta lid}$ (Fig 4.6A). In contrast the striking inhibitory effect of S17D on p53 expression was essentially absent when the S17D mutant was expressed in H1299 cells using the high expression vector pcDNA 3.1 (Fig 4.6B). This demonstrates the importance of using vectors which give more physiological protein levels when studying complex pathways. Further titrations of the pDEST 3.2 $MDM2^{S17D}$ construct revealed its striking ability to transrepress p53. Increasing titrations of pDEST 3.2 $MDM2^{S17D}$ from 15ng to 550ng resulted in transrepression of p53, with 15ng transrespressing p53 by around 50% (Fig 4.6C-left side of panel). To try and overcome this transrepression p53 was titrated in with fixed $MDM2^{S17D}$ (Fig 4.6C-middle of panel). This resulted in only partial rescue of transrepression unlike normal recovery seen with p53 only (Fig 4.6C-right side of panel).

In order to confirm it was a phospho-mimic specific mutation that was having this effect on MDM2's activity additional mutations were introduced at this site. An alanine mutation was introduced as a non polar amino acid, an asparagine was introduced which has neutral charge and glutamic acid was introduced as another

phospho-mimic amino acid. $MDM2^{S17A}$, $MDM2^{S17N}$ and $MDM2^{S17E}$ all lacked this striking inhibitory effect seen with $MDM2^{S17D}$. (Fig 4.7A) These mutations were only introduced to the pDEST 3.2 MDM2 as this was the construct which gave an over active MDM2. It was surprising that the other phospho-mimic S17E did not show an increase in activity in a manner similar to S17D but this could be due to its longer side chain which is slightly bigger than aspartic acid and perhaps does not mimic phosphate as well. Complimenting figure 4.3D, pcDNA3.1 $MDM2^{\Delta Lid}$ loses its transrepression ability which can be attributed to its thermo-sensitivity and lower expression levels (Fig 4.7B). To confirm that this striking effect seen was specifically due to mutation of S17D and not another spurious mutation missed by sequencing of the vector, the Asp17 mutation was reversed to a Ser. Reversal of this mutation returned MDM2s activity back to that of wild-type. (Fig 4.7C).

Mutation of Ser17 of MDM2 activates MDM2 towards p53 but only when expressed a low levels in the pDEST 3.2 expression vector and the activating mutation can be reversed by restoring the Ser17. We have shown that this activating effect is absent in the pcDNA 3.1 vector. This phospho-mimetic mutation causes an increase in p53 binding as shown by ELISA *in vitro* and an increase in p53 transrepression as seen *in vivo*.

4.2.4 The MDM2 lid may form the switch between MDM2 promoting p53 synthesis to degrading p53

We next wanted to see the effects that $MDM2^{WT}$, $MDM2^{S17D}$ and $MDM2^{\Delta lid}$ expressed in pDEST 3.2 had on p53 protein levels and down stream targets. To do this we used mouse embryonic fibroblasts which lacked both MDM2 and p53, this made it easier to see transfected MDM2 with the low expression vector.

Under these lower levels of $MDM2^{WT}$ production (pDEST 3.2), the $MDM2^{WT}$ protein enhanced the steady state synthesis of p53 and p21 protein (Fig 4.8A, lanes 3-6 vs lane 2). Conversely, the inhibitory effect of $MDM2^{S17D}$ on p53 activity is attributed to the enhanced instability of p53 protein after transfection into cells (Fig 4.8A, lanes 11-14 vs 3-6). p21 protein is similarly de-stabilized upon co-transfection of p53 with $MDM2^{S17D}$ (Fig 4.8A, lanes 7-10 vs 3-6). $MDM2^{\Delta lid}$ lost some of the enhanced steady state synthesis of p53 and p21 seen with $MDM2^{WT}$. This stimulatory effect of $MDM2^{WT}$ on p53 protein synthesis has been reported previously (Fahraeus et al., 1999) through binding of MDM2 and p53 RNA (Candeias et al., 2008) and can also be attributed to the chaperone functions of MDM2 (Wawrzynow et al., 2007).

As MDM4 is thought to work closely with MDM2 in regulating p53s functions we next evaluated whether pcDNA3.1 $MDM2^{S17D}$ exhibited enhanced binding to MDM4 and whether it effected the synthesis of the p53. The co-transfection of MDM2 or $MDM2^{S17D}$ and MDM4, followed by immuno-precipitation of the two proteins indicated that MDM4 was able to form a stable complex with either $MDM2^{WT}$ or $MDM2^{S17D}$ (Fig

4.8B). In contrast, p53 was attenuated in the formation of stable complex with MDM2 (Figure 4.8C) presumably due to de-stabilization of the p53 protein. Together, these data indicate that MDM2^{S17D} protein can selectively de-stabilize p53, without altering steady-state levels of MDM4 protein.

4.2.5 MDM2^{S17D} can transrepress and inhibit p53^{F19A}

One attribute of the dual site model of MDM2 function is that when the N-terminal hydrophobic pocket is "occupied" by ligand, MDM2 is able to inhibit p53^{F19A}, a p53 mutant normally refractory to inhibition by MDM2 due to mutation of the p53 BOX-I docking site required for MDM2 binding. (Wallace et al., 2006) (Fig 4.9C). In order to examine if MDM2^{S17D} could transrepress p53^{F19A} a dual luciferase assay was performed. Titration of pDEST 3.2 MDM2^{S17D} with p53^{WT}, and pDEST 3.2 MDM2^{S17D} with p53^{F19A} showed that pDEST 3.2 MDM2^{S17D} is able to transrepress p53^{F19A} (Fig 4.9A) compared to pDEST 3.2 MDM2^{WT} (last column Fig 4.9A), which is further consistent with the *in vitro* data that this mutant form of MDM2 has a higher affinity for p53. Like p53^{WT}, pDEST 3.2 MDM2^{S17D} can de-stabilize p53^{F19A} protein levels in cells (Fig 4.9B).

The data presented above showing that the phospho-mimetic S17D substitution of MDM2 inhibits p53, could be explained by two models which are consistent with the dual site docking model of MDM2 function (Wallace et al., 2006); Firstly the phospho-mimicking pseudo-substrate motif is indeed bound in the hydrophobic binding pocket

(McCoy et al., 2003), but is acting like Nutlin in a positive auto-allosteric manner (Wallace et al., 2006) or secondly that the S17D mutation orientates the pseudo-substrate motif in a position that stabilises the N-terminal domain of MDM2 in a conformation which is primed for allosteric activation. Further biochemical characterization of $MDM2^{S17D}$ was carried out in order to test these hypotheses. One method to examine whether the Asp^{17} mutation stabilizes the pseudo-substrate motif over the hydrophobic pocket of MDM2 would be to determine whether $MDM2^{S17D}$ is sensitive to Nutlin; it might be expected that the $MDM2^{S17D}$ is not able to interact with Nutlin (or the BOX-I domain of p53) if the Asp^{17} modified pseudo-substrate motif is stabilized over the hydrophobic pocket. However analysis of p53:MDM2 binding using ELISA showed that p53 binding to MDM2 was inhibited in the presence of Nutlin or BOX-Ia for both $MDM2^{WT}$ and $MDM2^{S17D}$ (Fig 4.10A and B). Similarly, BOX-Va and BOX-Vb inhibit formation of a complex but to a lesser extent. In a dual-luciferase assay MDM2 dependent transrepression of the p21 promoter can normally be rescued by Nutlin using the high expression vector pcDNA 3.1 MDM2 (Fig 4.10C). Using pDEST 3.2 $MDM2^{S17D}$ no rescue with Nutlin was seen suggesting that although Nutlin can inhibit the protein binding it is not having an effect on its cellular activity (Fig 4.10C). This data is not compatible with the model that the Asp^{17} substituted pseudo-substrate motif is stabilized over the hydrophobic pocket of MDM2. Rather, the data favours a model where by the Asp^{17} substitution does change the conformation of MDM2, but does so by "opening" the hydrophobic pocket and sensitizing MDM2 to BOX-I like

ligands. One model that can be formulated to explain this would be that the pseudo-substrate motif could contact an alternate site on MDM2 that facilitates this reaction.

4.2.6 MDM2^{S17D} binds with higher affinity to both the BOX-I and the BOX-V sites

If the MDM2^{S17D} protein does in fact have a more open conformation that stabilizes interactions with p53, it would be expected that MDM2^{S17D} would have a higher affinity for the BOX-I peptides from the N-terminus of p53. We tested this by ELISA, with the BOX-Ia or BOX-Ib peptides coated onto a 96 well plate. MDM2^{WT}, MDM2$^{\Delta lid}$ or MDM2^{S17D} were incubated over the peptide before detection of complex formation with the MDM2 specific antibody 2A10. In fact, as seen with the full-length p53, MDM2^{S17D} binds more stably to the BOX-I peptides, when compared to MDM2^{WT} (Fig 4.11A). The BOX-I peptide "a" is the naturally occurring peptide from p53, whilst BOX-I peptide "b" is the optimized higher affinity peptide named 12.1 identified using combinatorial peptide libraries (Bottger et al., 1996). Comparison of binding to BOX-Ia and BOX-Ib peptides by ELISA showed that this enhanced binding of MDM2^{S17D} to the BOX-I peptide from p53 is not compatible with the model that the Asp^{17} pseudo-substrate motif is stabilized over the hydrophobic pocket, as if this were the case, then MDM2^{S17D} should have a lower affinity for p53 (McCoy et al., 2003). MDM2$^{\Delta lid}$ was used as a control for BOX-I binding, MDM2$^{\Delta Lid}$ unable to form a stable complex with the BOX-I

peptide (Fig 4.11A), $MDM2^{\Delta Lid}$ was however able to form a stable complex with the ubiquitination signal in the BOX-V peptide highlighting the integrity of the acid domain is unaffected (Fig 4.11B). Furthermore, analysis of $MDM2^{WT}$ and $MDM2^{S17D}$ BOX-V binding showed that $MDM2^{S17D}$ is also more active in binding to the BOX-V peptide than $MDM2^{WT}$ (Fig 4.11B), which together explains in part why $MDM2^{S17D}$ binds better to p53. However, the higher affinity of $MDM2^{S17D}$ for Nutlin and BOX-I peptides cannot be explained by the current idea that the phospho-mimetic pseudo-substrate motif can be stabilized over the hydrophobic pocket and block the MDM2:p53 interaction.

4.2.7 Analysis of $MDM2^{WT}$ and $MDM2^{S17D}$ using a ProtoArray®

We wanted to see if $MDM2^{S17D}$ bound to a subset of proteins which was different from $MDM2^{WT}$. The ProtoArray® Human Protein Microarray is a high density protein microarray containing 8000 human proteins on its surface allowing for rapid and efficient detection of protein-protein interactions. Either $MDM2^{WT}$ or $MDM2^{S17D}$ was incubated over the array before being washed. Bound MDM2 was then detected using the MDM2 specific antibody 2A10 followed by Alexa Fluor® 647 labelled goat anti-mouse secondary antibody. Spots were then scored using computer programmes and assigned a score from A to E with A being a strong binding protein and E showing no binding. ProtoArray® revealed $MDM2^{S17D}$ has a higher affinity for a number of different proteins when compared to $MDM2^{WT}$ with potential to regulate many

pathways, specifically the ubiquitination pathway. Figure 4.11 B highlights a few proteins identified in this manner.

MDM2 can also ubiquitinate interferon regulatory factor 1 and 2 (IRF-1, IRF-2). They both contain potential BOX-I sites and a potential BOX-V sites (Data not shown). It is hypothesised that MDM2 degrades IRF-1 and IRF-2 using the same mechanism as for p53, the dual site mechanism. IRF-1 encodes interferon regulatory factor 1, a member of the interferon regulatory transcription factor family. IRF-1 promotes the expression of the toll-like receptor-3 protein (TLR-3) involved in innate immunity. IRF-2 negatively regulates IRF-1 and can inhibit this expression of TLR-3. Using the IRF-1 responsive promoter TLR-3, pDEST 3.2 $MDM2^{S17D}$ was shown to have similar transrepression effect as IRF-2 (Fig 4.13A). This can also be reproduced using the IRF-1 responsive TNF-related apoptosis-inducing ligand (TRAIL) derived promoter (Fig 4.13B). IRF-2 and pDEST 3.2 $MDM2^{WT}$ slightly reduces IRF-1 enhanced expression of TRAIL but pDEST 3.2 $MDM2^{S17D}$ has a marked increase in inhibition (Fig 4.13B). E2F1 is another protein with potential BOX-I and BOX-V motifs and transcriptional assays reveal it too can be repressed by pDEST 3.2 $MDM2^{S17D}$ (Fig 4.13C). $MDM2^{S17D}$ also bound to E2F1 with a higher affinity than $MDM2^{WT}$ and $MDM2^{\Delta lid}$ in an ELISA assay (Fig 4.13D).

This data identifies other targets of MDM2 which are repressed by the $MDM2^{S17D}$ protein. p53, IRF-1, IRF-2 and E2F1 are all transcription factors which function to regulate the transcription of various target genes. $MDM2^{S17D}$ can negatively

regulate all of them to a much larger extent than $MDM2^{WT}$. This highlights the phosphorylation of the MDM2 lid as a potential regulator of protein expression.

4.3 Discussion

MDM2 is a multi-domain E3 RING-finger ubiquitin ligase and represents a model protein with which to define mechanisms of substrate ubiquitination. The recent dual-site model for MDM2-mediated ubiquitination of p53 suggested an allosteric component to the E3 ubiquitin ligase function which invokes MDM2 docking to two distinct sites on p53; the *BOX-I* transactivation domain and a conformationally flexible motif in the *BOX-V* domain of p53. The allostery in the N-terminal domain that operates towards the acidic domain (Wallace et al., 2006) can be propagated presumably via the striking conformational flexibility of the N-terminal domain of MDM2 as defined by NMR (McCoy et al., 2003; Schon et al., 2004; Uhrinova et al., 2005). The unexpected feature of the dual site model was that the N-terminal hydrophobic pocket of MDM2 can act as an allosteric ligand binding site and that ligands like Nutlin can "activate" the E3 ubiquitin ligase function of MDM2 (Wallace et al., 2006). In order to test this model, the function of the poorly characterized MDM2 pseudo-substrate motif or 'Lid', in the MDM2:p53 complex interaction was evaluated, as this provides a potential physiological mechanism with which to regulate MDM2 conformation given the flexible motif proximity to the hydrophobic pocket of MDM2 (Fig 4.14).

These data also help to explain an apparent paradox in the MDM2:p53 regulatory loop. A large body of data clearly has indicated that MDM2 can function as a negative regulator of p53 (Toledo and Wahl, 2006). However, data has also indicated that MDM2 can function positively as a growth suppressor (Brown et al., 1998; Zhou et al., 2005), as a factor that can stimulate p53 protein synthesis (Candeias et al., 2008; Yin et al., 2002), and as a protein that can cooperate with HSP90 to co-chaperone and stimulate p53 function in an ATP-dependent manner (Wawrzynow et al., 2007). As suggested recently, more physiologically expressed levels of MDM2 protein might reveal regulation that is not seen by classic over-production methodologies (Clegg et al., 2008). In fact, by expressing very small amounts of $MDM2^{WT}$, an MDM2-dependent increase in p53 protein and p21 protein levels was observed. This can be explained by the recently identified model that MDM2 regulates p53 protein levels through the binding of the MDM2 RING to the BOX-I p53 RNA site (Candeias et al., 2008). By contrast, the transfection of $MDM2^{S17D}$ de-stabilizes p53 protein levels completely and thus recapitulates the standard function of MDM2 as a p53 inhibitor. These data described in this chapter therefore would suggest that phosphorylation of the pseudo-substrate motif of MDM2 would act as a physiological switch that would convert MDM2 from a positively acting chaperone to a negatively regulating factor that degrades p53. Figure 4.14 highlights the role of the lid within the Dual-site model. Under normal non-stressed conditions the lid is phosphorylated or in this case mutated to a phospho-mimic causing the lid to adopt a conformation compatible with enhance p53 binding and in tern enhance p53 ubiquitination , allowing p53 to be kept at low levels. (Fig 4.14A, B and C).

Accordingly, the kinases that activate MDM2 by this mechanism might function as oncogenic inhibitors of the p53 response by virtue of stimulating MDM2 function. Additional proteins that interact with MDM2 protein would also have the potential to become stabilized by such an activating phosphorylation of MDM2. A few of these proteins were highlighted in the ProtoArray®. More detailed analysis of this data and characterization of protein interactions are need. By contrast, de-phosphorylation of the pseudo-substrate motif would alter MDM2 dynamics and drive, amongst other events, the MDM2:HSP90-mediated folding of the native p53 tetramer and enhanced p53-dependent transcription maintained by the chaperone machinery (Candeias et al., 2008; Galigniana et al., 2004; Giannakakou et al., 2000; Pratt et al., 2004; Walerych et al., 2004; Wawrzynow et al., 2007).

MDM2 regulation, *in cis,* by a pseudo-substrate motif highlights the growing realization that many signal transduction events are modulated by relatively small unstructured polypeptide motifs. Although there are many well-defined globular protein domains that form folded independent compact structures, these globular domains represent only a fraction of the cellular polypeptide sequence repertoire. The remaining peptide sequences are intrinsically disordered and comprise linear motifs with weaker binding kinetics (Neduva et al., 2005). Thus, signal transduction among many components interacting via linear peptide motifs with weaker binding kinetics can provide specific and sensitive regulation of cellular signal transduction. Perturbations in these linear interaction motifs, for example by covalent modifications like phosphorylation, has the potential to drive signaling changes that mediate changes in

protein-protein interactions central to signal transduction. The ability of MDM2 to be modulated by such a flexible peptide motif opens the door to identify the physiological signals that regulate this conformational switch in MDM2 as well as novel pathways that respond to such an activated MDM2 conformation.

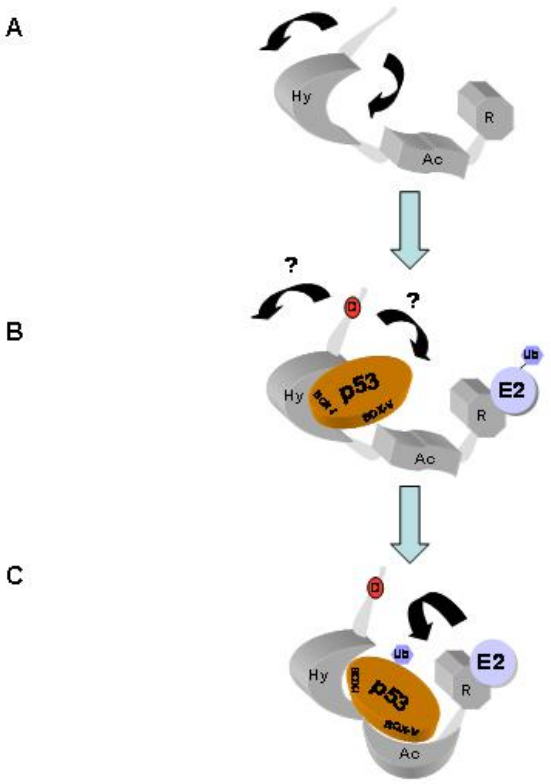

Figure 4.14 How does the Lid fit in with the Dual-Site model. (A) The MDM2 Lid is very flexible and is free to move around. **(B)** MDM2 binds the p53 BOX-I site through its hydrophobic pocket which is enhanced when serine 17 is mutated to aspartic acid. **(C)** Binding induces conformational changes in MDM2 allowing the docking of the acid domain to the BOX-V ubiquitination signal in the core of p53. This secondary interaction signals for the E2 mediated ubiquitin transfer to specific lysines within the p53 protein.

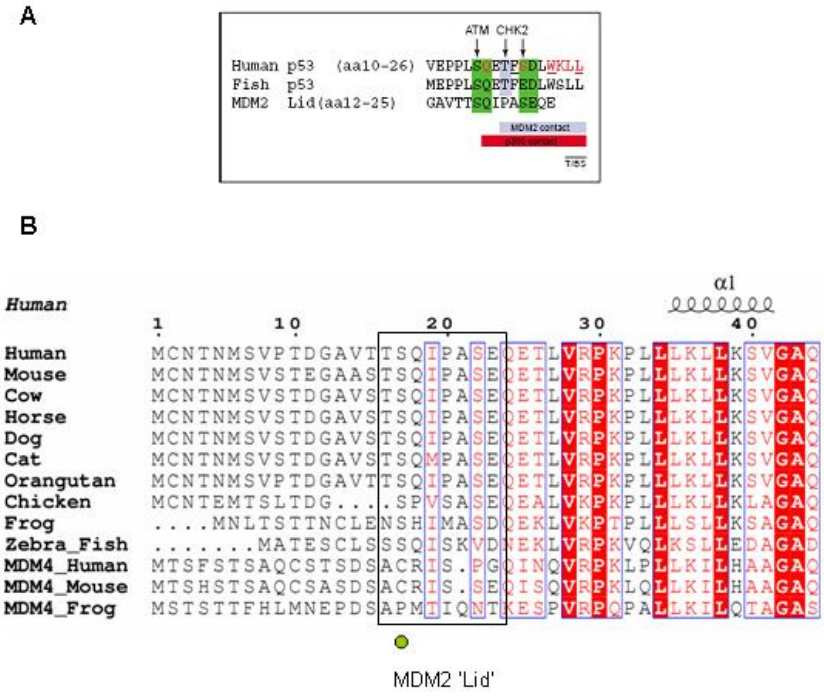

Figure 4.1 MDM2 lid sequence alignments (A) MDM2 Lid shows sequence homology to the p53-activation domain and contains a potential PI3 kinase phosphorylation site (Adapted from Shimizu and Hupp 2002) **(B)** The Lid is conserved among species, with the exception of the frog and chicken, and is not present in the MDM2 paralogue, MDM4.

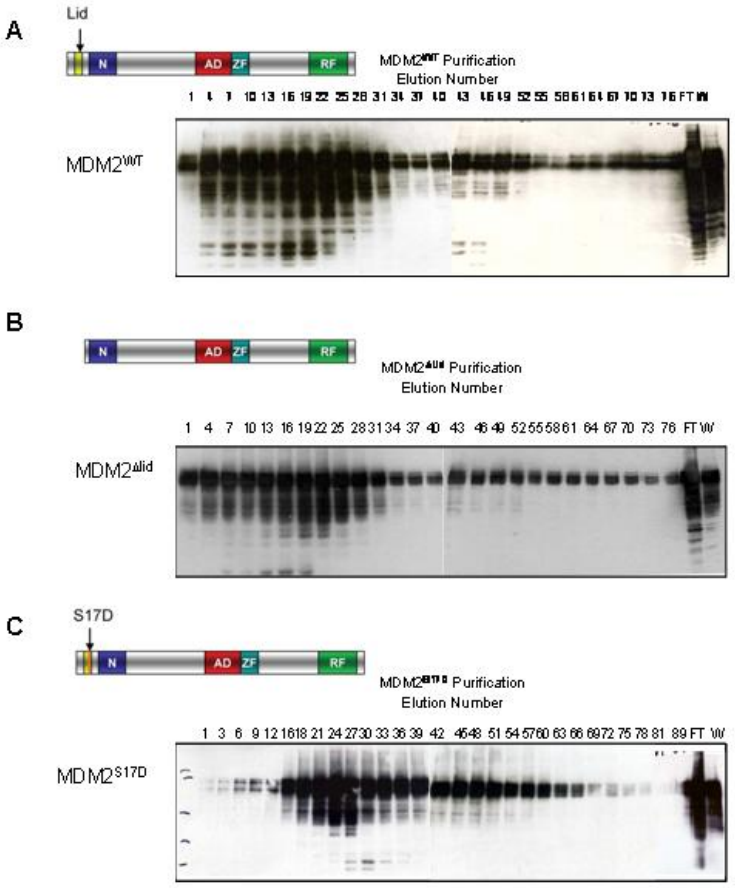

Figure 4.2 MDM2^{WT}, MDM2$^{\Delta lid}$ and MDM2^{S17D} purification. (A) MDM2^{WT} **(B)** a mutant lacking the first 26 amino acids encompassing the lid, MDM2$^{\Delta lid}$ and **(C)** a mutant with Ser17 mutated to aspartic acid by site directed mutagenesis, MDM2^{S17D} were cloned and purified from *E.coli* on a HiTrap FF-sp column. Every third fraction was resolved by 12% SDS-PAGE and proteins were transferred to nitrocellulose and detected with an MDM2 specific antibody, 2A10. FT: Flow through, W: Wash

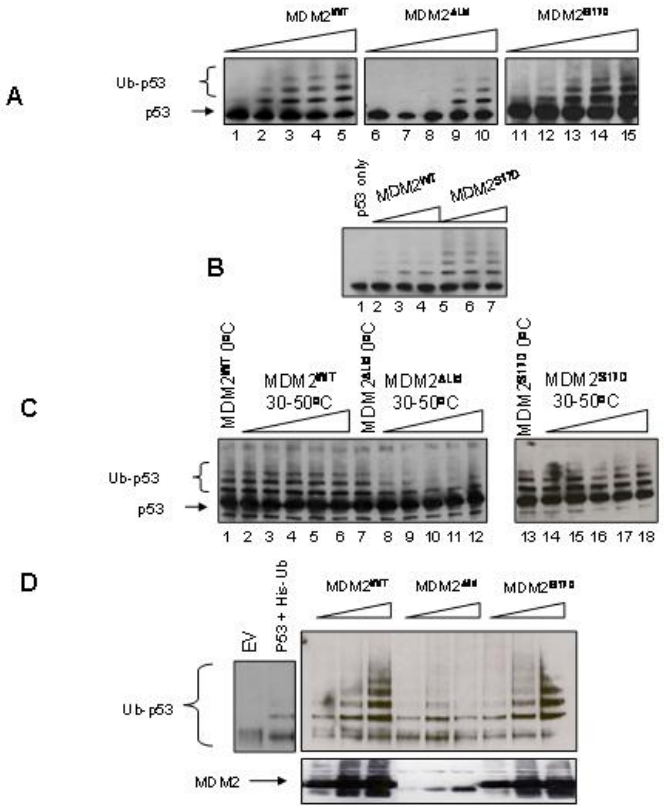

Figure 4.3 The MDM2 lid forms a positive regulatory motif. Protein was resolved on NOVEX 4-12% pre-cast gels unless otherwise stated. **(A)** 10 to 200 ng of purified $MDM2^{WT}$, $MDM2^{\Delta lid}$ and $MDM2^{S17D}$ were titrated into ubiquitination reactions using p53 as a substrate. After 15 minutes, the reactions were stopped and prepared for immunoblotting with the p53 specific antibody DO1 to measure the extent of p53 ubiquitination. **(B)** Ubiquitination assay created as in **(A)** with $MDM2^{WT}$ and $MDM2^{S17D}$ resolved using a NOVEX 4-12% gel. **(C)** $MDM2^{WT}$, $MDM2^{\Delta lid}$ and $MDM2^{S17D}$ were preincubated between 30°C and 50°C for 5 minutes before addition to the p53 ubiquitination assay. Extent of p53 ubiquitination was confirmed by immunobloting. **(D)** p53 was co-transfected into H1299 cells (1μg) with his-tagged ubiquitin (0.5μg) and vector control (lane 2) or increasing amounts of pCDNA3.1 MDM2 (lanes 3-5), $MDM2^{\Delta Lid}$ (lanes 6-8) or $MDM2^{S17D}$ (lanes 9-11) (0.5,1 and 2μg). His-ubiquitin immuno-precipitation was performed as described in materials and methods. The extent of p53 ubiquitination was confirmed by immunobloting.

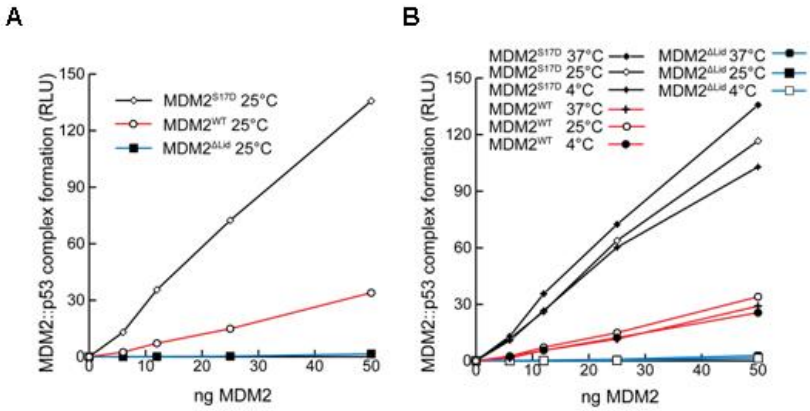

Figure 4.4 S17D mutation in the MDM2 lid stabilizes the MDM2:p53 complex. (A) Binding of $MDM2^{WT}$, $MDM2^{\Delta Lid}$, or $MDM2^{S17D}$ protein to p53 was assessed in an ELISA and $MDM2^{WT}$, $MDM2^{\Delta Lid}$, or $MDM2^{S17D}$ were titrated from 0-50 ng with fixed amounts of p53 on solid phase (50ng). The extent of MDM2 binding was quantified using the MDM2 specific antibody 2A10, and binding stability depicted using enhanced chemiluminescence in relative light units (RLU). **(B)** ELISA's were performed at distinct temperatures, as indicated, and MDM2 binding activity to p53 was measured as describe above in RLU.

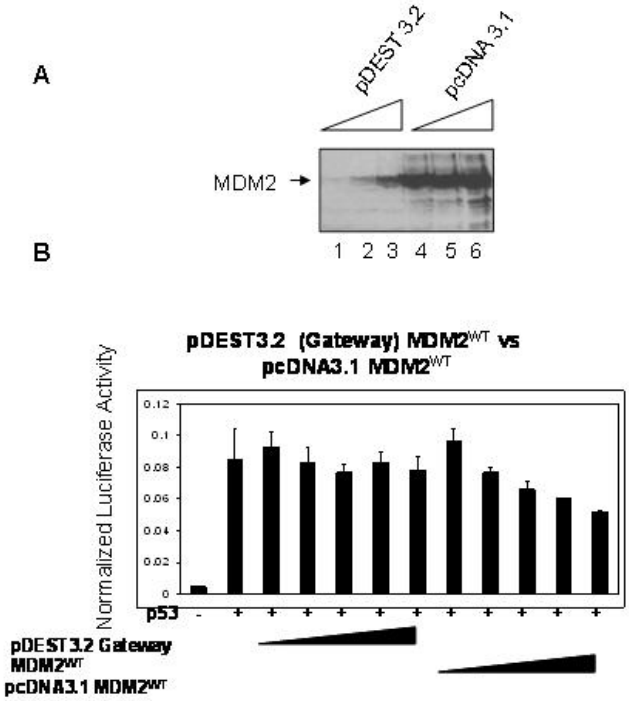

Figure 4.5 pDEST3.2 vectors produce more physiological levels of MDM2. (A) Mouse embryonic fibroblasts (MEFS) (p53-/- mdm2-/-) were transfected with MDM2 expressed from a Gateway pDEST3.2 expression vector (1-3, 0.5-2μg) or pcDNA3.1 vector (4-6, 0.5-2mg). MDM2 protein levels were quantified by immunoblotting with 2A10. **(B)** H1299 cells were co-transfected with vectors expressing a p53-responsive *luc* reporter, p53 (150 ng) and pDEST3.2 $MDM2^{WT}$ and pcDNA3.1 $MDM2^{WT}$ were titrated (75-500ng) in. p53 activity was measured as a function of normalized luciferase activity and expressed as RLU.

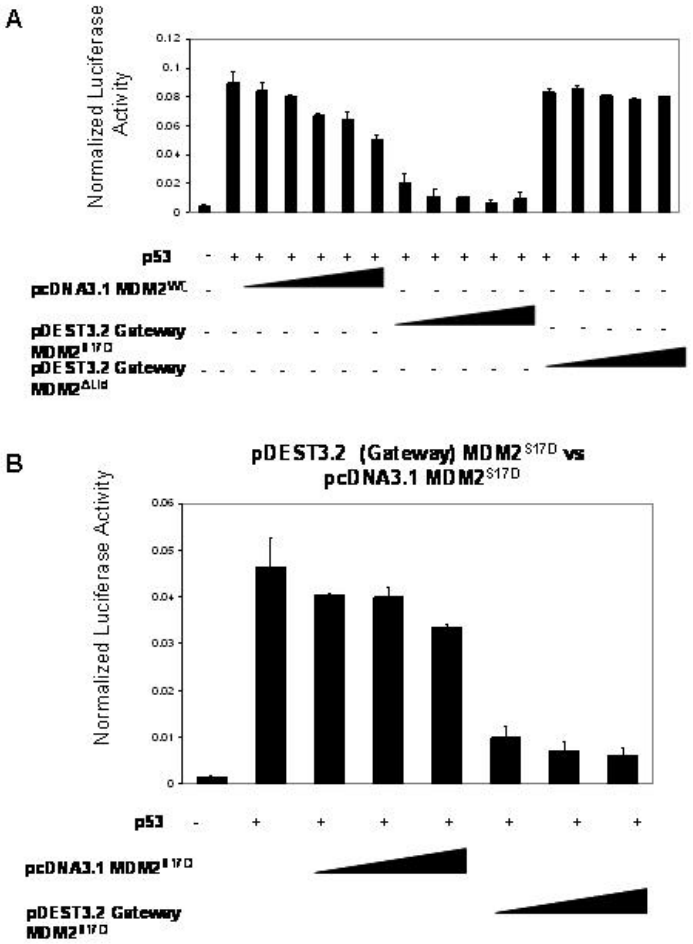
A
Normalized Luciferase Activity
0.12
0.1
0.08
0.06
0.04
0.02
0
p53
pcDNA3.1 MDM2WT
pDEST3.2 Gateway MDM2S17D
pDEST3.2 Gateway MDM2ΔLid
B
pDEST3.2 (Gateway) MDM2S17D vs pcDNA3.1 MDM2S17D
Normalized Luciferase Activity
0.06
0.05
0.04
0.03
0.02
0.01
0
p53
pcDNA3.1 MDM2S17D
pDEST3.2 Gateway MDM2S17D

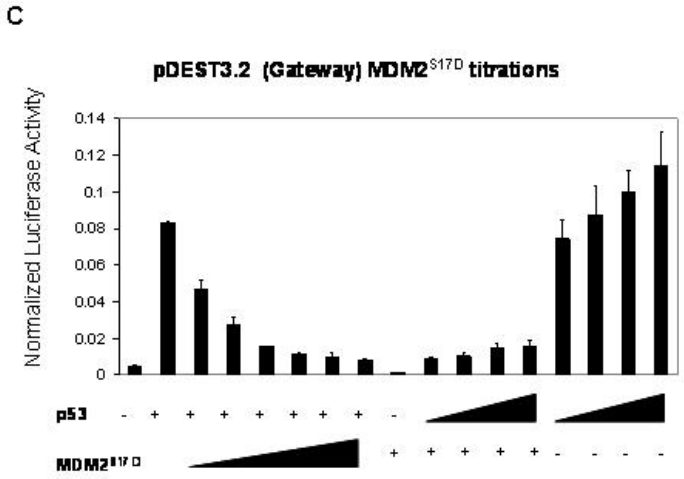

Figure 4.6 Effect of S17D mutation within the Lid of MDM2. (A) H1299 cells were co-transfected with vectors expressing a p53-responsive *luc* reporter, p53 (150 ng) and pcDNA3.1 $MDM2^{WT}$, pDEST $MDM2^{S17D}$ and pDEST $MDM2^{\Delta lid}$ were titrated (75-500ng) in. p53 activity was measured as a function of normalized luciferase activity and expressed as RLU. **(B)** H1299 cells were co-transfected with vectors expressing a p53-responsive *luc* reporter, p53 (150 ng) and pCDNA3.1 $MDM2^{S17D}$ and, pDEST $MDM2^{S17D}$ were titrated (75-500ng) in. **(C)** Further titrations of $MDM2^{S17D}$. H1299 cells were co-transfected with vectors expressing a p53-responsive *luc* reporter, p53 (150 ng) and pDEST3.2 $MDM2^{S17D}$ was titrated (15-550ng) in. The reverse was also performed with, fixed amounts of $MDM2^{S17D}$ (150ng) and increasing amounts of p53 (75-550ng). p53 activity was measured as a function of normalized luciferase activity and expressed as RLU

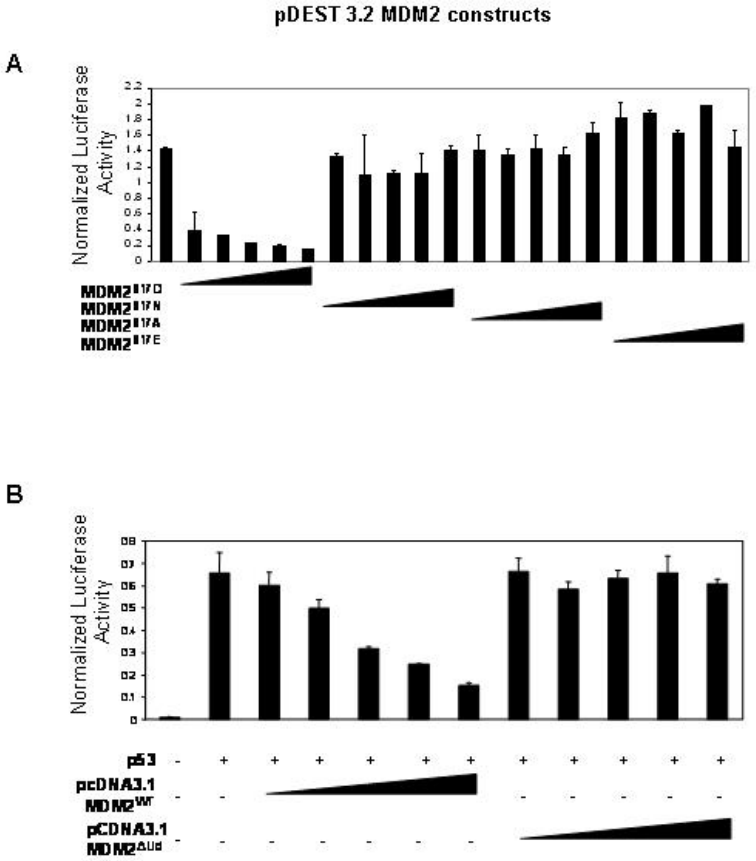
pDEST 3.2 MDM2 constructs
A
Normalized Luciferase Activity
MDM2Δ17D
MDM2Δ17N
MDM2Δ17A
MDM2Δ17E
B
Normalized Luciferase Activity
p53
pcDNA3.1 MDM2WT
pCDNA3.1 MDM2ΔUd

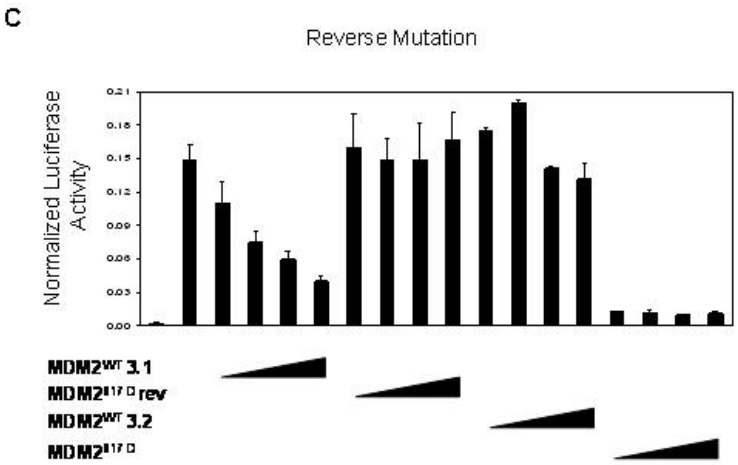

Figure 4.7 Effect of other mutations within the Lid **(A)** H1299 cells were co-transfected with vectors expressing a p53-responsive *luc* reporter, p53 (150 ng) and pDEST3.2 $MDM2^{S17D}$, $MDM2^{S17N}$, $MDM2^{S17A}$ and $MDM2^{S17E}$ were titrated in (75-500ng). p53 activity was measured as a function of normalized luciferase activity and expressed as RLU. **(B)** H1299 cells were co-transfected with vectors expressing a p53-responsive *luc* reporter, p53 (150 ng) and pcDNA3.1 $MDM2^{WT}$ and $MDM2^{\Delta lid}$ were titrated (75-500ng) in. p53 activity was measured as a function of normalized luciferase activity and expressed as RLU. **(C)** H1299 cells were co-transfected with vectors expressing a p53-responsive *luc* reporter, p53 (150 ng) and pcDNA3.1 $MDM2^{WT}$, pDEST3.2 $MDM2^{D17S}$, $MDM2^{WT}$ and $MDM2^{S17D}$ were titrated in (75-500ng). p53 activity was measured as a function of normalized luciferase activity and expressed as RLU.

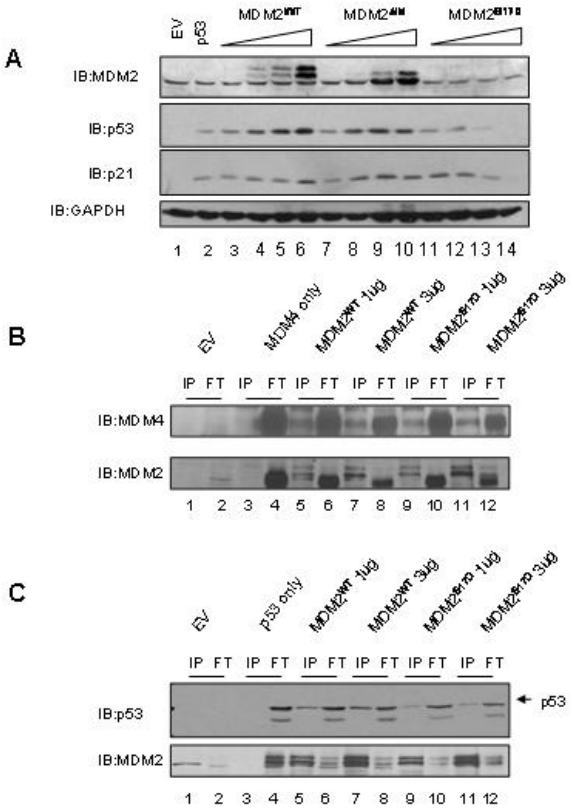

Figure 4.8 . The Effect of MDM2 mutants on p53 protein stability. (A) MEFS (p53-/-mdm2-/-) were co-transfected with vectors expressing p53 (150 ng) and increasing amounts of pDEST3.2 MDM2 expression vectors (250-2000ng): $MDM2^{WT}$ (lanes 3-6), $MDM2^{\Delta lid}$ (lanes 7-10) and $MDM2^{S17D}$ (lanes 11-14). Cell lysates were immunoblotted, as indicated to measure steady state levels of MDM2, p53, p21, and GAPDH. **(B)** H1299 cells were transfected with fixed concentrations of HA-MDM4 and two concentrations of pCDNA3.1 $MDM2^{WT}$ or $MDM2^{S17D}$ as indicated. Co-immunoprecipitation (Co-IP) was used to evaluate MDM2-MDM4 complexes. Co-IPs were resolved by SDS-PAGE and imunobloted using anti-HA antibody. MDM2 levels were confirmed using anti-MDM2 antibody 2A10. EV: Empty vector, IP: Immuno-precipitation, FT: Flow through **(C)** As in **(B)** but fixed p53 instead of MDM4. IPs were resolved by SDS-PAGE and immunoblotted using anti-p53 antibody CM1.

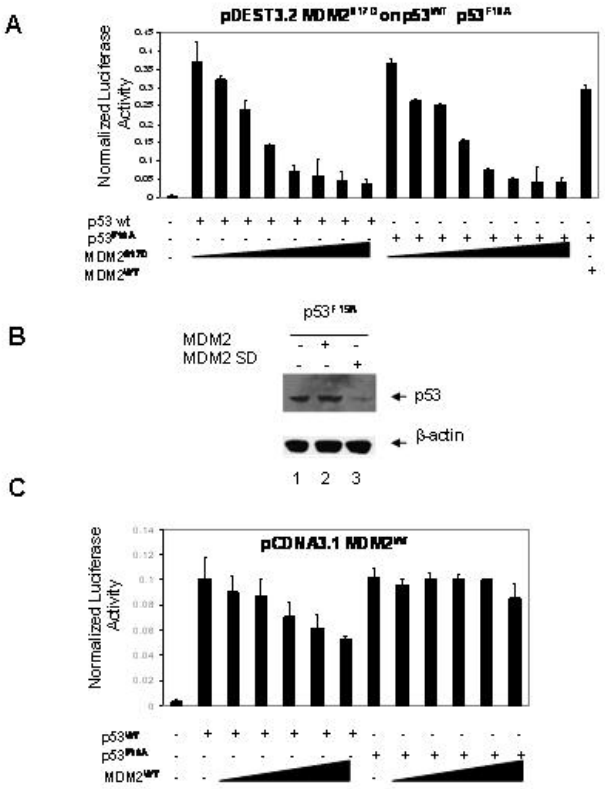

Figure 4.9 Effects of MDM2^{S17D} on p53^{F19A} activity. (A) pDEST3.2 vectors. H1299 cells were co-transfected with vectors expressing a p53-responsive *luc* reporter, p53^{WT} or *p53^{F19A}* (150 ng) and MDM2^{S17D} were titrated in (15-550ng). A fixed MDM2^{WT} (550ng) was included as a control. p53 activity was measured as a function of normalized luciferase activity and expressed as RLU. **(B)** MEFS (p53-/- mdm2-/-) were co-transfected p53^{F19A} (150 ng) and pDEST3.2 MDM2^{WT} or pDEST3.2 MDM2^{S17D} (300ng). Cell lysates were immunoblotted, as indicated to measure steady state levels of p53, and β-actin. **(C)** pcDNA3.1 vectors. H1299 cells were co-transfected with vectors expressing a p53-responsive *luc* reporter, p53^{WT} or p53^{F19A} (150ng) and pCDNA3.1 MDM2^{WT} or MDM2^{S17D} were titrated in (75-550ng). p53 activity was measured as a function of normalized luciferase activity and expressed as RLU.

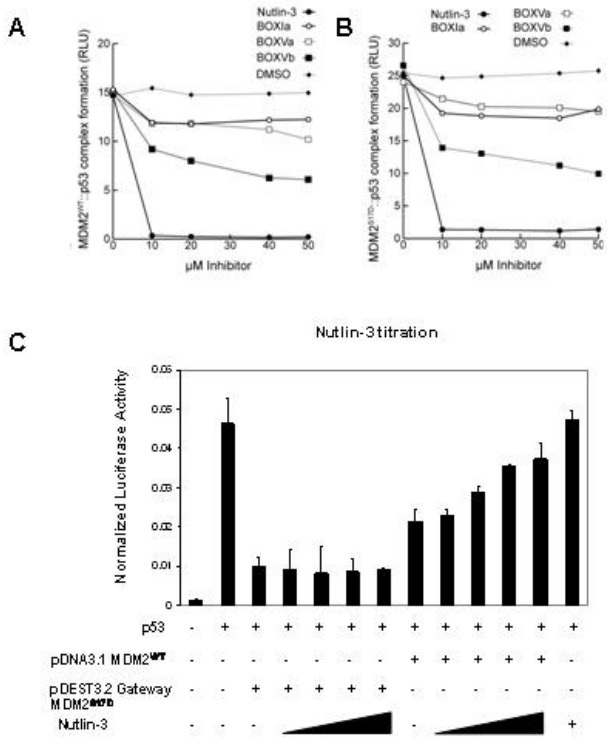

Figure 4.10 MDM2^{S17D} is not immune to destabilization onto p53 by Nutlin . MDM2^{WT} **(A)** or MDM2^{S17D} (25ng) **(B)** was assembled into reactions containing the indicated ligand: BOX-I peptide, BOX-V peptide, or Nutlin. The mixture was added to p53 protein on the solid phase and the amount of MDM2 bound stably to p53 was quantified using the MDM2 monoclonal antibody 2A10. The stability of the MDM2:p53 complex is depicted in relative light units. **(C)** H1299 cells were co-transfected with vectors expressing a p53-responsive *luc* reporter, with fixed p53 (75ng) and fixed pDEST MDM2^{S17D} (100ng) or pCDNA MDM2^{WT} (100ng) with nutlin titrated in(1.5-12µM). p53 activity was measured as a function of normalized luciferase activity and expressed as RLU

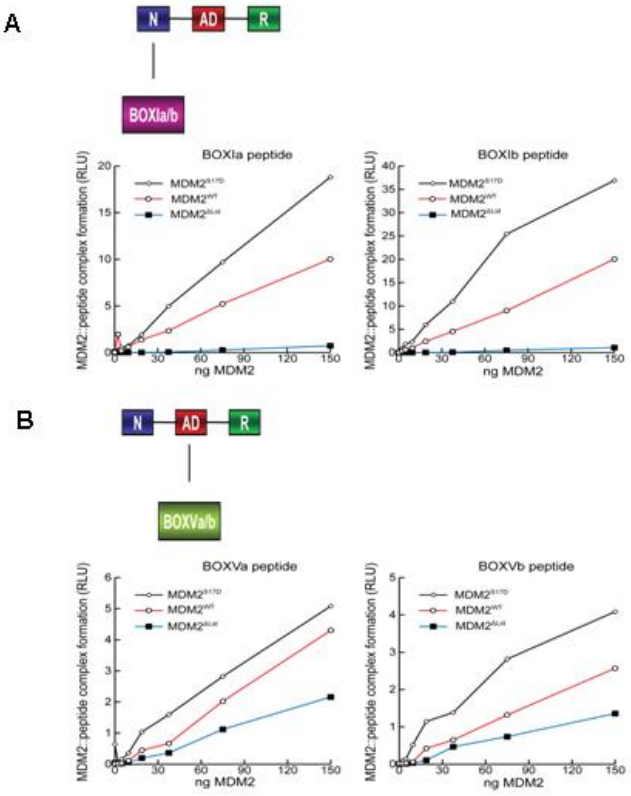

Figure 4.11 Characterization of BOX-I and BOX-V interactions. (A) The schematic highlights the interaction between the N-terminal MDM2 domain (N) and the p53 BOX-I motif which is being assayed. $MDM2^{WT}$, $MDM2^{\Delta Lid}$, or $MDM2^{S17D}$ proteins were titrated into reaction buffer and incubated onto the solid phase containing BOX-Ia peptide (left panel) and BOX-Ib peptide (right panel). The amount of MDM2 stably bound to the p53 peptides was quantified using an the MDM2 monoclonal antibody 2A10. The stability of the MDM2:p53 complex is depicted in relative light units. **(B)** The shematic highlights the interaction between the acid domain of MDM2 (AD) and the BOX-V motif of p53 being assayed. $MDM2^{WT}$, $MDM2^{\Delta Lid}$, or $MDM2^{S17D}$ proteins were titrated into reaction buffer and incubated onto the solid phase containing BOX-Va peptide (left panel) and BOX-Vb peptide (right panel). The amount of MDM2 bound stably to the p53 peptides was quantified as above.

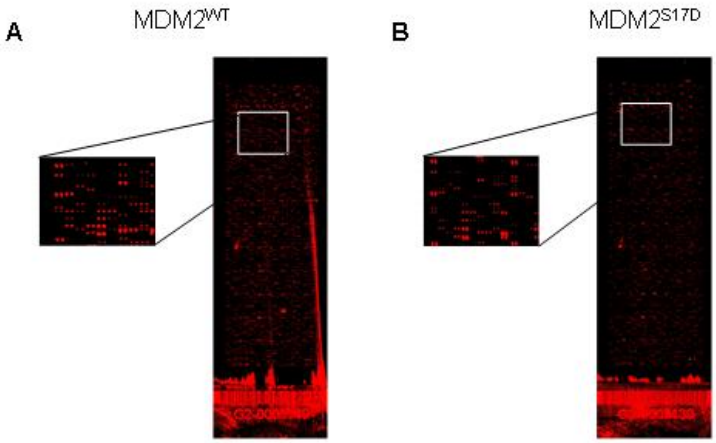

C

	MDM2WT	MDM2S17D
Pim-2 Oncogene (PIM2)	E	A
Casein Kinase 2 Alpha	E	A
Ubiquitin-Conjugating Enzyme E2 L 6 (UBE2L6)	E	B
Ubiquitin-Conjugating Enzyme E2-like	E	B
Interferon Regulatory Factor-1 (IRF-1)	E	C

Figure 4.12 ProtoArray® Human Protein Microarray. (A) and **(B)** 500nM of indicated protein was incubated over microarray for 1 hour on ice then washed. Bound protein was detected using Alexa Fluor® 647 Goat Anti-Mouse IgG. Data was gathered and analysed. **(C)** Table of selected proteins which preferentially bound to $MDM2^{S17D}$. Binding proteins were scored on their ability to bind to MDM2 with very strong binding proteins scoring an A and very week to no binding scoring an E with many falling in between.

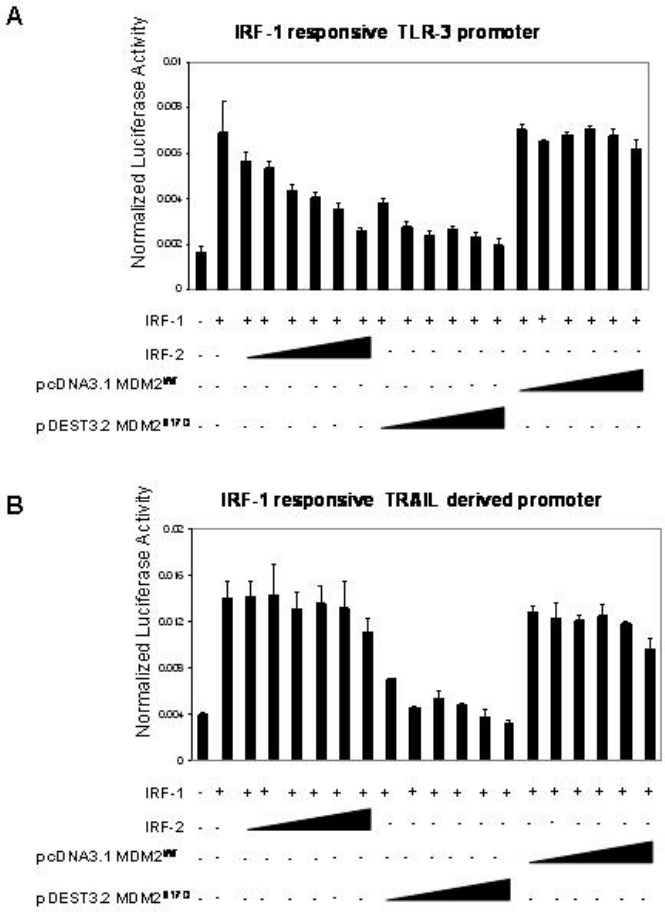
A
IRF-1 responsive TLR-3 promoter
Normalized Luciferase Activity
0.01
0.008
0.006
0.004
0.002
0
IRF-1 - + + + + + + + + + + + + + + + + +
IRF-2 - -
pcDNA3.1 MDM2FL - - - - - - - - - - - - - - - - -
pDEST3.2 MDM2 ΔRING - - - - - - - - - - - - - - - - -
B
IRF-1 responsive TRAIL derived promoter
Normalized Luciferase Activity
0.02
0.016
0.012
0.008
0.004
0
IRF-1 - + + + + + + + + + + + + + + + + +
IRF-2 - -
pcDNA3.1 MDM2FL - - - - - - - - - - - - - - - - -
pDEST3.2 MDM2 ΔRING - - - - - - - - - - - - - - - - -

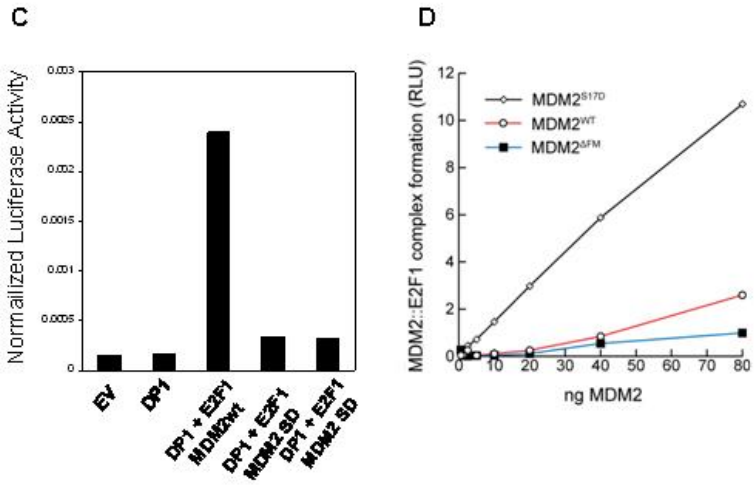

Figure 4.13 Effects of MDM2S17D on non-p53 responsive promoters **(A)** H1299 cells were co-transfected with vectors expressing a IRF1-responsive *luc* reporter (TLR-3), fixed IRF1 (150ng) and IRF2, pDEST3.2 $MDM2^{S17D}$ or pCDNA3.1 MDM2 were titrated in (15-550ng). IRF1 activity was measured as a function of normalized luciferase activity and expressed as RLU. **(B)** Same as **(A)** but with TRAIL derived *luc* reporter. **(C)** H1299 cells were co-transfected with vectors expressing an E2F1-responsive *luc* reporter, with fixed DP1 (100ng) and two different concentrations of $MDM2^{S17D}$ (250ng and 500ng). E2F1 activity was measured as a function of normalized luciferase activity and expressed as RLU. **(D)** $MDM2^{WT}$, $MDM2^{\Delta Lid}$, or $MDM2^{S17D}$ protein was titrated from 0-50ng into an ELISA reaction where fixed amounts E2F1 were on solid phase (100ng). The extent of MDM2 binding was quantified using the anti-MDM2 monoclonal antibody 2A10, and binding stability depicted using enhanced chemiluminescence in relative light units (RLU).

Chapter 5

AN EQUILIBRIUM MODEL FOR THE CONTROL OF MDM2 ACTIVITY BY ITS N-TERMINAL PSEUDO-SUBSTRATE MOTIF OR 'LID'

5.1 Introduction

Data from the previous chapter highlighted the activating effect that a phospho-mimetic mutation at S17 had on MDM2's activity towards p53. The current data do not fit with the present model in which the pseudo-substrate motif or 'lid', upon phosphorylation, binds into the hydrophobic pocket of MDM2 and blocks the interaction with p53 (Mcoy et al 2003). A new mechanism was needed to explain this apparent contradiction in findings.

A model to resolve this paradox invokes an equilibrium mechanism that involves the ability of the pseudo-substrate motif to exist in distinct conformations (Fig 5.1). The pseudo-substrate motif can be positioned over the hydrophobic pocket which is not compatible with p53 peptide binding but can also adopt conformations directed away from the pocket which are compatible with p53 peptide binding (Fig 5.1). NMR

analysis of the MDM2 N-terminal *apo*-structure revealed a narrower binding groove in the hydrophobic pocket of MDM2 as a result of the closer association of the two the lid and the hydrophobic pocket of MDM2. (Uhrinova et al., 2005). As suggested previously (McCoy et al., 2003), MDM2 residues 18-24 have helical character that can partially occlude the shallow end of the p53 binding cleft, although this region is not highly structured and the remainder of the binding pocket is not occupied by the remainder of the pseudo-substrate motif (McCoy et al., 2003). This conformation of the C-terminal region of the pseudo-substrate motif and p53 binding to the N-terminal domain of MDM2 are mutually exclusive (Fig 5.2A); p53 peptide binding must be preceded by the displacement of residues 19-25 of the lid from one end of the binding groove. The observation in this study that $MDM2^{S17D}$ induces a conformation primed for p53 peptide binding raises the possibility that this binding is achieved by inducing a conformational change within the pseudo-substrate motif which displaces it from the binding groove. In this model, the Asp^{17}-pseudo-substrate motif would bind to a region of the N-terminal domain of MDM2 which is distinct from the binding groove, displacing the region of the pseudo-substrate motif occluding the end binding pocket, and facilitating p53 binding.

Inspection of the NMR *apo*-MDM2 structure reveals that the conformationally heterogeneous pseudo-substrate motif may be in close proximity to a basic pair of amino acids ($Arg^{97}Lys^{98}$) which could form a complex with acidic residues (Fig 5.2B). Thus, the Asp^{17}-pseudo-substrate motif might exist in equilibrium between its positioning over the hydrophobic pocket of MDM2 (Fig 5.2A) and with a second contact site on MDM2 (Fig 5.2B). If the "phospho-mimetic" pseudo-substrate motif was stabilized by the

interaction with this arginine/lysine pair then this would suggest that the pseudo-substrate motif can exist in equilibrium between two relatively stable states.

In regards to this equilibrium model, it is interesting to note that the $Arg^{97}Lys^{98}$ residues are not present in MDM4 and are replaced by serine and proline residues. (Fig 5.3 and 5.4)(Baker et al., 2001; Gouet et al., 1999). This is interesting as the surrounding region of MDM4 is highly conserved with MDM2. This might give clues to residues that have co-evolved with the MDM2 pseudo-substrate motif.

5.2 Results

5.2.1 Mutating the basic region on MDM2 to MDM4 equivalent abolishes the activating effect of $MDM2^{S17D}$

To test the hypothesis that mutating the basic region on MDM2 to the MDM4 equivalent abolishes the activating effect of MDM2S17D we mutated the basic region of MDM2 at positions 97 and 98 to the equivalent residues of MDM4 and examined the effect in protein binding to p53 and in transcriptional assays. This MDM2 mutant therefore contains the $Arg^{97}Lys^{98}$ mutated to $Ser^{97}Pro^{98}$. MDM4 has been shown to have a conserved structure with MDM2 and can bind to p53 peptides in the same manner as MDM2 and with comparable affinities (Popowicz et al., 2007). Analysis of $MDM2^{R97S:K98P}$ binding to p53 by ELISA showed that in spite of the basic substitutions

at positions 97 and 98, the mutant MDM4 form of MDM2 was still able to bind to p53 and binding was the same as $MDM2^{WT}$.(Fig 5.5A). By contrast, the enhanced binding of $MDM2^{S17D}$ to p53 is completely eliminated by mutation of residues 97 and 98 to MDM4 and the $MDM2^{S17D:R98S:K98P}$ triple mutant was unable to bind p53 at any concentration tested (Fig 5.5B). We next went on to examine the impact that mutation of these residues had on MDM2s function *in vivo* using transrepression assays. In H1299 cells the presence of pDEST 3.2 $MDM2^{WT}$, p53 dependent transrepression is not effected (Fig 5.5C-Red). However as shown in chapter 4 pDEST 3.2 $MDM2^{S17D}$ does repress transcription (Fig 5.5C-Black). Surprisingly the introduction of mutations at residues 97 and 98 had no effect on p53 dependent transcription, however mutating these residues in the presence of S17D abolishes $MDM2^{S17D}$s ability to transrepress p53 dependent transcription and p53 transcription of the luciferase reporter in the presence of pDEST 3.2 $MDM2^{S17D:R97S:K98P}$ was comparable to pDEST 3.2 $MDM2^{R97S:K98P}$ (Fig 5.5C). These data indicate that the integrity of $Arg^{97}Lys^{98}$ residues of MDM2 are important in maintaining the activating effect of the Asp^{17} mutation and favours the equilibrium model of MDM2 pseudo-substrate motif function. In spite of the difference in model presented, these data are consistent with the observations of McCoy and colleagues (McCoy et al., 2003) that the pseudo-substrate motif of the Asp^{17} MDM2 mutant has a higher affinity for MDM2, yet this increase in affinity is not due to increased binding within the hydrophobic pocket.

A final prediction of this equilibrium model would be that the $MDM2^{S17D:R97S:K98P}$ triple mutant would be unable to form a stable interaction between

the pseudo-substrate motif and the $Arg^{97}Lys^{98}$ region. This would favour the stabilization of the Asp^{17}- pseudo-substrate motif over the hydrophobic pocket, perhaps by interacting with His^{73} or Lys^{94} residues as suggested (McCoy et al., 2003), and this in turn would render the $MDM2^{S17D:R98S:K98P}$ triple mutant unable to bind to BOX-I like ligands (Fig 5.6A). To test this we examined the ability of these mutants to interact with the BOX-I and BOX-V peptides of p53 in an ELISA. Comparison of $MDM2^{WT}$ and $MDM2^{R97S:K98P}$ showed that they were still able to bind to the BOX-I peptide (Fig 5.7A). Binding was however reduced by 50% maybe indicating the binding differences between the MDM2 and MDM4 hydrophobic pockets. In contrast the $MDM2^{S17D:R97S:K98P}$ mutant showed that introducing mutations at residues 97 and 98 completely abolished $MDM2^{S17D}$s ability to bind to the BOX-I peptide (Fig 5.7B) indicating that the $Ser^{97}Pro^{98}$ mutation overcomes the activating effect of the Asp^{17}-pseudo-substrate motif mutation. In order to show that the loss in binding of the $MDM2^{S17D:R97S:K98P}$ mutant was not due to global misfolding of the protein we examined binding to the BOX-V peptide. If we could show that the integrity of the acid domain binding is still working then the loss of binding to the N-terminus is solely due to the mutations. The $MDM2^{S17D:R97S:K98P}$ triple mutant maintains the ability to bind to the BOX-V peptide as well as $MDM2^{S17D}$ and $MDM2^{WT}$ (Fig 5.7C and D).

The inability of the $MDM2^{S17D:R98S:K98P}$ triple mutant to form a stable complex with p53 in a manner similar to $MDM2^{WT}$ (Fig 5.5B) can be explained by the phospho-mimetic pseudo-substrate motif contacting an alternate site and hindering access to the hydrophobic binding pocket (Fig 5.6A). Residues His^{73}, Lys^{94} (as suggested (McCoy et

al., 2003)) or His^{96} surround the hydrophobic binding pocket could interact with Asp^{17}. These data indicate that the integrity of $Arg^{97}Lys^{98}$ region is important to maintain the activating effect of the Asp^{17} mutation within the lid domain and favours the model that the MDM2 pseudo-substrate motif function accommodates a potentially activating effect in the event of lid phosphorylation.

5.2.2 Activated $MDM2^{S17D}$ de-stabilizes mutant p53 protein in cells

A recent physiological pathway has been identified, using genetic studies, whereby mutant forms of the p53 protein was unexpectedly ubiquitinated in murine transgenes in an MDM2-dependent pathway (Terzian et al., 2008). Ubiquitination of mutant p53 was attributed to the second MDM2 binding site in p53 in the BOX-V domain which is known to sensitize mutant p53 to ubiquitination in cells (Shimizu et al., 2002; Shimizu et al., 2006). These mutants are $p53^{R175H}$ and $p53^{F270A}$ which are hyper-ubiquitinated in cells.

We thus evaluated the ability of the mutant $MDM2^{S17D}$ protein to degrade or de-stabilize the mutant p53 protein under conditions where $MDM2^{WT}$ was not able to degrade the mutant p53. When pDEST 3.2 $MDM2^{S17D}$ was transiently transfected into cells co-transfected with mutant p53 isoforms containing the R175H or F270A alleles, the $MDM2^{S17D}$ was able to destabilize and deplete ubiquitinated-mutant p53 in H1299 cells (Fig 5.8A lanes 3 and 6 vs 2 and 5 and quantified in C) as seen by the depletion of

p53. MDM2^{S17D} was also able to deplete the mutant proteins in MEFs (Fig 5.7B lanes 3 and 6 vs 2 and 5 and quantified in C). These data indicate that MDM2^{S17D} protein can have dominant effects on either the more "unstable" wt-p53 or on the more "stable" mutant p53 with implications for how changes in phosphorylation of the MDM2 lid can function as dominant regulator of the p53 response.

The alternate splice isoform of p53, p47 was also attenuated in the formation of a stable complex with MDM2 presumably due to de-stabilization of the p47 protein (Fig 5.9A, B and quantified in C). p47 lacks the conventional BOX-I binding site so this de-stabilization due to MDM2^{S17D} must act either through reduced protein expression due to the inability of MDM2^{S17D} to bind to p53 mRNA (Candeias et al., 2008) or through the interaction with the acid domain.

MDM2^{S17D} is able to degrade both mutant p53 and p47, suggesting that the phosphorylation of Ser^{17} allows MDM2 to regulate p53 forms which are normally refractory to MDM2 control.

5.2.3 Mutations in the β-sheet are dominant and restore p53 protein induction by MDM2^{S17D} acid domain mutants

Studies have shown that the MDM2^{S17D} protein has enhanced interactions with the BOX-V domain of p53 presumably via the acidic domain (Yu et al., 2006b). In order to determine whether the activating effects of the Asp^{17} mutation could be inhibited we

introduced mutations in the acid domain that have the potential to alter the flexibility of this region. The MDM2 acid domain contains a putative β-strand which is thought to be an interface for protein-protein interactions with many proteins (Bothner et al 2001). Using a secondary structure prediction programme, mutations were designed to either stabilize or de-stabilized this β-strand, and mutations were introduced at codons 237 and 240 which were predicted to stabilize or de-stabilize the β-strand respectively (Fig 5.10). Indeed, mutating codon 237 from a serine to a phenylalanine or phenylalanine 240 to a lysine resulted in a mutant form $MDM2^{S17D}$ protein which had lost the ability to inhibit p53 protein shown by loss of transrepression in pDEST 3.2 (Fig 5.11A). These codon changes also switched the pDEST 3.2 $MDM2^{S17D}$ protein to a more wild-type like MDM2 protein resulting in enhanced steady-state levels of p53 and p21 proteins. This was seen by $MDM2^{S17D}$ dependent decrease in p53 and p21 proteins, whereas the β-strand mutants stimulate p53 and p21 as seen in chapter 4 with pDEST 3.2 $MDM2^{WT}$ (Fig 5.11B). These two mutants also lost the ability to ubiquitinate p53 when co-transfected into H1299 cells in the pcDNA 3.1 vector (Fig 5.11C). This was seen by a decrease in high molecular weight forms of p53 in comparison to $MDM2^{WT}$. The activating mutation at codon 237 resulted in a reduction in ubiquitination seen in $MDM2^{WT}$ and in $MDM2^{S17D}$ backgrounds where as the destabilizing mutation at 240 resulted in almost complete loss of ubiquitination. Slightly more ubiquitination was seen in the activating mutation in $MDM2^{WT}$ compared to $MDM2^{S17D}$ which may reflect some conformational changes within MDM2 having some effect of the N-terminal binding pocket. These data indicate that the integrity of the acidic domain is required

for optimal activating effect of the MDM2^{S17D} protein on p53 degradation. Further, as the RING domain is central to the stimulatory effect of MDM2 on p53 protein levels (Candeias et al., 2008), these data are consistent with distinct domains of MDM2 being involved in p53 protein degradation or its synthesis.

5.3 Discussion

A novel model can be developed that incorporates the various biochemical and biophysical studies of the flexible N-terminal domain of MDM2 and which supports an equilibrium model for pseudo-substrate motif function. As originally suggested (McCoy et al., 2003) and later confirmed in the NMR structure of *apo*-MDM2 (Showalter et al., 2008; Uhrinova et al., 2005), the N-terminal segment of MDM2 can partially occlude the shallow end of the p53-binding cleft; however, this motif is not well structured and the remainder of the binding pocket remains empty, at least in the non-phosphorylated state. In this conformation, Ile^{19} occupies much of the space taken up by Pro^{27} of the p53 peptide chain (Kussie et al., 1996) and as such excludes the mutual occupancy of the pseudo-substrate motif and p53. Interestingly, Ile^{19} is the only residue in the N-terminal region that exhibits any significant interaction with the rest of *apo*-MDM2 (Uhrinova et al., 2005), forming hydrophobic contacts with His^{96}, Arg^{97} and Tyr^{100} in the N-terminal part of helix α2′. In some NMR conformers, Ile^{19} is displaced from the site occupied by Pro^{27}, forming a more intimate association with the N-terminal region of helix α2′.

Based on this we have proposed that the pseudo-substrate motif exists in dynamic equilibrium between states that are incompatible with or compatible with p53 peptide binding; p53 can only bind when the pseudo-substrate motif has dissociated from the hydrophobic binding site. In favor of this equilibrium, both NMR studies indicated several residues within the pseudo-substrate domain and the region surrounding helix α2′ that behaved as though in slow conformational exchange (McCoy et al., 2003) (Uhrinova et al., 2005). Furthermore, it is interesting to note that a shorter p53 peptide, lacking residues 27-29 which share an overlapping binding site with the pseudo-substrate motif, bind to MDM2 with a ten fold higher affinity (Schon et al., 2004).

Thus, in order for p53 to bind to MDM2, the following events need to occur possibly in a concerted fashion. Firstly residues 19-25 forming the pseudo-substrate motif must dissociate from one end of the hydrophobic pocket groove and be replaced by residues 27-29 of the incoming p53. Next the two MDM2 sub-domains, the lid and the hydrophobic pocket, swing apart from one another by 3-4 Å and during the process of p53 binding, strand β3' is formed, completing the terminal (β1, β2, β3') sheet that caps one end of the groove and helps to hold the two sub-domains in their new more rigid conformation. However, deletion of the flexible lid de-stabilizes the N-terminal domain of p53, so this motif must have a positive role to play in the MDM2:p53 interaction. In addition to these ordered and sequential changes in MDM2-substrate binding, evidence has suggested an activating model for the function of the flexible pseudo-substrate motif upon phosphorylation. This is thought to enhance the displacement of the pseudo-substrate domain by altering its equilibrium between open

and closed states, thus opening the groove to stabilize p53-peptide binding to MDM2. This conformational change upon hydrophobic pocket occupation by its ligand then appears to be propagated to the central acidic domain of MDM2 resulting in enhanced MDM2 interactions with p53. Figure 5.12 summarizes the above events, firstly upon phosphorylation (or phospho-mimetic mutation) the lid is directed away from the hydrophobic pocket allowing it to come into contact with a basic region (Fig 5.12A and B). Displacement of the lid then permits increased binding to the hydrophobic pocket and in turn, increases signaling from the acid domain for ubiquitination of the p53 protein (Fig 5.12C)

We have proposed a model here in which MDM2 can adopt a conformation which as well as degrading wild type p53 can also degrade mutant forms of p53. It may be the case that this form of MDM2 can even bind phosphorylated forms of p53 which are normally unable to bind to MDM2. This could provide a mechanism in which MDM2 could quickly switch off the p53 pathway once cellular stress has passed allowing the cell to re-enter the cell cycle. It might be of benefit to target this basic region on MDM2 in order to prevent this active form of MDM2 degrading p53.

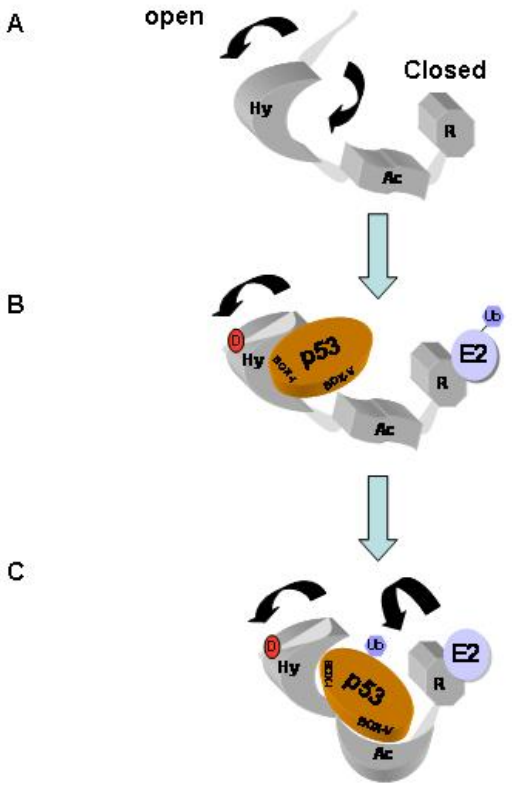

Figure 5.12 Phospho-mimic mutation at Ser17 activates the Dual-Site mechanism. (A) Under normal physiological conditions the MDM2 lid is in a slow equilibrium between and open and closed state. **(B)** Upon phosphorylation after some sort of stimulus, by an as yet unknown kinase, the equillibrium is shifted towards a more open conformation, increasing binding of substrates (in this case p53) to the hydrophobic pocket and **(C)** the acid domain leading to ubiquitination.

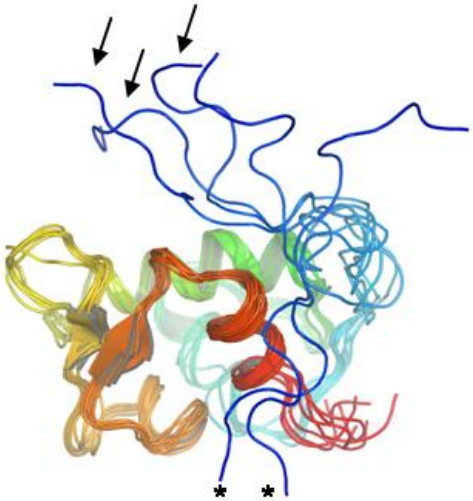

Figure 5.1 Flexibility of the MDM2 Lid. The NMR structure of the non-liganded N-terminal p53 binding domain of MDM2 (PDB ID 1Z1M, residues 10-109; *apo*-MDM2 (Uhrinova, Uhrin et al. 2005) reveals a large degree of conformational heterogeneity in the N-terminal 20 residues (Colored from blue (N-terminal) to red (C-terminal)). Pseudo-substrate motif conformations acting like a lid to cover the MDM2 hydrophobic pocket are highlighted with arrows and conformations with the pseudo-substrate motif interacting with the MDM2 surface are highlighted with asterisks.

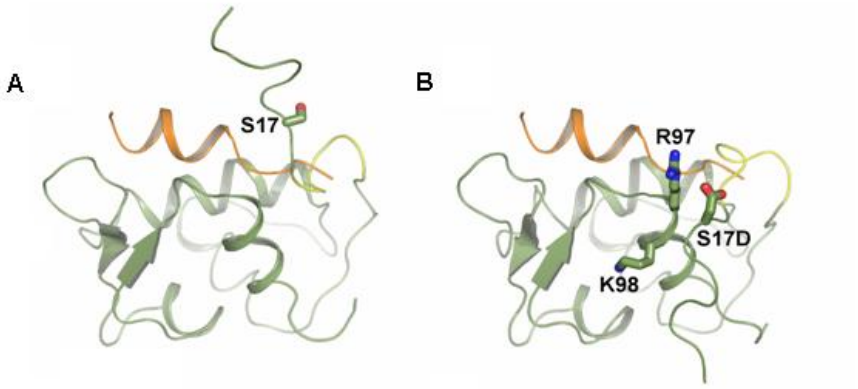

Figure 5.2 MDM2 Lid can be placed over hydrophobic pocket and directed away from it. (A) The C-terminal region of the pseudo-substrate domain (residues 18-24; colored yellow) can have helical character and occupy the shallow end of the hydrophobic binding pocket as reported previously (McCoy, Gesell et al. 2003), (p53 peptide from PDB structure 1YCR (Kussie, Gorina et al. 1996) shown for comparison, colored orange). **(B)** The pseudo-substrate motif can also exist displaced from the binding pocket with Ser17 (S17D mutation shown for illustration) in proximity to a basic region at the N-terminal of helix α2' composed of Arg97/Lys98. Based on this, it is postulated that the S17D (mimicking phosphorylation of Ser17) mutation could stabilise the N-terminal domain of MDM2 in a conformation primed for p53 binding by forming electrostatic interactions with residues Arg97/Lys98. Structural figures generated with PyMol (www.pymol.org).

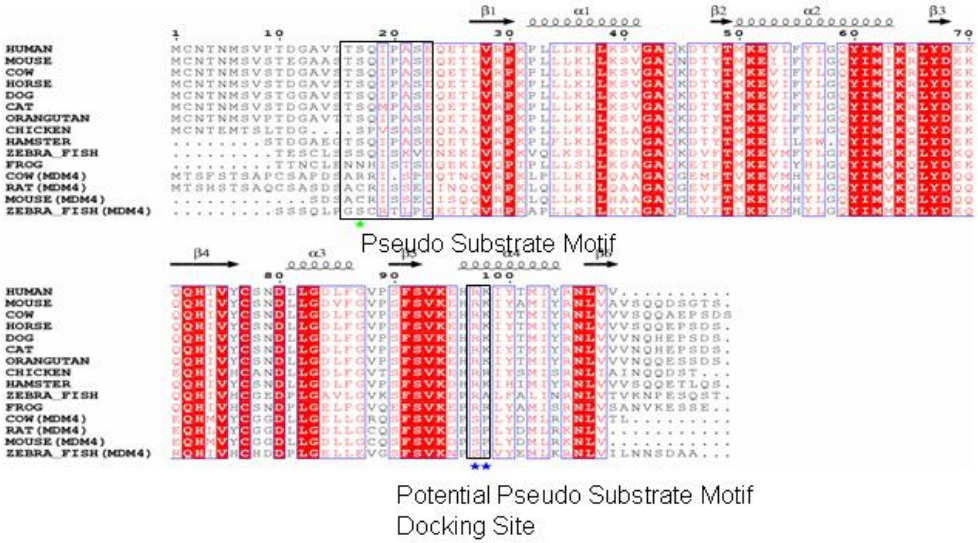

Figure 5.3 Sequence Alignment. Multiple sequence alignment of MDM2 and MDM4 highlighting the evolutionary divergence between MDM2 and MDM4 at the pseudo-substrate motif (aa 16-23) and at the potential pseudo-substrate motif basic docking site for acidic residues (i.e. Asp, phosphate) at amino acid residues 97-98. Alignment figure was generated with ESPript (Gouet, Courcelle et al. 1999) .

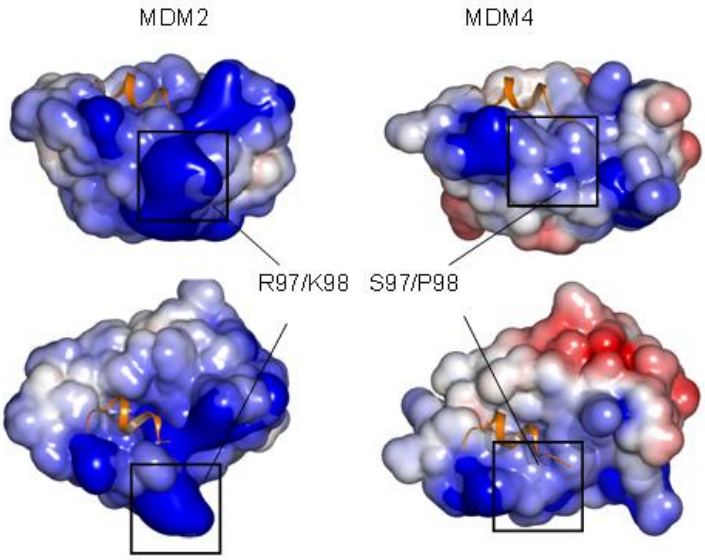

Figure 5.4 MDM4 lacks basic region. Electrostatic potential mapped onto the solvent accessible surface. Positive and negative charged regions colored blue and red respectively. The electrostatic calculations were performed with APBS (Baker, Sept et al. 2001) and highlighted is $MDM2^{WT}$ with R97/K98 and MDM4 equivalent S97/P98.

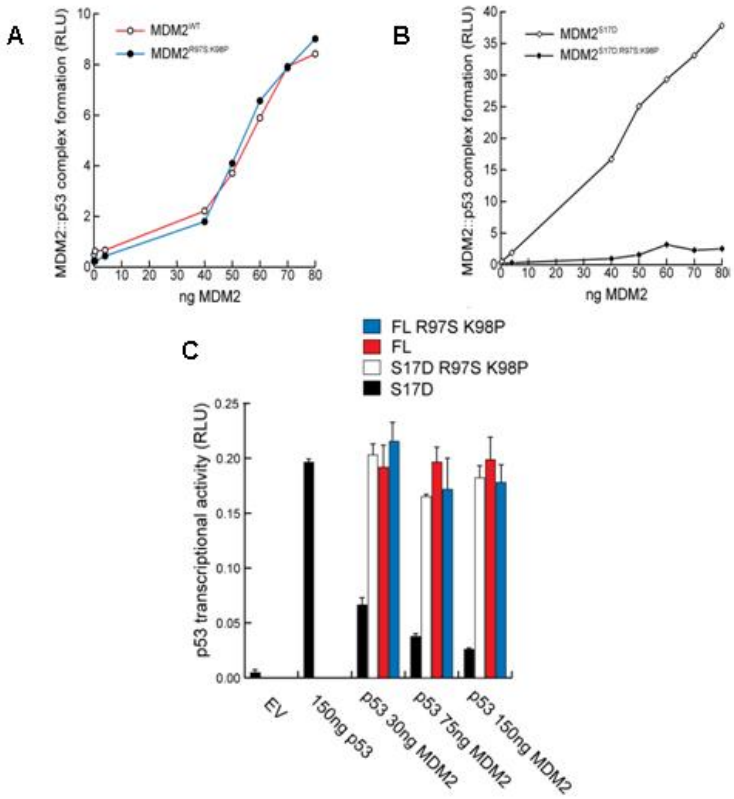

Figure 5.5 Selective de-stabilization of the activated MDM2^{S17D}:p53 complex by mutation of surface basic residues. **(A)** Increasing amounts of the indicated MDM2 protein (MDM2^{WT} or MDM2$^{R97S:K98P}$) were titrated into reactions where fixed amounts of p53 (50ng) were bound to the solid phase. The extent of MDM2 binding was quantified using an anti-MDM2 monoclonal antibody (2A10) and binding stability depicted using enhanced chemiluminescence in relative light units (RLU). **(B)** Reactions composed as in **(A)** but increasing amounts of MDM2^{S17D} or MDM2$^{S17D:R97S:K98P}$ were titrated into reactions. **(C)** H1299 cells were co-transfected with vectors expressing a p53-responsive luc reporter, p53 (150 ng) and the indicated amounts of pDEST 3.2 MDM2 expression vectors: MDM2^{WT}, MDM2$^{R97S:K98P}$, MDM2^{S17D}, or MDM2$^{S17D:R97S:K98P}$. p53 activity was measured as a function of normalized luciferase activity and expressed as RLU.

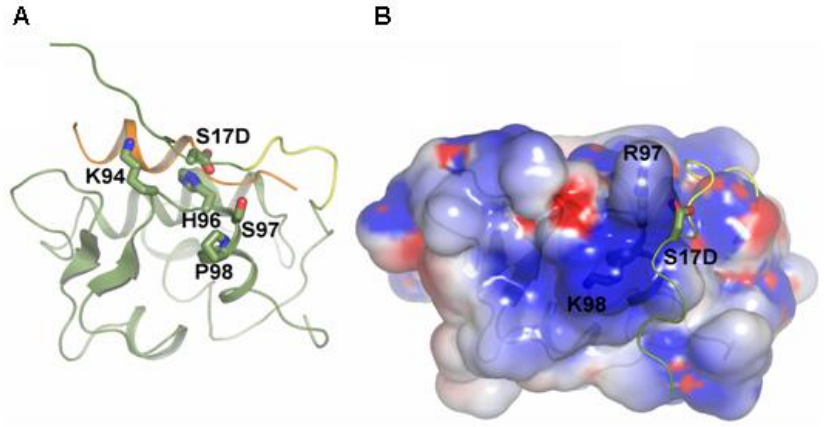

Figure 5.6 MDM2$^{S17D:R97S:K98P}$ mutant forces the Lid over the pocket. (A) In the MDM2$^{S17D:R98S:K98P}$ triple mutant, the phospho-mimetic pseudo-substrate motif may bind other basic regions of the MDM2 surface such as Lys94/His96 which line the hydrophobic binding pocket and explain why the MDM2 triple mutant (MDM2$^{S17D:R97S:K98P}$) binds p53 with a substantially lower affinity than does the MDM2 double mutant (MDM2$^{R97S:K98P}$). **(B)** Electrostatic potential mapped onto the solvent accessible surface. Positive and negative charged regions colored blue and red respectively. The alignment figure was generated with ESPript (Gouet, Courcelle et al. 1999). Structural figures generated with PyMol (www.pymol.org). The electrostatic calculations were performed with APBS (Baker, Sept et al. 2001).

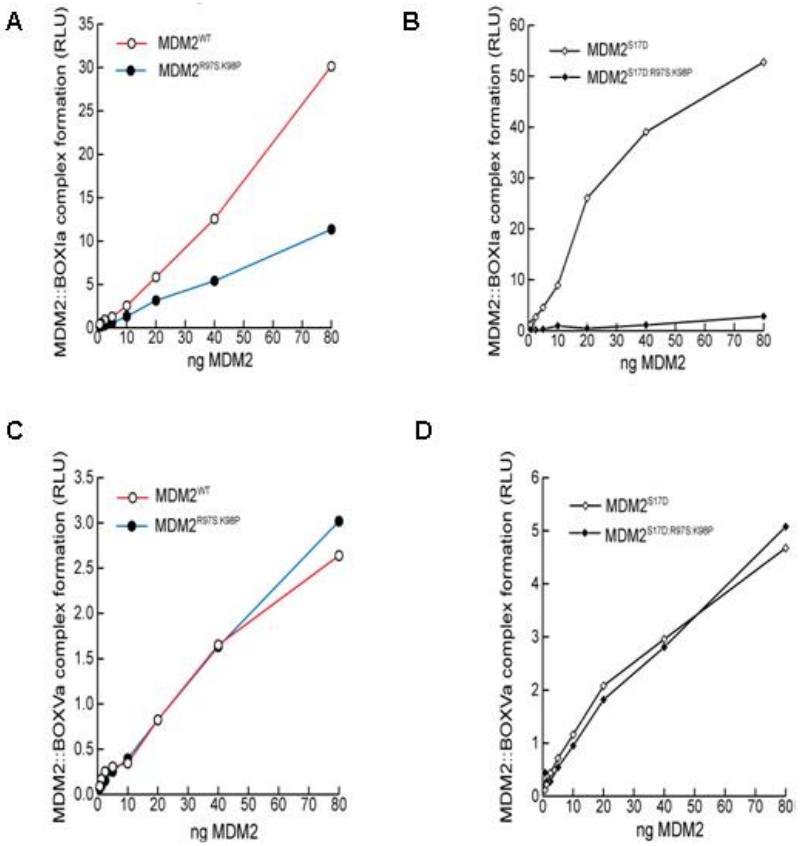

Figure 5.7 The effects of MDM2 codon 97-98 residue mutation to the MDM4 equivalent on MDM2:BOX-I peptide complex stability. (A and B) Increasing amounts of the indicated MDM2 protein (**A**; $MDM2^{WT}$ and $MDM2^{R97S:K98P}$ or **B**; $MDM2^{S17D}$ and $MDM2^{S17D:R97S:K98P}$ proteins) were titrated into reactions containing fixed amounts of the BOX-I peptide bound to the solid phase. The extent of MDM2 binding was quantified using an anti-MDM2 monoclonal antibody (2A10) and binding stability depicted using enhanced chemiluminescence in relative light units (RLU). **(C and D)** $MDM2^{WT}$ and $MDM2^{R97S:K98P}$ or $MDM2^{S17D}$ and $MDM2^{S17D:R97S:K98P}$ proteins were titrated into reaction buffer and incubated onto the solid phase containing BOX-V peptide. The amount of MDM2 bound stably to the p53 peptides was quantified as before.

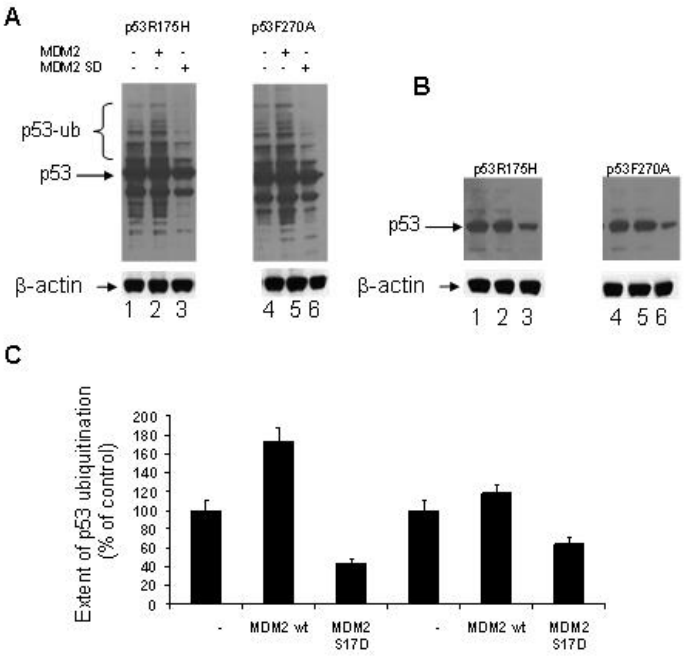

Figure 5.8 Effects of MDM2^{S17D} on mutant p53 protein ubiquitination in vivo. (A) H1299 cells were co-transfected with vectors expressing the indicated mutant p53 allele and either pDEST 3.2 MDM2^{WT} or pDEST3.2 MDM2^{S17D}. Cell lysates were immunoblotted as indicated to measure steady state levels of ubiquitinated p53 and actin. **(B)** Effects of pDEST 3.2 MDM2^{S17D} on mutant p53 protein degradation in vivo. MEFS (p53-/- mdm2-/-) were co-transfected with vectors the indicated mutant p53 allele and either pDEST 3.2 MDM2^{WT} or pDEST 3.2 MDM2^{S17D}. Cell lysates were immunoblotted, as indicated to measure steady state levels of ubiquitinated p53 and actin. **(C)** Quantification of **(A)**

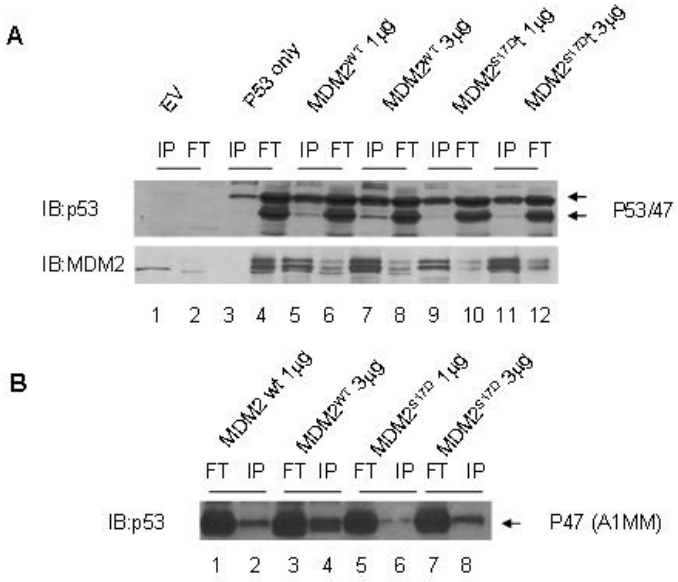

Figure 5.9 Effects of MDM2^{S17D} on p47:MDM2 complex stability. (A and B) MEFS (p53-/-mdm2-/-) were co-transfected with vectors expressing the indicated pCDNA3.1 expression vectors for p53 (lanes 3-12), MDM2^{WT} (lanes 5-8), and/or MDM2^{S17D} (lanes 9-12). After immunoprecipitating MDM2 with an anti-MDM2 monoclonal Ab, the cell lysates were immunoblotted, as indicated to measure steady state levels of p53, MDM2 and p47.

Figure 5.10 Mutating MDM2 acid domain. **(A)** Protein secondary structure prediction programme was used to identify potential β-strand within the acid domain of MDM2. **(B)** Potential stabilizing β-strand mutation introduced at codon 237. **(C)** Potential de-stabilizing mutation introduced at codon 240. The numbers represent the confidence of structure prediction with 1 being low and 10 being high and are represented by the black blocks . The letters B indicate the prediction is a β-strand and a dash is disordered. Predictions were made using JPred3 (http://www.compbio.dundee.ac.uk/~www-jpred/index.html)

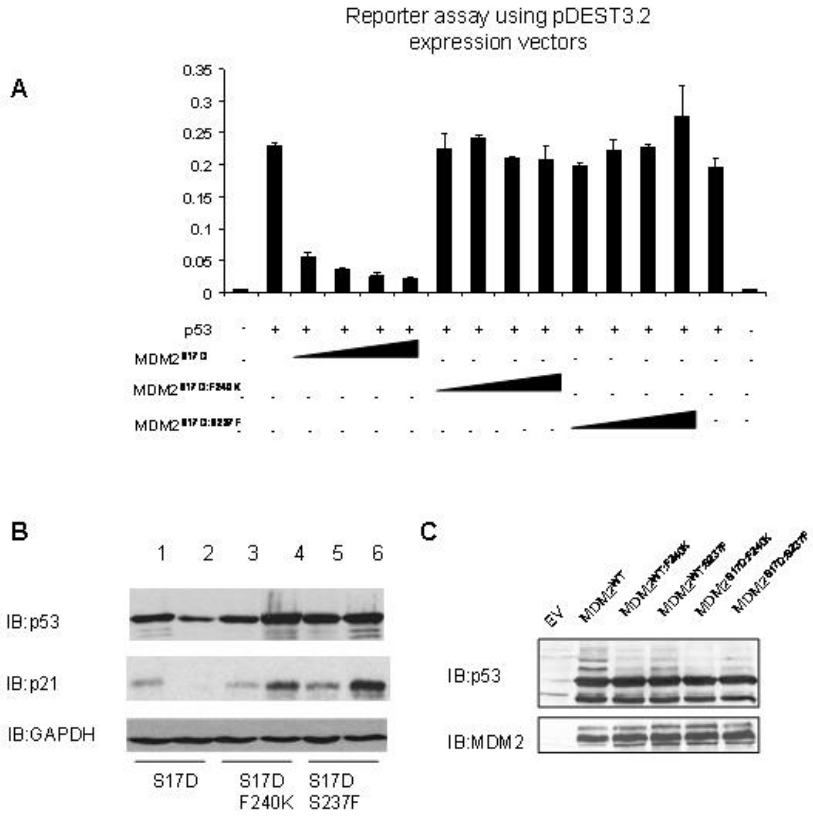

Figure 5.11 Effects of β-strand mutations on MDM2^{S17D} activity. (A) H1299 cells were co-transfected with vectors expressing a p53-responsive luc reporter, p53 (150 ng) and the pDEST 3.2 MDM2 expression vectors were titrated in: MDM2^{WT}, MDM2^{S17D}, double mutant MDM2$^{S17D:F240K}$, and double mutant MDM2$^{S17D:S237F}$. p53 activity was measured as a function of normalized luciferase activity and expressed as RLU. **(B).** Effects of β-strand mutations in p53 protein steady state-levels in cells. H1299 cells were co-transfected with vectors expressing p53 (0.25μg,lanes 1-6) and fixed amount (1μg) of MDM2 pDEST3.2 expression vectors MDM2^{S17D} (lane 2), double mutant MDM2$^{S17D:F240K}$ (lane 4) and double mutant MDM2$^{S17D:S237F}$ (lane 6), compared to no MDM2 (lanes 1, 3 and 5. Cell lysates were immunoblotted, as indicated to measure steady state levels of p53, p21, and GAPDH. **(C)** H1299 cells were co-transfected with p53 (0.5μg) and MDM2 (2μg) mutants in pcDNA3.1 expression vectors as indicated. Lysates were immunoblotted for p53 and MDM2. EV: empty vector

Chapter 6

GENERATION AND CHARACTERIZATION OF PHOSPHO-MDM2^{Ser17} MONOCLONAL ANTIBODIES WITH MORAVIAN BIOTECHNOLOGY

6.1 Introduction

Until relatively recently, the only way to study protein phosphorylation was through the use of radiolabelled ATP assays, both by *in vivo* labelling which looks at global phosphorylation states and *in vitro* kinase assays where a purified kinase phosphorylates a purified target protein. More complicated methods of studying protein phosphorylation include phospho-peptide mapping where a protein is purified from cell lysate, then digested with trypsin and the fragments are analysed by isoelectric focusing (using radiolabelled ATP) or by mass spectrometry. Methods to study protein phosphorylation have come along way since its discovery nearly 55 years ago (Burnett and Kennedy, 1954). Phosphorylation is a reversible process which is achieved by over 2000 kinases and reversed by considerably less phosphatases. Phosphorylation generally leads to one of two things, either phosphorylation induces conformational changes within a protein changing its protein function, or phosphorylation can provide a

platform for further protein-protein interactions inducing multi-protein complexes (Mandell, 2003). The importance of phosphorylation is also highlighted in gene regulation; many transcription factors are phosphorylated and this can have a direct effect on gene expression. Phosphorylation has also been brought into the field of protein degradation through phosphorylation-dependent proteolysis (Willems et al., 1999). It was quoted that "the reversible phosphorylation of proteins regulates nearly every aspect of cell life" (Cohen, 2002). Protein phosphorylation controls the decision of whether a cell should die, differentiate or divide and is evident in the cell cycle in which every step is controlled by the phosphorylation of the cyclin dependent protein kinases (Nurse, 2000; Zhou and Elledge, 2000). Given this fact, it is not surprising that studying the phosphorylation states of proteins within a cell at a given point, be it after stress or during development, is of major importance in today's science.

One major tool for studying protein phosphorylation is phospho-specific antibodies. These antibodies will only bind to the target epitope within a protein when it is phosphorylated and can be used in many techniques including western analysis or by immunohistochemistry. Phospho-specific antibodies were discovered in the 1980's accidently when scientists were trying to generate antibodies towards neurofilament fibres (Sternberger and Sternberger, 1983). The 1980s also witnessed the development of monoclonal and polyclonal antibodies, specific for phosphotyrosine and phosphothreonine residues which can identify any protein phosphorylated at either amino-acid (Glenney et al., 1988; Heffetz et al., 1989; Ross et al., 1981).

The 1990s saw the beginning of a more targeted approach to development of sequence-specific phospho antibodies. The first site-specific phospho-monoclonal antibody was generated against phosphorylated forms of glial fibrillary acidic protein (GFAP) by injecting mice with a phosphorylated peptide and subsequently screening the serum from hybridomas with phospho and non-phospho peptides (Yano et al., 1991). This was followed by the generation of polyclonal antisera from rabbits. This is a far less labor intensive process but does require an additional purification step to rid sera of non-phospho specific antibodies (Czernik et al., 1991). As 'easy' as it is to make a phospho-specific antibody, it is also possible to make non-phospho specific antibodies. This procedure is essentially the same as for phospho-specific antibodies except the immunogen is a non-phospho peptide and sera is first passed through a column of phospho-peptide to remove all antibodies that can bind the phospho form, thus leaving only antibodies specific for non-phospho forms of peptide. Today hundreds of different phospho-specific antibodies are commercially available to study all different kinds of pathways.

The first step in generating a phospho-specific antibody is obtaining a peptide containing a specific sequence with a phosphorylated amino-acid. The peptide is then conjugated to keyhole limpet hemocyanin (KLH), a carrier protein that helps stimulate the immune response upon injection. Other carrier proteins can be used such as BSA, however KLH elicits a stronger immune response due to its large mass and complexity (Moravian biotech). The conjugated phospho-peptide is then injected into BALB/C mice in complete Freund's adjuvant. Freund's adjuvant also helps to stimulate the

immune response of the mice. After 21 days the mice are re-injected with a further dose of KLH-coupled peptide in incomplete Freund's adjuvant and tail bleeds are taken to test the serum via dot-blot against phospho-peptide. The same procedure is repeated after 42 days prior to two injections of KLH conjugated peptide on days 45 and 46. On day 47 the mice were prepared for fusion with myeloma cells. A summarization of the process can be seen in figure 6.1.

The spleen cells are recovered from the mice and fused with SP2 myeloma cells. Splenocytes are mixed with myeloma cells and grown in media containing Azaserine-Hypoxanthine which will kill unfused cells, therefore only splenocytes fused with SP2 cells can grow. Fifteen 96 well plates are then seeded and grown for 7 days before antibody screening begins. Supernatant is screened for immunoglobulin (Ig) production and against BSA-coupled phospho-peptide. Only those positive for both Ig and phospho-peptide are taken forward for large scale production.

In this study I describe the generation and characterization of phospho-specific antibodies towards the MDM2 lid to study the physiological conditions in which the lid is phosphorylated.

6.2 Results

6.2.1 Screening Phospho-MDM2^{Ser17} Antibodies

In order to study the phosphorylation state of MDM2 at Ser^{17}, we developed a panel of monoclonal antibodies with the help from Moravian Biotechnology in the Czech Republic. The mice were immunised with phospho-peptide coupled to KLH as described above before splenocytes were removed and fused with myeloma cells and seeded into 96 well plates. Over a two week period, the fifteen 96 well plates were monitored daily and wells in which fusions showed good growth, the media was screened for the presence of Ig and phospho-peptide specificity. Figure 6.2A indicates all the supernatants screened on day 3. The supernatants were scored according to their response; a yellow mark indicates a positive Ig blot and a red mark indicates a positive phospho-peptide blot. Those wells which showed good response to both were highlighted in green and taken forward for further screening. From this initial screen, 5B5 and 9G11 both tested positive for both and were taken forward for further analysis, the other positive fusions failed to grow when subcultured. Figure 6.2B shows the screening on day 4 where 3A6 was identified, once again, other positive failed to grow when subcultured.

The positive hybridomas were grown up in larger plates where higher quantities of media could be obtained. 9G11, 5B5 and 3A6 supernatants were then screened against phospho-peptide in an ELISA format against phospho and non-phospho peptide (Fig 6.3A). This revealed that all three clones have a higher affinity for phospho-peptide than non-phospho peptide and in particular 3A6 seemed to be the best at detecting phospho-peptide over non-phospho peptide. Next the serums were screened against full length MDM2 proteins to test their cross-reactivity. Aspartic acid is a good mimic of

phosphorylation, so it was hypothesised that the phospho-specific antibodies would preferentially bind to $MDM2^{S17D}$. All the antibodies showed good specificity towards $MDM2^{S17D}$ but not to $MDM2^{WT}$. $MDM2^{\Delta lid}$ was used as a control which should not be detected due to lack of the epitope (Fig 6.3B). To test 9G11 further it was screened against protein in an ELISA format and showed $MDM2^{S17D}$ specificity at 1:100 dilution (Fig 6.3C). 9G11 showed the most consistent response in all assays performed and was therefore purified and used to screen against lysates.

In order to further characterise 9G11, we attempted to phosphorylate purified recombinant MDM2 with endogenous kinases. To do this we first fractionated MEFs (p53-/-mdm2-/-) via anion exchange chromatography. The double knockout MEFs were chosen as they are MDM2 deficient and so endogenous MDM2 wouldn't obscure our observations. MDM2 was incubated with fractions obtained from chromatography and the reaction products were resolved and transferred and probed for the presence of phospho-Ser^{17} using 9G11. A clear and distinct peak of phospho-Ser^{17} was detected in the presence of fractions 14-30 suggesting these contain kinases which target the Ser^{17} residue. Interestingly whole cell lysate weakens the signal suggesting phosphatase activity which de-phosphorylates Ser^{17} is also present (Fig 6.4)

A375 cell lysates were also analysed for the presence of endogenous phosho-Ser^{17} MDM2 (Fig 6.5). A375 cells were used because they have been shown to contain an intact MDM2-p53 regulatory network. A titration of cell lysate was probed for total MDM2 or phospho-Ser^{17} MDM2. Comparison of the profile for both antibodies shows the 9G11 antibody gave rise to a similar pattern of banding seen by the MDM2 specific

antibody 2A10, suggesting that the phospho-specific antibody was detecting MDM2 (Fig 6.5). Having previously shown that 9G11 does not bind to recombinant $MDM2^{WT}$ by western blotting, this result indicated the 9G11 antibody was detecting phospho-Ser^{17} MDM2. To further characterize the 9G11 antibody, physiological conditions in which the phosphorylation state of this site changes need to be identified.

Having developed a phospho-$MDM2^{Ser17}$ antibody and confirming that recombinant protein can be phosphorylated at this site and that phospho MDM2 can be detected in A375 cell lysates, we went on to characterize the physiological conditions in which the phosphorylation state might change.

6.2.2 Characterization of 9G11 *In Vivo*

In order to define the physiological situations in which the MDM2 lid phosphorylation might operate, the response to DNA damage was evaluated. p53 protein is classically stabilized by cellular X-irradiation and this is paralleled by increases in MDM2 protein through induction of MDM2 gene expression (Fig 6.6A). This increase begins at 2 hrs and peaks at 5 hrs returning to basal levels by 24 hrs (Fig 6.6A and C). Surprisingly, analysis of phospho-Ser^{17} MDM2 in these lysates after X-irradiation showed basal levels of MDM2 lid phosphorylation begin to decrease under conditions where p53 and MDM2 protein levels begin to accumulate (Fig 6.6A). Phospho-Ser^{17} levels decrease by 20% after 2 hrs and decrease to a max of 60% at 5 hrs and didn't fully recover up to 24

hrs (Fig 6.6A and B). MDM2 hypo-phosphorylation is reported to occur transiently after ionizing radiation, as observed by masking of the 2A10 epitope via ATM phosphorylation (Maya et al., 2001) and the loss of this epitope after IR is taken to represent phosphorylation at Ser^{395} of MDM2; indeed this increase in phosphorylation at the ATM site occurs under conditions where lid hypo-phosphorylation was observed, as seen by the parallel decrease in phospho-Ser^{17} and 2A10 (Fig 6.7A, quantified in 6.7C). At later times after X-irradiation when MDM2 protein is not phosphorylated at the ATM site and the 2A10 signal is recovered (Fig 6.7A), lid hypo-phosphorylation appeared to be maintained as seen by the decrease in signal vs 0 hr (Fig 6.7A, B and C). These data suggest that hypo-phosphorylation of the MDM2 lid occurs when p53 protein is activated, which is consistent with the data indicating that phospho-mimetic lid MDM2 is activated as a p53 inhibitor in cells (Chapter 4, figure 4.6A).

Another physiological condition in which p53 protein activity is known to be attenuated is under conditions of high cell density (Bar et al., 2004). This stress was suggested to represent the microenvironment of tumor cells and could place stress on p53 pathway inactivation in human cancers *in vivo*. Accordingly, the ratio of MDM2 lid-phosphorylation to p53 protein levels as cells are grown to high density were evaluated. When cell monolayers are subconfluent at 24 hrs after seeding, a basal ratio of phospho-MDM2 lid to total MDM2 and p53 can be defined by high levels of MDM2 and p53 and low levels of phospho-Ser^{17} MDM2 (Fig 6.8A). When cells begin to form highly dense monolayers from 48 hrs after seeding, de-stabilization of p53 protein levels is observed under conditions where MDM2 lid phosphorylation is elevated (Fig 6.8A, and D vs B).

Normalisation of phospho-Ser^{17} MDM2, MDM2 and p53 to actin levels at various stages of confluency clearly demonstrates these differences (Fig 6.8B, C, D, and E). Total MDM2 at 96 hrs was 40% of MDM2 at 24 hrs whilst phospho-Ser^{17} MDM2 was considerably higher than phospho-Ser^{17} at 24 hr (Fig 6.8A and B). The ratio of phospho-Ser^{17} MDM2 vs MDM2 total also follows and increasing trend (Fig 6.8E). De-stabilization of p53 protein under conditions where elevated levels of lid phosphorylation are present is further consistent with our data indicating that phospho-mimetic lid MDM2 is hyperactive as a p53 inhibitor in cells.

Our findings show lid-phosphorylation is observed at times when p53 and MDM2 protein levels are low (Fig 6.8A, B, C and D) and is repressed when these proteins are high (Fig 6.6 and 6.7). These results are consistent with previous transfection data where MDM2^{S17D} de-stabilizes p53 protein in cells (Chapter 4, figure 4.8A). The next step to confirm the effect was due to S17D mutation and the support the phospho-antibody data was to generate stable inducible cell lines containing MDM2^{WT} and MDM2^{S17D}. A375 cells were co-transfected with vectors expressing the Tet-repressor and either MDM2^{WT} or MDM2^{S17D} and treated with tetracycline for 48 hours. The production of stable inducible cell lines similarly demonstrate that induction of MDM2^{WT} protein expression following the treatment with tetracycline can increase basal expression of p53, p47 and p21 proteins (Fig 6.9A, B, D and E), whilst the induction of MDM2^{S17D} protein results in de-stabilization in the steady-state levels of p53, p47, and p21 protein (Fig 6.9A, quantified in C, D and E).

We have managed to recapitulate the transfection results seen in chapter 4 and 5 using a phospho-antibody and inducible cells, in that when phospho-MDM2^{Ser17} levels are high as with transfection of MDM2^{S17D}, p53 and p21 levels are reduced. However, when MDM2 is not phosphorylated at this site as with transfection of MDM2^{WT}, p53 and p21 levels increased.

6.2.3 Developing a New Phospho-MDM2^{Ser17} Antibody to an optimized Lid Peptide

Although the phospho-lid antibody 9G11 proved successful in detecting phospho-Ser17 MDM2 *in vitro* an *in vivo,* it was not easy to work with. Once purified we realised the 9G11 antibody was an IgM class of antibody rather than IgG. This class of antibody is less stable than IgG and also tends to be more 'sticky' and non-specific. They also tend to be required to be used at higher concentrations to be effective; we found 1:50 dilution worked best. Due to these problems a new optimized peptide was synthesized and used to immunize further mice. Instead of using the old peptide which contained Ser^{17} quite close to the N-terminus, a new peptide was synthesized which containing Ser^{17} in a more central location in the hope that this will provide a better platform for generating a phospho-specific antibody (Fig10A). The same immunization and screening protocol used to generate 9G11 were performed. An ELISA using phospho and non-phospho peptide and MDM2^{WT} and MDM2^{S17D} protein identified a few hybridomas with high

specificity for the new phospho-peptide and purified MDM2^{S17D} protein (Fig 6.10B and C respectively). This specificity was also confirmed by dot-blot analysis comparing phospho or non-phospho peptide coupled to BSA (Fig 6.10D and E). Figure 6.10B and D clearly shows hybridomas 17,18 and 23-26 have high reactivity to the optimized phospho-peptide and very little cross-reactivity with the non-phospho peptide. Hybridoma supernatants 17 and 18 were analysed further by ELISA and titrations of sera revealed the high specificity to phospho peptide compared to non-phospho peptide at dilutions as low as 1:128 (Fig 6.10F and G). Supernatant 17 and 18 originate from the same hybridoma and are currently being grown and purified for further characterization.

6.3 Discussion

The development of phospho-specific monoclonal antibodies in the 1980s has made research into phosphorylation states at specific amino acids in proteins possible. Phosphorylation states at distinct points in cellular pathways after stress or during development can now be studied with relative ease without the need for the use of radiolabelled ATP. This chapter has focused on the production of a monoclonal antibodies towards phospho-Ser^{17} MDM2 specific antibody with help from Moravian Biotechnology, Brno, Czech Republic.

9G11 was isolated from a panel of potential Ser^{17} MDM2 specific antibodies using various screening techniques such as peptide ELISA's, protein ELISA's, dot-blots,

and by western blotting against mutant recombinant protein. Previous studies have also shown that phospho-specific antibodies can recognise the phospho-mimic amino acid Aspartic acid. In this study they show that a phospho-specific antibody for HSP27 at Ser78 could also detect a band when the serine was replaced with an aspartic acid (Kubisch et al., 2004). Phospho-Ser^{17} MDM2 antibody has led to the identification of conditions when MDM2^{Ser17} is phosphorylated and how this correlates with the state of p53. From transfection studies using the mutated form of MDM2, MDM2^{S17D} it was found that when MDM2^{S17D} is present at high levels, p53 is destabilized and accordingly so is p21. Agreeing with these findings phospho-Ser^{17} MDM2 is found at high levels in circumstances when p53 and MDM2 are destabilized and conversely, at low levels when p53 and MDM2 are stabilized.

MDM2 can be phosphorylated at multiple sites by a myriad of protein kinases and these modifications have very different consequences (Meek and Knippschild, 2003). CK1 and CK2, along with other kinases, can phosphorylate MDM2 within the acidic domain leading to increased p53 degradation, presumably by increasing binding between the acid domain and the p53 ubiquitination signal (Gotz et al., 1999; Winter et al., 2004). This phosphorylation could occur in concert with lid phosphorylation which also leads to p53 degradation. The SQ motif within the lid forms a potential DNA-PK/ATM phosphorylation site. It was previously shown that this site could potentially be phosphorylated by DNA-PK *in vitro* (Mayo et al., 1997), but has not since been shown.

During cellular growth, the PI3-K/Akt pathway regulates cell cycle and proliferation (Lawlor and Alessi, 2001). Through a series of kinase cascades, Akt is phosphorylated and released from the membrane, allowing it to interact and phosphorylate substrates such as IKK, p21 and p27, leading to cell survival. Akt can phosphorylate MDM2 at serines 166 and 186 which reside in close proximity to the nuclear localisation sequence (NLS) and stimulates entry into the nucleus (Mayo and Donner, 2001). Phosphorylation at these residues within MDM2 leads to the increased ubiquitination of p53 and increased binding to p300 (Ogawara et al., 2002; Zhou et al., 2001). The activation of MDM2 by the PI3-K/Akt pathway leads, in turn, to increased turn over of p53 and thus reduced intracellular levels of MDM2 (Ogawara et al., 2002; Zhou et al., 2001). Phosphorylation at serines 166 and 186 could also coincide with lid phosphorylation as during cell growth and contact inhibition, lid phosphorylation was found to increase as p53 and MDM2 protein levels fall. Full activation of the Akt pathway requires amongst others, phosphorylation of Akt by DNA-PK which could also phosphorylate the lid in the same conditions in which it phosphorylates Akt (Boehme et al., 2008).

In conclusion, the MDM2 lid, exists in dynamic equilibrium between an open and a closed state (Fig 6.12A), during cellular stress, such as contact inhibition, the lid becomes phosphorylated opening the hydrophobic pocket of MDM2 and allowing binding of p53 which is reversed by x-ray (Fig 6.12B). This activates the dual-site model of MDM2 allowing MDM2 to degrade p53 (Fig 6.12C). These findings highlight the fact that a post translational modification (PTM) occur in the lid domain of MDM2

in response to a variety of stresses. The intra-cellular pathways and kinases which control this phosphorylation need to be elucidated. This will enhance our understanding of the already large MDM2/p53 signaling network within the cell.

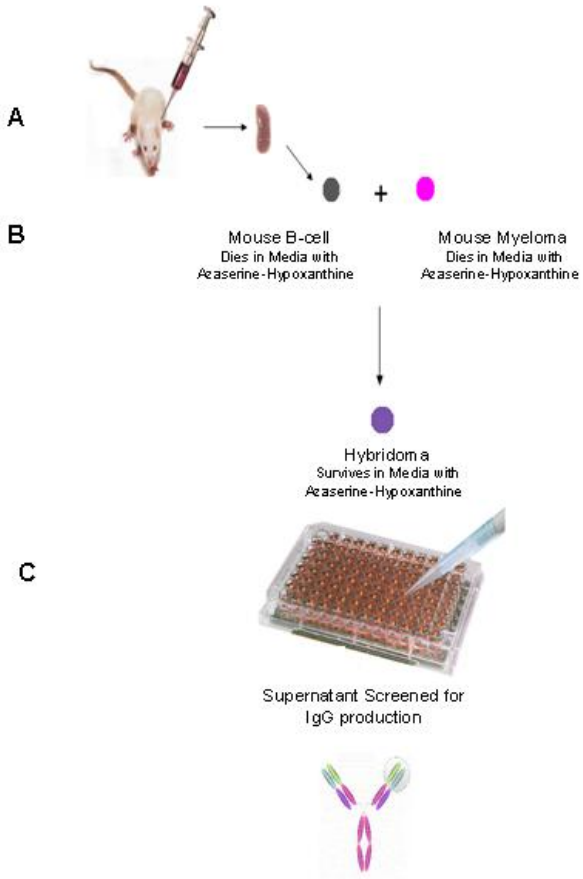

Figure 6.1 Monoclonal antibody production (A) Mice are injected with antigen over a period of 47 days. **(B)** B-cells are isolated from the mouse spleen and mixed with myeloma cells in media containing Azaserine-Hypoxanthine. Only cells fused together can grow in this media. **(C)** Hybridoma supernatants are screened gor IgG production and screened against antigen raised against. Positives can then be grown up and purified.

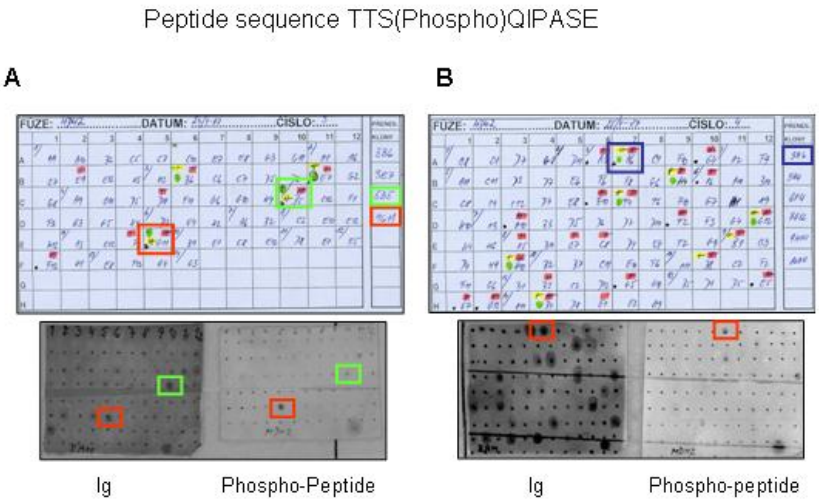

Figure 6.2 Hybridoma Screening. In the top left corner of 1A is a number 1 which indicates which 96 well plate the following supernatants were taken from and written in the centre of the box is the position in the plate. **(A) and (B)** Hybridomas were selected from 15 96 well plates as indicated and screened for reaction against Ig and phospho^{Ser17} peptide. Those which reacted to Ig were scored with a yellow dot, phospho-peptide with a red dot and both with a green dot. **(A)** Four positives were identified from screen 3 but only 9G11 and 5B5 survived. **(B)** Six positives were identified from screen 4 but only 3A6 survived. In total three positive clones were isolated and taken further.

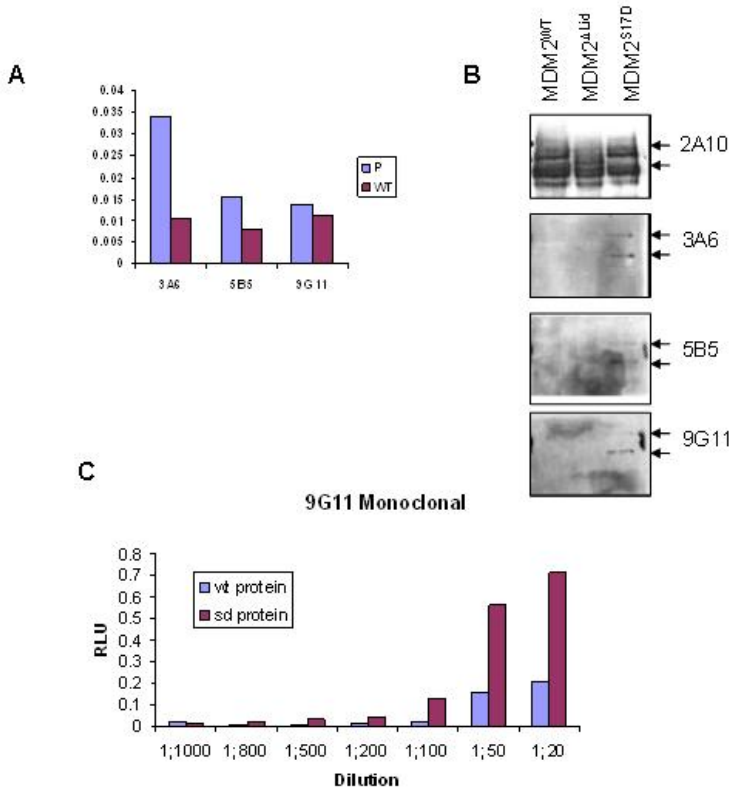

Figure 6.3 Screening positive clones (A) Using an ELISA format with either phospho-peptide or non-phospho peptide coated onto the wells the antibodies were screened for phospho-specificity. P: phospho-peptide, WT: non-phospho-peptide. **(B)** Recombinant protein, either $MDM2^{WT}$, $MDM2^{\Delta lid}$ or $MDM2^{S17D}$ were resolved by SDS-PAGE and transferred to nitrocellulose and prepared for blotting with phospho-antibodies. Phospho-antibodies show specificity to the phospho-mimic $MDM2^{S17D}$. **(C)** 9G11 was screened against $MDM2^{WT}$ and $MDM2^{S17D}$ using an ELISA with the protein bound to the plate.

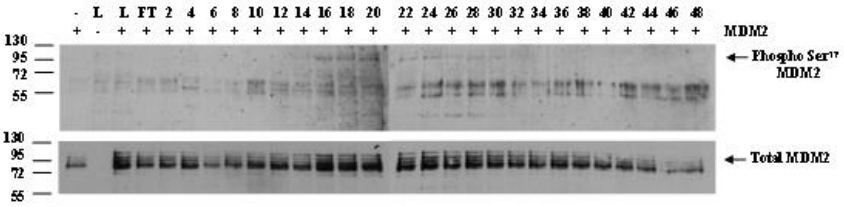

Figure 6.4 9G11 can detect in vitro phosphorylation of recombinant protein MEF (p53-/-mdm2-/-) lysate was fractionated using a mono-Q column and added to an in vitro kinase reaction containing ATP and purified recombinant MDM2. After 30 minutes at 30°C the reaction was stopped by addition of sample buffer and reaction products were resolved by SDS-PAGE then prepared for blotting with 9G11 (1:50). Equal loading of recombinant MDM2 to reactions was detected by re-probing the membranse with 2A10. L: Lysate, FT: Unbound column flow through. (Data courtesy of Dr Jenny Fraser)

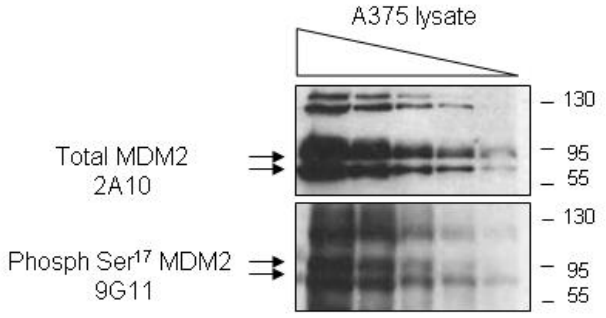

Figure 6.5 9G11 detects a similar banding pattern to the MDM2 specific antibody 2A10. A titration of A375 lysate from 80 to 5 µg was resolved by SDS-PAGE and prepared for blotting with 9G11 (1:50) or 2A10.

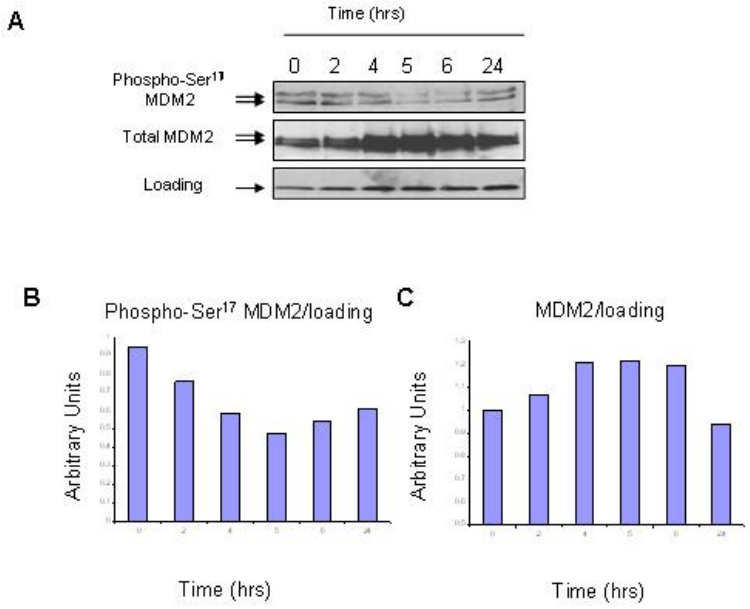

Figure 6.6 The effects of 5 Gy X-Irradiation on MDM2 lid phosphorylation (A) A375 cells were irradiated with 5Gy irradiation and left for 2 to 6 hours. Lysates were resolved by SDS-PAGE and prepared for blotting for phospho-Ser17 MDM2 and total MDM2. **(B)** Phospho-Ser17 MDM2 levels quantified, divided by loading. **(C)** Total MDM2 levels following X-irradiation quantified, divided by loading.

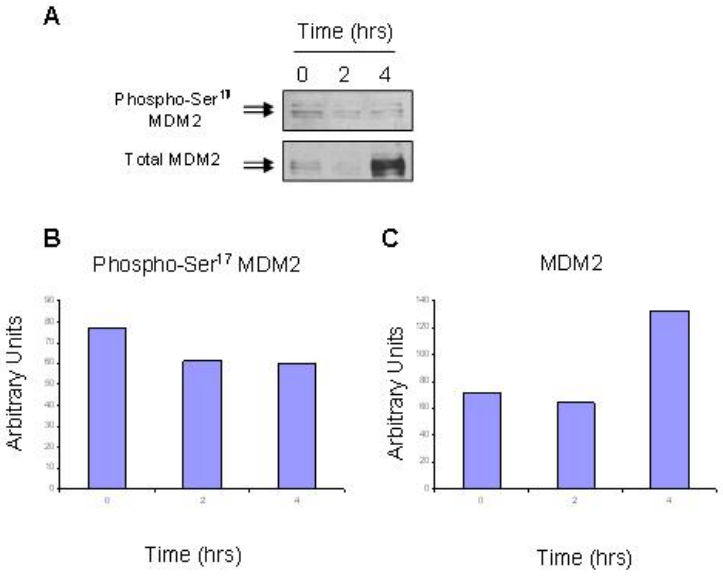

Figure 6.7 Effects 5Gy X-Irradiation on ATM-site phosphorylation of MDM2. **(A)** A375 cells were irradiated with 5Gy X-irradiation and the lysates were processed from early and late times post X-irradiation for blotting to define changes in MDM2-lid phosphorylation or ATM site phosphorylation of MDM2 (as defined by epitope masking of the 2A10 epitope). **(B)** Phospho-Ser^{17} MDM2 levels quantified. **(C)** Total MDM2 levels quantified.

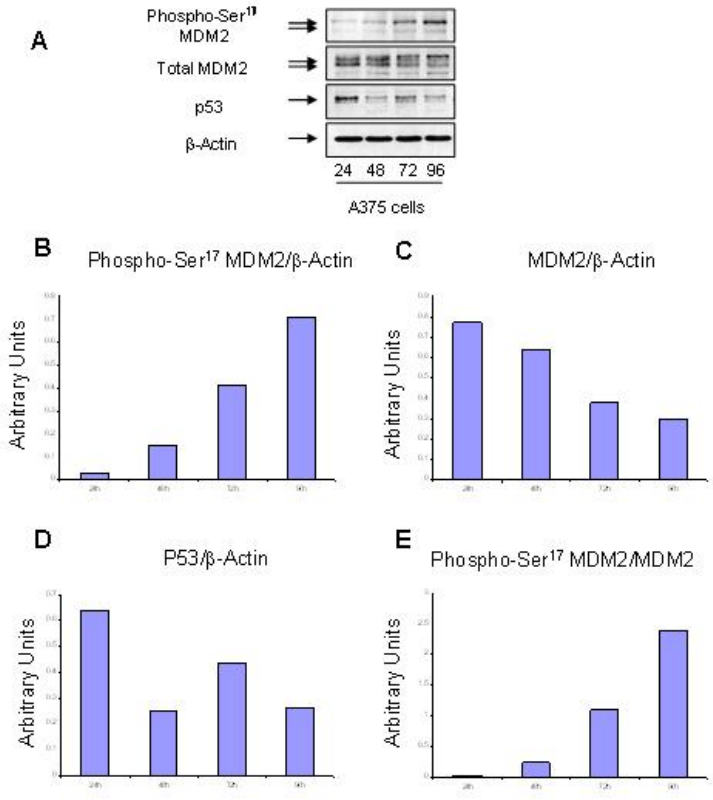

Figure 6.8 Effects of cell density on MDM2-lid phosphorylation. (A) A375 cells were grown to increasingly high density and cell lysates were processed for immunoblotting in order to determine the ratio of phospho-MDM2:MDM2:p53, as indicated. **(B)** Phospho-Ser17 levels increase with higher cell density as quantified divided by β-Actin. **(C and D)** Total MDM2 and p53 levels fall with increasing cell desity as quantified divided by β-Actin. **(E)** The ratio between phosphoSer17 MDM2 and total MDM2 increases with time quite dramatically as quantified (Data courtesy of Anne-Sophie Huart).

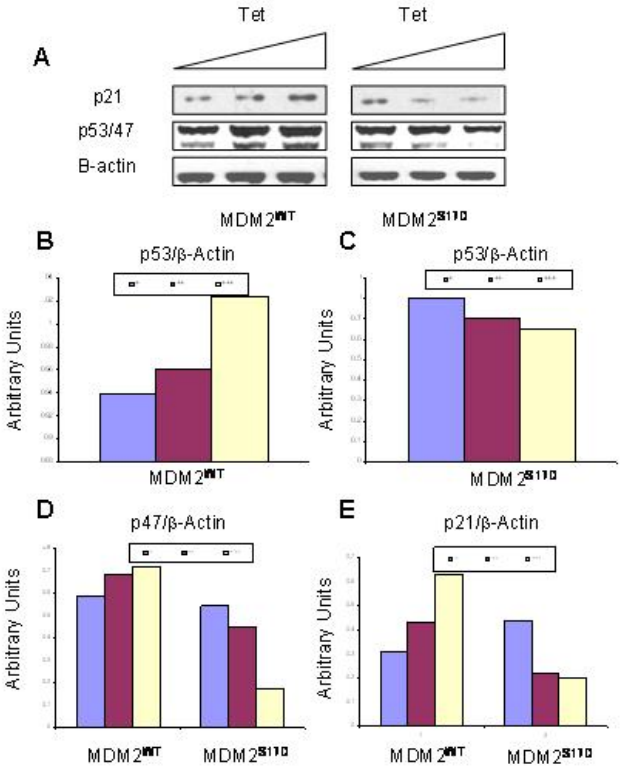

Figure 6.9 Stable Inducible Cells. (A) A375 cells (containing wtp53) were co-transfected with vectors expressing the TET-repressor (pcDNA.6/TR) and MDM2 expression vectors expressing either $MDM2^{WT}$ or $MDM2^{S17D}$ under control of the TET repressor (pT-REx-DEST). Cells transfected to drug resistance were chosen and analyzed for changes in p53 pathway activity after MDM2 induction using tetracycline: Left panel depicts increases in endogenous p53/p47 and p21 proteins after inducing $MDM2^{WT}$ expression and the right panel depicts decreases in p53/p47 and p21 proteins after inducing the activated $MDM2^{S17D}$. Quantitation in the changes in steady state levels of p53, p21 or p47 isoform as a function of MDM2 isoform induction can be seen in **(B) – (E).**

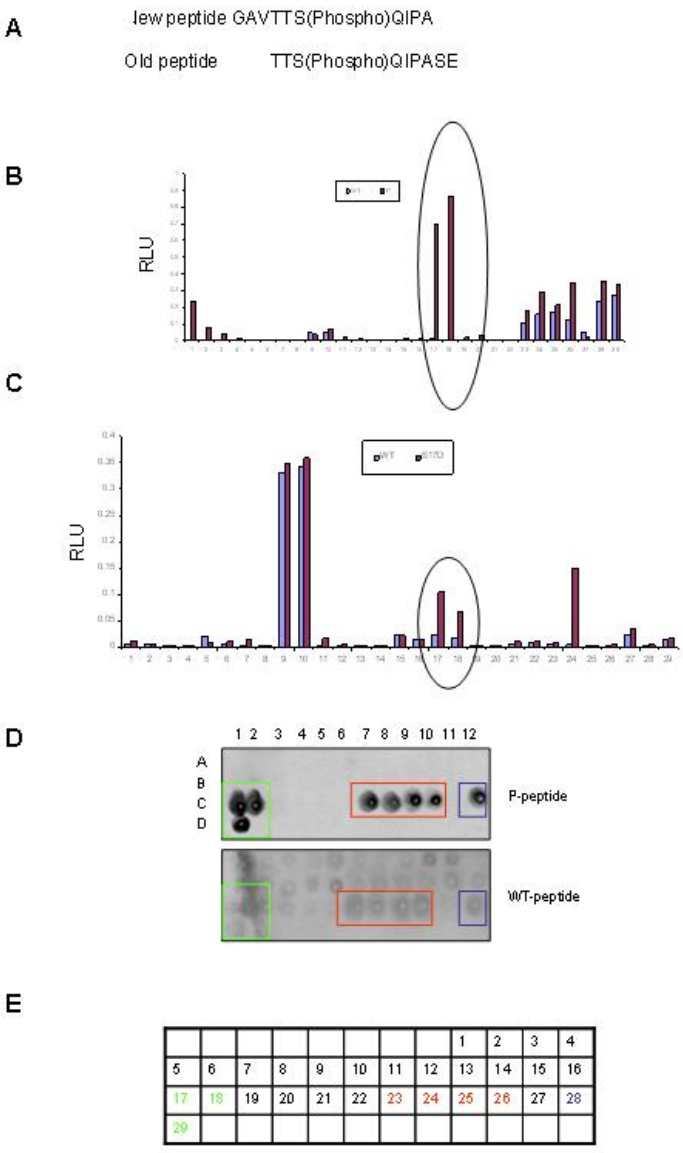
A
lew peptide GAVTTS(Phospho)QIPA
Old peptide TTS(Phospho)QIPASE
B
RLU
C
RLU
D
1 2 3 4 5 6 7 8 9 10 11 12
A
B
C
D
P-peptide
WT-peptide
E
1 2 3 4
5 6 7 8 9 10 11 12 13 14 15 16
17 18 19 20 21 22 23 24 25 26 27 28
29

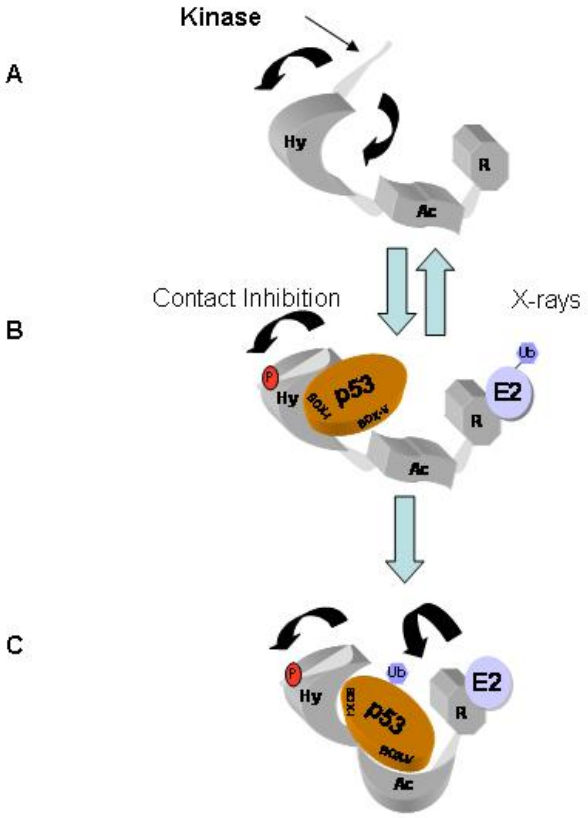

Figure 6.11 Phosphorylation of Ser17 activates the Dual-Site mechanism. **(A)** Under normal physiological conditions the MDM2 lid is in a slow equillibrium between and open and closed state. **(B)** Upon phosphorylation by an as yet unknown kinase the quillibrium is shifted towards a more open conformation increasing binding of substrates (in this case p53) to the hydrophobic pocket and **(C)** the acid domain leading to ubiquitination.

Chapter 7

CONCLUSIONS AND FUTURE PERSPECTIVES

p53 is a tumor suppressor that plays a pivotal role in the regulation of the cell cycle. It activates the cell cycle inhibitor p21, arresting cell growth and also activates genes involved in DNA repair and/or apoptosis. p53 is negatively regulated by the E3 ligase MDM2 which targets it for proteasomal degradation by ubiquitination. The mechanism of MDM2 catalysed ubiquitination was largely undefined before this study. We have identified a dual-site model in which ubiquitination of p53 occurs through binding of MDM2 and p53 through more central regions. This binding provides the signal which elicits the ubiquitination of p53 (Chapter 3). Initially binding occurs through the p53 transactivation domain to the MDM2 hydrophobic pocket and this induces conformational changes within MDM2 which allows the acid domain of MDM2 to bind to the more central BOX-V region of p53, which encompasses the ubiquitination signal (Fig 7.1A).

This study has also built on this dual-site model of MDM2 dependent ubiquitination of p53 and incorporated the lid domain of MDM2 in p53 ubiquitination, to which there was no previous function assigned. This was accomplished using various biochemical, biophysical and cell biological techniques. We have shown that a phospho-mimetic substitution within the lid at Ser^{17} enhances MDM2s binding to p53

compared to $MDM2^{WT}$ using *in vitro* protein binding assays and also that this mutation has an inhibitory effect on p53 protein levels *in vivo* (Chapter 4). It is also shown that $MDM2^{S17D}$ can degrade mutant forms of p53 which are normally refractory to degradation by MDM2 (Chapter 5). Previous studies have suggested that phosphorylation of the MDM2 lid allows it to adopt a conformation which occludes the hydrophobic pocket (McCoy et al., 2003). Using previously published NMR data we have predicted that when phosphorylated, it can bind to a region outwith the hydrophobic pocket of MDM2, adopting a conformation which is compatible with p53 binding. In fact, we propose a model where the MDM2 lid is in dynamic equilibrium between an open and closed state, adopting conformations which both occlude the pocket and leave the pocket in a more open state (Fig 7.1B). During this study, a paper was published which supported our equilibrium model, suggesting the lid was in equilibrium between an "open" and "closed" conformation (Showalter et al., 2008). We built upon this and found a basic region in MDM2 (Arginine (R) 97 and Lysine 98 (K)) with the potential to form a docking site for the phosphorylated Ser^{17} within the lid. This basic region is absent from MDM4, which also does not contain the lid, perhaps highlighting residues that have co-evolved with the MDM2 lid (Chapter 5).

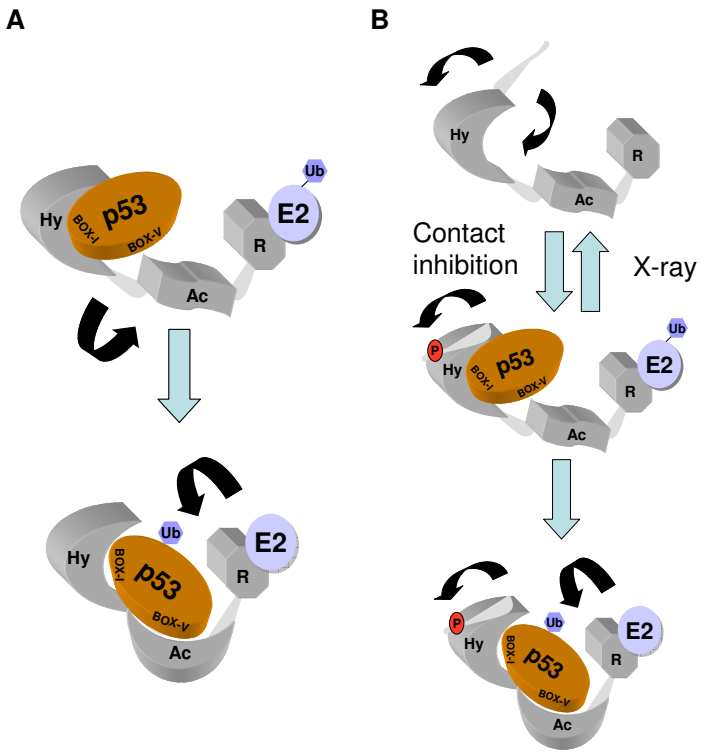

Figure 7.1 The Dual-Site Mechanism for MDM2 Catalyzed Ubiquitination of p53. **(A)** The hydrophobic pocket of MDM2 binds to the BOX-I site in p53 triggering a conformational change within MDM2 inducing binding of the acid domain of MDM2 to the BOX-V region of p53. This secondary binding triggers a signal which catalyzes the ubiquitination of p53. **(B)** The lid can function within the dual-site model by opening or closing MDM2s hydrophobic pocket. Phosphorylation of the lid at Ser17 induced p53 binding and subsequent ubiquitination.

Having identified a possible function for the phosphorylation at MDM2 Ser^{17} in negatively regulating p53 levels and identifying a potential mechanism, we also went on to develop phospho-specific antibodies to the Ser^{17} epitope (Chapter 6). These antibodies supported previous transfection data suggesting that in the presence of high levels of transfected $MDM2^{S17D}$, p53 levels were reduced, as in situations where

phospho-MDM2^{Ser17} was high then p53 and p21 levels were low and visa versa (Chapter 4).

There is growing evidence in the MDM2:p53 field that MDM2 can regulate the translation of p53. MDM2 has been shown to interact with many ribosomal proteins including L5, L11, L23 and S7, primarily through the acid domain of MDM2 (Ofir-Rosenfeld et al., 2008). The MDM2 acid domain is central in the ubiquitination of p53 and thus the binding of these ribosomal proteins to the acid domain of MDM2 inhibits the degradation of p53 and stabilizes it. This association of MDM2 with multiple ribosomal proteins has implicated MDM2 in the translation of proteins and is also highlighted by the fact that MDM2 can be found in complex with the polysomes (Candeias et al., 2008). These interactions are shown to increase when ribosome biogenesis is disrupted, a process called 'ribosomal biogenesis stress'(Ofir-Rosenfeld et al., 2008).

Our studies have shown that when MDM2 is transfected in a low expression vector, or is induced in stable A375 cell lines then p53 levels increase. This observation is not accepted in the wider community, with many peers suggesting this observation may be due to the activation of the p53 pathway by the transfection of DNA. However in our experiments I routinely control for the impact of transfection by using empty vector, and we found the transfection data is corroborated by inducible cell systems which also suggests these observations are not due to the effect of transient transfection causing cellular stress and instead specific expression levels of MDM2. The scientific community find it difficult to accept that 'MDM2-the negative regulator of p53' can in

fact stimulate p53s synthesis. MDM2 clearly has a role in degrading p53 via ubiquitination, but coupled to this is its ability to regulate the translation of the protein. This is highlighted by the effect of our $MDM2^{S17D}$ phospho-mimetic protein in switching the stimulation of p53 by $MDM2^{WT}$ to degradation of the p53 protein.

A couple of recent papers have bought this regulation of p53 translation by MDM2 to the forefront again, although they both differ slightly. One model proposes MDM2 mediates protein translation through binding to ribosomal proteins, specifically L26. L26 can bind to the 5' untranslated region (5' UTR) of p53 mRNA and stimulate its translation upon exposure to DNA damage, contributing to the stress-induced increase in p53 protein levels (Takagi et al., 2005). L26 is also a target for MDM2 degradation via the proteasome and thus the degradation of L26 by MDM2 leads to a reduction in L26 mediated p53 mRNA translation. MDM2 can either be inhibited from ubiquitinating p53 protein through the direct binding of L26 to the acid domain of MDM2 which results in p53 translation or it can degrade L26 via acting as an E3 ligase leading to the loss of L26 enhanced translation of p53 mRNA. Phosphorylation of $MDM2^{Ser17}$ could increase ubiquitination of L26, resulting in loss of L26 enhanced translation of p53. One aspect of this model which does not fit with our data is that we observe stimulation of p53 protein levels following transfection of MDM2 and p53 expression vectors. The transfected p53 plasmid does not contain the 5' UTR which is required for L26 to bind so its translation cannot be depend of L26. This does not entirely rule out the possibility that L26 does play a role in p53 translation as we also see

stimulation of p53 protein levels in inducible cell systems with endogenous p53, but it suggests there must be another route in which MDM2 can stimulate p53 translation.

Another paper highlighting MDM2s role in stimulating p53 synthesis suggests that it is the MDM2 protein that binds the p53 mRNA directly at the polysomes and enhances its translation (Candeias et al., 2008). They show that MDM2 binds to p53 mRNA through a RNA binding site within the RING of MDM2. This RNA binding region within the MDM2 RING binds the p53 mRNA at the site which encodes the MDM2 binding domain, termed the MDM2 binding domain encoding sequence (MDM-ES). Using quantitative real time PCR, the authors show that mutating the RNA binding site or deleting the RING domain reduces p53 mRNA binding to the MDM2 protein (Candeias et al., 2008). In support of this, we used the same assay to show that mutation of Ser^{17} to Asp^{17} prevents MDM2 binding to the p53 mRNA in a manner similar to removing the RING domain of MDM2 (Fig 7.2). This suggests that perhaps phophorylation of the MDM2 lid functions to control cellular levels of p53.

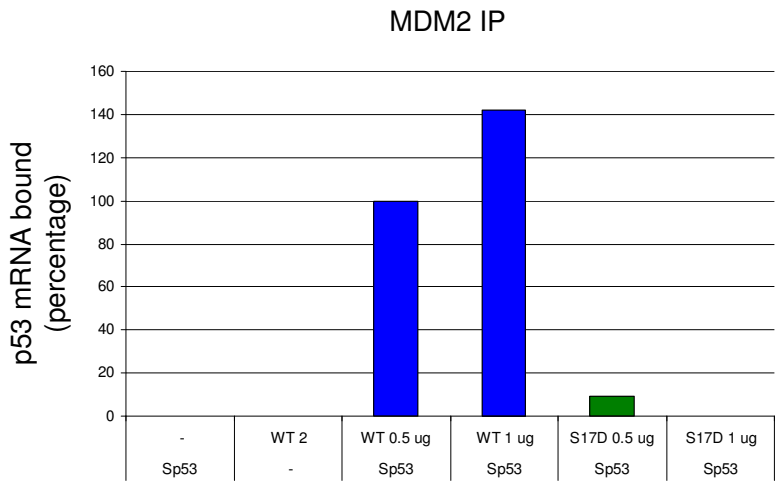

Figure 7.2 MDM2^{S17D} is unable to bind p53 mRNA. Immunoprecipitation was carried out as described in materials and methods followed by proteinase K treatment and RNA extraction. qRT-PCR was performed using p53 and control primers (Data courtesy of Magda Maslon).

Phosphorylation of MDM2^{Ser17} may therefore form the switch which could control MDM2s functions towards p53. Under normal conditions, MDM2 is phosphorylated at Ser^{17} which results in a MDM2 form which does not bind p53 mRNA and favours the ubiquitination of p53. Upon cellular stress MDM2^{Ser17} becomes dephosphorylated by an as yet unknown mechanism, activating MDM2s p53 mRNA binding ability and enhancing p53 translation. Thus phosphorylation of the lid at Ser^{17}, provides a switch between the p53 degradation and p53 promoting functions of MDM2.

To date, most drugs aimed at inhibiting the MDM2:p53 interaction have been modelled to fit within the hydrophobic pocket of MDM2. We have shown that drugs that bind within the hydrophobic pocket do not inhibit the ubiquitination of p53, and can in fact stimulate p53 ubiquitination. Due to this observation it may therefore be of benefit to design drugs around the BOX-V/Rb1 peptides which target the acid domain

instead of the hydrophobic pocket as these would both stabilize p53 and inhibit p53 ubiquitination. As well as targeting the acid domain of MDM2 it might also be an advantage to inhibit the flexibility of the lid as this would freeze the MDM2 conformation and prevent activation. If drugs could inhibit binding of the lid to the basic region formed by Arg97 and Lys98 through Ser^{17}, then it is possible that they would prevent MDM2 from adopting an activated conformation and would be unable to degrade p53, either through ubiquitination, or through decreased p53 mRNA binding.

Further *in vivo* characterization of the phospho-$MDM2^{Ser17}$ antibodies is required in order to enhance our understanding of signals involved in targeting the lid. The identification of additional cellular stress's which can alter the phosphorylation state of Ser^{17} and even the kinases or phosphatases responsible for phosphorylation or de-phosphorylation at this site need to be elucidated. Only then will we fully understand the signalling network which operates through this region and understand the complex signalling pathways which feed into and control MDM2/p53. Only then will we be able to generate drugs which target the control signals when they are deregulated following mutation and tumourogenic transformation.

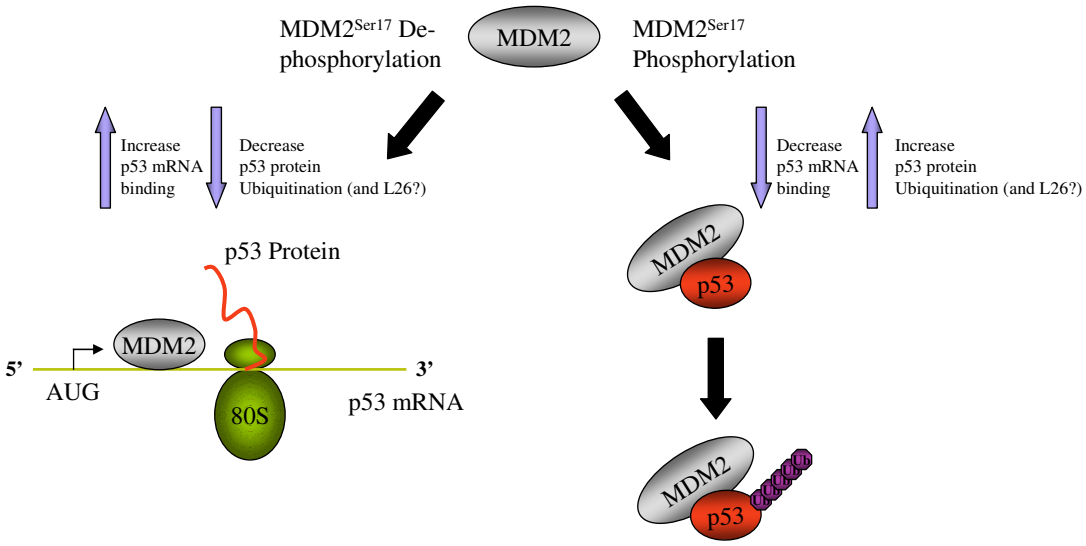

Figure 7.3 The Dual Function of MDM2. When MDM2^{Ser17} is unphosphorylated, MDM2 functions to regulate p53 mRNA synthesis through mRNA binding and its E3-ligase activities are silenced. Upon phosphorylation, MDM2 switches from p53 mRNA binding to p53 protein

REFERENCES

Adams, J. (2004) The proteasome: a suitable antineoplastic target. Nat Rev Cancer, 4(5), 349-360.

Ahn, J., and Prives, C. (2001) The C-terminus of p53: the more you learn the less you know. Nat Struct Biol, 8(9), 730-732.

Allende-Vega, N., McKenzie, L., and Meek, D. (2008) Transcription factor TAFII250 phosphorylates the acidic domain of Mdm2 through recruitment of protein kinase CK2. Mol Cell Biochem, 316(1-2), 99-106.

Appella, E., and Anderson, C.W. (2001) Post-translational modifications and activation of p53 by genotoxic stresses. Eur J Biochem, 268(10), 2764-2772.

Arva, N.C., Gopen, T.R., Talbott, K.E., Campbell, L.E., Chicas, A., White, D.E., Bond, G.L., Levine, A.J., and Bargonetti, J. (2005) A chromatin-associated and transcriptionally inactive p53-Mdm2 complex occurs in mdm2 SNP309 homozygous cells. J Biol Chem, 280(29), 26776-26787.

Baker, N.A., Sept, D., Joseph, S., Holst, M.J., and McCammon, J.A. (2001) Electrostatics of nanosystems: application to microtubules and the ribosome. Proc Natl Acad Sci U S A, 98(18), 10037-10041.

Bar, J., Cohen-Noyman, E., Geiger, B., and Oren, M. (2004) Attenuation of the p53 response to DNA damage by high cell density. Oncogene, 23(12), 2128-2137.

Baumeister, W., Walz, J., Zuhl, F., and Seemuller, E. (1998) The proteasome: paradigm of a self-compartmentalizing protease. Cell, 92(3), 367-380.

Benchimol, S., Lamb, P., Crawford, L.V., Sheer, D., Shows, T.B., Bruns, G.A., and Peacock, J. (1985) Transformation associated p53 protein is encoded by a gene on human chromosome 17. Somat Cell Mol Genet, 11(5), 505-510.

Bhat, K.P., Itahana, K., Jin, A., and Zhang, Y. (2004) Essential role of ribosomal protein L11 in mediating growth inhibition-induced p53 activation. Embo J, 23(12), 2402-2412.

Blattner, C., Hay, T., Meek, D.W., and Lane, D.P. (2002) Hypophosphorylation of Mdm2 augments p53 stability. Mol Cell Biol, 22(17), 6170-6182.

Blaydes, J.P., and Wynford-Thomas, D. (1998) The proliferation of normal human fibroblasts is dependent upon negative regulation of p53 function by mdm2. Oncogene, 16(25), 3317-3322.

Bode, A.M., and Dong, Z. (2004) Post-translational modification of p53 in tumorigenesis. Nat Rev Cancer, 4(10), 793-805.

Boehme, K.A., Kulikov, R., and Blattner, C. (2008) p53 stabilization in response to DNA damage requires Akt/PKB and DNA-PK. Proc Natl Acad Sci U S A, 105(22), 7785-7790.

Bond, G.L., Hu, W., Bond, E.E., Robins, H., Lutzker, S.G., Arva, N.C., Bargonetti, J., Bartel, F., Taubert, H., Wuerl, P., Onel, K., Yip, L., Hwang, S.J., Strong, L.C., Lozano, G., and Levine, A.J. (2004) A single nucleotide polymorphism

in the MDM2 promoter attenuates the p53 tumor suppressor pathway and accelerates tumor formation in humans. Cell, 119(5), 591-602.

Bothner, B., Lewis, W.S., DiGiammarino, E.L., Weber, J.D., Bothner, S.J., and Kriwacki, R.W. (2001) Defining the molecular basis of Arf and Hdm2 interactions. J Mol Biol, 314(2), 263-277.

Bottger, A., Bottger, V., Sparks, A., Liu, W.L., Howard, S.F., and Lane, D.P. (1997) Design of a synthetic Mdm2-binding mini protein that activates the p53 response in vivo. Curr Biol, 7(11), 860-869.

Bottger, V., Bottger, A., Howard, S.F., Picksley, S.M., Chene, P., Garcia-Echeverria, C., Hochkeppel, H.K., and Lane, D.P. (1996) Identification of novel mdm2 binding peptides by phage display. Oncogene, 13(10), 2141-2147.

Brooks, C.L., and Gu, W. (2006) p53 ubiquitination: Mdm2 and beyond. Mol Cell, 21(3), 307-315.

Brown, D.R., Thomas, C.A., and Deb, S.P. (1998) The human oncoprotein MDM2 arrests the cell cycle: elimination of its cell-cycle-inhibitory function induces tumorigenesis. Embo J, 17(9), 2513-2525.

Burch, L., Shimizu, H., Smith, A., Patterson, C., and Hupp, T.R. (2004) Expansion of protein interaction maps by phage peptide display using MDM2 as a prototypical conformationally flexible target protein. J Mol Biol, 337(1), 129-145.

Burch, L.R., Midgley, C.A., Currie, R.A., Lane, D.P., and Hupp, T.R. (2000) Mdm2 binding to a conformationally sensitive domain on p53 can be modulated by RNA. FEBS Lett, 472(1), 93-98.

Burnett, G., and Kennedy, E.P. (1954) The enzymatic phosphorylation of proteins. J Biol Chem, 211(2), 969-980.

Buschmann, T., Lerner, D., Lee, C.G., and Ronai, Z. (2001) The Mdm-2 amino terminus is required for Mdm2 binding and SUMO-1 conjugation by the E2 SUMO-1 conjugating enzyme Ubc9. J Biol Chem, 276(44), 40389-40395.

Butler, J.S., and Loh, S.N. (2003) Structure, function, and aggregation of the zinc-free form of the p53 DNA binding domain. Biochemistry, 42(8), 2396-2403.

Candeias, M.M., Malbert-Colas, L., Powell, D.J., Daskalogianni, C., Maslon, M.M., Naski, N., Bourougaa, K., Calvo, F., and Fahraeus, R. (2008) p53 mRNA controls p53 activity by managing Mdm2 functions. Nat Cell Biol.

Carvajal, D., Tovar, C., Yang, H., Vu, B.T., Heimbrook, D.C., and Vassilev, L.T. (2005) Activation of p53 by MDM2 antagonists can protect proliferating cells from mitotic inhibitors. Cancer Res, 65(5), 1918-1924.

Cernac, A., Lincoln, C., Lammer, D., and Estelle, M. (1997) The SAR1 gene of Arabidopsis acts downstream of the AXR1 gene in auxin response. Development, 124(8), 1583-1591.

Chen, L., and Chen, J. (2003) MDM2-ARF complex regulates p53 sumoylation. Oncogene, 22(34), 5348-5357.

Chene, P. (2003) Inhibiting the p53-MDM2 interaction: an important target for cancer therapy. Nat Rev Cancer, 3(2), 102-109.

Chene, P., Fuchs, J., Bohn, J., Garcia-Echeverria, C., Furet, P., and Fabbro, D. (2000) A small synthetic peptide, which inhibits the p53-hdm2 interaction, stimulates the p53 pathway in tumour cell lines. J Mol Biol, 299(1), 245-253.

Cho, Y., Gorina, S., Jeffrey, P.D., and Pavletich, N.P. (1994) Crystal structure of a p53 tumor suppressor-DNA complex: understanding tumorigenic mutations. Science, 265(5170), 346-355.

Ciechanover, A. (1998) The ubiquitin-proteasome pathway: on protein death and cell life. Embo J, 17(24), 7151-7160.

Clegg, H.V., Itahana, K., and Zhang, Y. (2008) Unlocking the Mdm2-p53 loop: ubiquitin is the key. Cell Cycle, 7(3), 287-292.

Cohen, P. (2002) The origins of protein phosphorylation. Nat Cell Biol, 4(5), E127-130.

Craig, A.L., Burch, L., Vojtesek, B., Mikutowska, J., Thompson, A., and Hupp, T.R. (1999) Novel phosphorylation sites of human tumour suppressor protein p53 at Ser20 and Thr18 that disrupt the binding of mdm2 (mouse double minute 2) protein are modified in human cancers. Biochem J, 342 (Pt 1), 133-141.

Czernik, A.J., Girault, J.A., Nairn, A.C., Chen, J., Snyder, G., Kebabian, J., and Greengard, P. (1991) Production of phosphorylation state-specific antibodies. Methods Enzymol, 201, 264-283.

Dai, M.S., and Lu, H. (2004) Inhibition of MDM2-mediated p53 ubiquitination and degradation by ribosomal protein L5. J Biol Chem, 279(43), 44475-44482.

Dai, M.S., Zeng, S.X., Jin, Y., Sun, X.X., David, L., and Lu, H. (2004) Ribosomal protein L23 activates p53 by inhibiting MDM2 function in response to ribosomal perturbation but not to translation inhibition. Mol Cell Biol, 24(17), 7654-7668.

Dastidar, S.G., Lane, D.P., and Verma, C.S. (2008) Multiple Peptide Conformations Give Rise to Similar Binding Affinities: Molecular Simulations of p53-MDM2. J Am Chem Soc.

Deshaies, R.J. (1999) SCF and Cullin/Ring H2-based ubiquitin ligases. Annu Rev Cell Dev Biol, 15, 435-467.

Dias, S.S., Milne, D.M., and Meek, D.W. (2006) c-Abl phosphorylates Hdm2 at tyrosine 276 in response to DNA damage and regulates interaction with ARF. Oncogene, 25(50), 6666-6671.

Duncan, S.J., Cooper, M.A., and Williams, D.H. (2003) Binding of an inhibitor of the p53/MDM2 interaction to MDM2. Chem Commun (Camb)(3), 316-317.

Dyson, H.J., and Wright, P.E. (2002) Coupling of folding and binding for unstructured proteins. Curr Opin Struct Biol, 12(1), 54-60.

el-Deiry, W.S., Kern, S.E., Pietenpol, J.A., Kinzler, K.W., and Vogelstein, B. (1992) Definition of a consensus binding site for p53. Nat Genet, 1(1), 45-49.

Elenbaas, B., Dobbelstein, M., Roth, J., Shenk, T., and Levine, A.J. (1996) The MDM2 oncoprotein binds specifically to RNA through its RING finger domain. Mol Med, 2(4), 439-451.

Elmen, J., Thonberg, H., Ljungberg, K., Frieden, M., Westergaard, M., Xu, Y., Wahren, B., Liang, Z., Orum, H., Koch, T., and Wahlestedt, C. (2005) Locked nucleic acid (LNA) mediated improvements in siRNA stability and functionality. Nucleic Acids Res, 33(1), 439-447.

Fahraeus, R., Fischer, P., Krausz, E., and Lane, D.P. (1999) New approaches to cancer therapies. J Pathol, 187(1), 138-146.

Fang, S., Jensen, J.P., Ludwig, R.L., Vousden, K.H., and Weissman, A.M. (2000) Mdm2 is a RING finger-dependent ubiquitin protein ligase for itself and p53. J Biol Chem, 275(12), 8945-8951.

Friedler, A., Veprintsev, D.B., Freund, S.M., von Glos, K.I., and Fersht, A.R. (2005) Modulation of binding of DNA to the C-terminal domain of p53 by acetylation. Structure, 13(4), 629-636.

Friedman, P.N., Chen, X., Bargonetti, J., and Prives, C. (1993) The p53 protein is an unusually shaped tetramer that binds directly to DNA. Proc Natl Acad Sci U S A, 90(8), 3319-3323.

Galigniana, M.D., Harrell, J.M., O'Hagen, H.M., Ljungman, M., and Pratt, W.B. (2004) Hsp90-binding immunophilins link p53 to dynein during p53 transport to the nucleus. J Biol Chem, 279(21), 22483-22489.

Giannakakou, P., Sackett, D.L., Ward, Y., Webster, K.R., Blagosklonny, M.V., and Fojo, T. (2000) p53 is associated with cellular microtubules and is transported to the nucleus by dynein. Nat Cell Biol, 2(10), 709-717.

Gill, G. (2003) Post-translational modification by the small ubiquitin-related modifier SUMO has big effects on transcription factor activity. Curr Opin Genet Dev, 13(2), 108-113.

Glenney, J.R., Jr., Zokas, L., and Kamps, M.P. (1988) Monoclonal antibodies to phosphotyrosine. J Immunol Methods, 109(2), 277-285.

Goldberg, A.L. (2007) Functions of the proteasome: from protein degradation and immune surveillance to cancer therapy. Biochem Soc Trans, 35(Pt 1), 12-17.

Gostissa, M., Hengstermann, A., Fogal, V., Sandy, P., Schwarz, S.E., Scheffner, M., and Del Sal, G. (1999) Activation of p53 by conjugation to the ubiquitin-like protein SUMO-1. Embo J, 18(22), 6462-6471.

Gotz, C., Kartarius, S., Scholtes, P., Nastainczyk, W., and Montenarh, M. (1999) Identification of a CK2 phosphorylation site in mdm2. Eur J Biochem, 266(2), 493-501.

Gouet, P., Courcelle, E., Stuart, D.I., and Metoz, F. (1999) ESPript: analysis of multiple sequence alignments in PostScript. Bioinformatics, 15(4), 305-308.

Grasberger, B.L., Lu, T., Schubert, C., Parks, D.J., Carver, T.E., Koblish, H.K., Cummings, M.D., LaFrance, L.V., Milkiewicz, K.L., Calvo, R.R., Maguire, D., Lattanze, J., Franks, C.F., Zhao, S., Ramachandren, K., Bylebyl, G.R., Zhang, M., Manthey, C.L., Petrella, E.C., Pantoliano, M.W., Deckman, I.C., Spurlino, J.C., Maroney, A.C., Tomczuk, B.E., Molloy, C.J., and Bone, R.F. (2005) Discovery and cocrystal structure of benzodiazepinedione HDM2 antagonists that activate p53 in cells. J Med Chem, 48(4), 909-912.

Grossman, S.R., Deato, M.E., Brignone, C., Chan, H.M., Kung, A.L., Tagami, H., Nakatani, Y., and Livingston, D.M. (2003) Polyubiquitination of p53 by a ubiquitin ligase activity of p300. Science, 300(5617), 342-344.

Grossman, S.R., Perez, M., Kung, A.L., Joseph, M., Mansur, C., Xiao, Z.X., Kumar, S., Howley, P.M., and Livingston, D.M. (1998) p300/MDM2 complexes participate in MDM2-mediated p53 degradation. Mol Cell, 2(4), 405-415.

Gu, W., and Roeder, R.G. (1997) Activation of p53 sequence-specific DNA binding by acetylation of the p53 C-terminal domain. Cell, 90(4), 595-606.

Gu, W., Shi, X.L., and Roeder, R.G. (1997) Synergistic activation of transcription by CBP and p53. Nature, 387(6635), 819-823.

Guedat, P., and Colland, F. (2007) Patented small molecule inhibitors in the ubiquitin proteasome system. BMC Biochem, 8 Suppl 1, S14.

Harris, S.L., and Levine, A.J. (2005) The p53 pathway: positive and negative feedback loops. Oncogene, 24(17), 2899-2908.

Hay, T.J., and Meek, D.W. (2000) Multiple sites of in vivo phosphorylation in the MDM2 oncoprotein cluster within two important functional domains. FEBS Lett, 478(1-2), 183-186.

Heffetz, D., Fridkin, M., and Zick, Y. (1989) Antibodies directed against phosphothreonine residues as potent tools for studying protein phosphorylation. Eur J Biochem, 182(2), 343-348.

Hershko, A., and Ciechanover, A. (1998) The ubiquitin system. Annu Rev Biochem, 67, 425-479.

Hershko, A., Heller, H., Eytan, E., and Reiss, Y. (1986) The protein substrate binding site of the ubiquitin-protein ligase system. J Biol Chem, 261(26), 11992-11999.

Hupp, T.R., and Lane, D.P. (1994a) Allosteric activation of latent p53 tetramers. Curr Biol, 4(10), 865-875.

Hupp, T.R., and Lane, D.P. (1994b) Regulation of the cryptic sequence-specific DNA-binding function of p53 by protein kinases. Cold Spring Harb Symp Quant Biol, 59, 195-206.

Hupp, T.R., Meek, D.W., Midgley, C.A., and Lane, D.P. (1992) Regulation of the specific DNA binding function of p53. Cell, 71(5), 875-886.

Jackson, M.W., and Berberich, S.J. (2000) MdmX protects p53 from Mdm2-mediated degradation. Mol Cell Biol, 20(3), 1001-1007.

Jackson, P.K., and Eldridge, A.G. (2002) The SCF ubiquitin ligase: an extended look. Mol Cell, 9(5), 923-925.

Jeffrey, P.D., Gorina, S., and Pavletich, N.P. (1995) Crystal structure of the tetramerization domain of the p53 tumor suppressor at 1.7 angstroms. Science, 267(5203), 1498-1502.

Jenuwein, T., and Allis, C.D. (2001) Translating the histone code. Science, 293(5532), 1074-1080.

Jimenez, G.S., Khan, S.H., Stommel, J.M., and Wahl, G.M. (1999) p53 regulation by post-translational modification and nuclear retention in response to diverse stresses. Oncogene, 18(53), 7656-7665.

Jin, A., Itahana, K., O'Keefe, K., and Zhang, Y. (2004) Inhibition of HDM2 and activation of p53 by ribosomal protein L23. Mol Cell Biol, 24(17), 7669-7680.

Joazeiro, C.A., and Weissman, A.M. (2000) RING finger proteins: mediators of ubiquitin ligase activity. Cell, 102(5), 549-552.

Joazeiro, C.A., Wing, S.S., Huang, H., Leverson, J.D., Hunter, T., and Liu, Y.C. (1999) The tyrosine kinase negative regulator c-Cbl as a RING-type, E2-dependent ubiquitin-protein ligase. Science, 286(5438), 309-312.

Jones, S.N., Roe, A.E., Donehower, L.A., and Bradley, A. (1995) Rescue of embryonic lethality in Mdm2-deficient mice by absence of p53. Nature, 378(6553), 206-208.

Kamijo, T., Weber, J.D., Zambetti, G., Zindy, F., Roussel, M.F., and Sherr, C.J. (1998) Functional and physical interactions of the ARF tumor suppressor with p53 and Mdm2. Proc Natl Acad Sci U S A, 95(14), 8292-8297.

Kisselev, A.F., Callard, A., and Goldberg, A.L. (2006) Importance of the different proteolytic sites of the proteasome and the efficacy of inhibitors varies with the protein substrate. J Biol Chem, 281(13), 8582-8590.

Kisselev, A.F., and Goldberg, A.L. (2001) Proteasome inhibitors: from research tools to drug candidates. Chem Biol, 8(8), 739-758.

Kitayner, M., Rozenberg, H., Kessler, N., Rabinovich, D., Shaulov, L., Haran, T.E., and Shakked, Z. (2006) Structural basis of DNA recognition by p53 tetramers. Mol Cell, 22(6), 741-753.

Koblish, H.K., Zhao, S., Franks, C.F., Donatelli, R.R., Tominovich, R.M., LaFrance, L.V., Leonard, K.A., Gushue, J.M., Parks, D.J., Calvo, R.R., Milkiewicz, K.L., Marugan, J.J., Raboisson, P., Cummings, M.D., Grasberger, B.L., Johnson, D.L., Lu, T., Molloy, C.J., and Maroney, A.C. (2006) Benzodiazepinedione inhibitors of the Hdm2:p53 complex suppress human tumor cell proliferation in vitro and sensitize tumors to doxorubicin in vivo. Mol Cancer Ther, 5(1), 160-169.

Koegl, M., Hoppe, T., Schlenker, S., Ulrich, H.D., Mayer, T.U., and Jentsch, S. (1999) A novel ubiquitination factor, E4, is involved in multiubiquitin chain assembly. Cell, 96(5), 635-644.

Kohler, A., Cascio, P., Leggett, D.S., Woo, K.M., Goldberg, A.L., and Finley, D. (2001) The axial channel of the proteasome core particle is gated by the Rpt2 ATPase and controls both substrate entry and product release. Mol Cell, 7(6), 1143-1152.

Kojima, K., Konopleva, M., Samudio, I.J., Shikami, M., Cabreira-Hansen, M., McQueen, T., Ruvolo, V., Tsao, T., Zeng, Z., Vassilev, L.T., and Andreeff, M. (2005) MDM2 antagonists induce p53-dependent apoptosis in AML: implications for leukemia therapy. Blood, 106(9), 3150-3159.

Kouzarides, T. (2000) Acetylation: a regulatory modification to rival phosphorylation? Embo J, 19(6), 1176-1179.

Kubisch, C., Dimagno, M.J., Tietz, A.B., Welsh, M.J., Ernst, S.A., Brandt-Nedelev, B., Diebold, J., Wagner, A.C., Goke, B., Williams, J.A., and Schafer, C. (2004) Overexpression of heat shock protein Hsp27 protects against cerulein-induced pancreatitis. Gastroenterology, 127(1), 275-286.

Kussie, P.H., Gorina, S., Marechal, V., Elenbaas, B., Moreau, J., Levine, A.J., and Pavletich, N.P. (1996) Structure of the MDM2 oncoprotein bound to the p53 tumor suppressor transactivation domain. Science, 274(5289), 948-953.

Laney, J.D., and Hochstrasser, M. (1999) Substrate targeting in the ubiquitin system. Cell, 97(4), 427-430.

Lawlor, M.A., and Alessi, D.R. (2001) PKB/Akt: a key mediator of cell proliferation, survival and insulin responses? J Cell Sci, 114(Pt 16), 2903-2910.

Lin, J., Chen, J., Elenbaas, B., and Levine, A.J. (1994) Several hydrophobic amino acids in the p53 amino-terminal domain are required for transcriptional activation, binding to mdm-2 and the adenovirus 5 E1B 55-kD protein. Genes Dev, 8(10), 1235-1246.

Linares, L.K., Kiernan, R., Triboulet, R., Chable-Bessia, C., Latreille, D., Cuvier, O., Lacroix, M., Le Cam, L., Coux, O., and Benkirane, M. (2007) Intrinsic ubiquitination activity of PCAF controls the stability of the oncoprotein Hdm2. Nat Cell Biol, 9(3), 331-338.

Linke, K., Mace, P.D., Smith, C.A., Vaux, D.L., Silke, J., and Day, C.L. (2008) Structure of the MDM2/MDMX RING domain heterodimer reveals dimerization is required for their ubiquitylation in trans. Cell Death Differ, 15(5), 841-848.

Liu, W.L., Midgley, C., Stephen, C., Saville, M., and Lane, D.P. (2001) Biological significance of a small highly conserved region in the N terminus of the p53 tumour suppressor protein. J Mol Biol, 313(4), 711-731.

Lohrum, M.A., Woods, D.B., Ludwig, R.L., Balint, E., and Vousden, K.H. (2001) C-terminal ubiquitination of p53 contributes to nuclear export. Mol Cell Biol, 21(24), 8521-8532.

Lomax, M.E., Barnes, D.M., Hupp, T.R., Picksley, S.M., and Camplejohn, R.S. (1998) Characterization of p53 oligomerization domain mutations isolated from Li-Fraumeni and Li-Fraumeni like family members. Oncogene, 17(5), 643-649.

Maclaine, N.J., Oster, B., Bundgaard, B., Fraser, J.A., Buckner, C., Lazo, P.A., Meek, D.W., Hollsberg, P., and Hupp, T.R. (2008) A central role for CK1 in catalysing phosphorylation of the P53 transactivation domain at serine 20 after HHV-6B viral infection. J Biol Chem.

Mandell, J.W. (2003) Phosphorylation state-specific antibodies: applications in investigative and diagnostic pathology. Am J Pathol, 163(5), 1687-1698.

Mani, A., and Gelmann, E.P. (2005) The ubiquitin-proteasome pathway and its role in cancer. J Clin Oncol, 23(21), 4776-4789.

Marechal, V., Elenbaas, B., Piette, J., Nicolas, J.C., and Levine, A.J. (1994) The ribosomal L5 protein is associated with mdm-2 and mdm-2-p53 complexes. Mol Cell Biol, 14(11), 7414-7420.

Marine, J.C., and Jochemsen, A.G. (2005) Mdmx as an essential regulator of p53 activity. Biochem Biophys Res Commun, 331(3), 750-760.

May, P., and May, E. (1999) Twenty years of p53 research: structural and functional aspects of the p53 protein. Oncogene, 18(53), 7621-7636.

Maya, R., Balass, M., Kim, S.T., Shkedy, D., Leal, J.F., Shifman, O., Moas, M., Buschmann, T., Ronai, Z., Shiloh, Y., Kastan, M.B., Katzir, E., and Oren, M. (2001) ATM-dependent phosphorylation of Mdm2 on serine 395: role in p53 activation by DNA damage. Genes Dev, 15(9), 1067-1077.

Mayo, L.D., and Donner, D.B. (2001) A phosphatidylinositol 3-kinase/Akt pathway promotes translocation of Mdm2 from the cytoplasm to the nucleus. Proc Natl Acad Sci U S A, 98(20), 11598-11603.

Mayo, L.D., Turchi, J.J., and Berberich, S.J. (1997) Mdm-2 phosphorylation by DNA-dependent protein kinase prevents interaction with p53. Cancer Res, 57(22), 5013-5016.

McCoy, M.A., Gesell, J.J., Senior, M.M., and Wyss, D.F. (2003) Flexible lid to the p53-binding domain of human Mdm2: implications for p53 regulation. Proc Natl Acad Sci U S A, 100(4), 1645-1648.

Meek, D.W., and Knippschild, U. (2003) Posttranslational modification of MDM2. Mol Cancer Res, 1(14), 1017-1026.

Meulmeester, E., Frenk, R., Stad, R., de Graaf, P., Marine, J.C., Vousden, K.H., and Jochemsen, A.G. (2003) Critical role for a central part of Mdm2 in the ubiquitylation of p53. Mol Cell Biol, 23(14), 4929-4938.

Michael, D., and Oren, M. (2003) The p53-Mdm2 module and the ubiquitin system. Semin Cancer Biol, 13(1), 49-58.

Miyauchi, Y., Yogosawa, S., Honda, R., Nishida, T., and Yasuda, H. (2002) Sumoylation of Mdm2 by protein inhibitor of activated STAT (PIAS) and RanBP2 enzymes. J Biol Chem, 277(51), 50131-50136.

Moll, U.M., and Petrenko, O. (2003) The MDM2-p53 interaction. Mol Cancer Res, 1(14), 1001-1008.

Momand, J., Jung, D., Wilczynski, S., and Niland, J. (1998) The MDM2 gene amplification database. Nucleic Acids Res, 26(15), 3453-3459.

Murray, J.K., and Gellman, S.H. (2007) Targeting protein-protein interactions: lessons from p53/MDM2. Biopolymers, 88(5), 657-686.

Nalepa, G., Rolfe, M., and Harper, J.W. (2006) Drug discovery in the ubiquitin-proteasome system. Nat Rev Drug Discov, 5(7), 596-613.

Neduva, V., Linding, R., Su-Angrand, I., Stark, A., de Masi, F., Gibson, T.J., Lewis, J., Serrano, L., and Russell, R.B. (2005) Systematic discovery of new recognition peptides mediating protein interaction networks. PLoS Biol, 3(12), e405.

Newman, D.J., Cragg, G.M., and Snader, K.M. (2003) Natural products as sources of new drugs over the period 1981-2002. J Nat Prod, 66(7), 1022-1037.

Nurse, P. (2000) A long twentieth century of the cell cycle and beyond. Cell, 100(1), 71-78.

Ofir-Rosenfeld, Y., Boggs, K., Michael, D., Kastan, M.B., and Oren, M. (2008) Mdm2 regulates p53 mRNA translation through inhibitory interactions with ribosomal protein L26. Mol Cell, 32(2), 180-189.

Ogawara, Y., Kishishita, S., Obata, T., Isazawa, Y., Suzuki, T., Tanaka, K., Masuyama, N., and Gotoh, Y. (2002) Akt enhances Mdm2-mediated ubiquitination and degradation of p53. J Biol Chem, 277(24), 21843-21850.

Oliner, J.D., Pietenpol, J.A., Thiagalingam, S., Gyuris, J., Kinzler, K.W., and Vogelstein, B. (1993) Oncoprotein MDM2 conceals the activation domain of tumour suppressor p53. Nature, 362(6423), 857-860.

Osaka, F., Saeki, M., Katayama, S., Aida, N., Toh, E.A., Kominami, K., Toda, T., Suzuki, T., Chiba, T., Tanaka, K., and Kato, S. (2000) Covalent modifier NEDD8 is essential for SCF ubiquitin-ligase in fission yeast. Embo J, 19(13), 3475-3484.

Pickart, C.M. (2001) Mechanisms underlying ubiquitination. Annu Rev Biochem, 70, 503-533.

Picksley, S.M., Vojtesek, B., Sparks, A., and Lane, D.P. (1994) Immunochemical analysis of the interaction of p53 with MDM2;--fine mapping of the MDM2 binding site on p53 using synthetic peptides. Oncogene, 9(9), 2523-2529.

Popowicz, G.M., Czarna, A., Rothweiler, U., Sszwagierczak, A., Krajewski, M., Weber, L., and Holak, T.A. (2007) Molecular Basis for the Inhibition of p53 by Mdmx. Cell Cycle, 6(19).

Poyurovsky, M.V., Priest, C., Kentsis, A., Borden, K.L., Pan, Z.Q., Pavletich, N., and Prives, C. (2007) The Mdm2 RING domain C-terminus is required for supramolecular assembly and ubiquitin ligase activity. Embo J, 26(1), 90-101.

Pratt, W.B., Galigniana, M.D., Harrell, J.M., and DeFranco, D.B. (2004) Role of hsp90 and the hsp90-binding immunophilins in signalling protein movement. Cell Signal, 16(8), 857-872.

Puppo, F., Murdaca, G., Ghio, M., and Indiveri, F. (2005) Emerging biologic drugs for the treatment of rheumatoid arthritis. Autoimmun Rev, 4(8), 537-541.

Reiss, Y., Heller, H., and Hershko, A. (1989) Binding sites of ubiquitin-protein ligase. Binding of ubiquitin-protein conjugates and of ubiquitin-carrier protein. J Biol Chem, 264(18), 10378-10383.

Ren, R. (2005) Mechanisms of BCR-ABL in the pathogenesis of chronic myelogenous leukaemia. Nat Rev Cancer, 5(3), 172-183.

Rodenhuis, S. (1992) ras and human tumors. Semin Cancer Biol, 3(4), 241-247.

Rohaly, G., Chemnitz, J., Dehde, S., Nunez, A.M., Heukeshoven, J., Deppert, W., and Dornreiter, I. (2005) A novel human p53 isoform is an essential element of the ATR-intra-S phase checkpoint. Cell, 122(1), 21-32.

Ross, A.H., Baltimore, D., and Eisen, H.N. (1981) Phosphotyrosine-containing proteins isolated by affinity chromatography with antibodies to a synthetic hapten. Nature, 294(5842), 654-656.

Rosser, M.F., Washburn, E., Muchowski, P.J., Patterson, C., and Cyr, D.M. (2007) Chaperone functions of the E3 ubiquitin ligase CHIP. J Biol Chem, 282(31), 22267-22277.

Saito, S., Goodarzi, A.A., Higashimoto, Y., Noda, Y., Lees-Miller, S.P., Appella, E., and Anderson, C.W. (2002) ATM mediates phosphorylation at multiple p53 sites, including Ser(46), in response to ionizing radiation. J Biol Chem, 277(15), 12491-12494.

Saito, S., Yamaguchi, H., Higashimoto, Y., Chao, C., Xu, Y., Fornace, A.J., Jr., Appella, E., and Anderson, C.W. (2003) Phosphorylation site interdependence of human p53 post-translational modifications in response to stress. J Biol Chem, 278(39), 37536-37544.

Sakaguchi, K., Sakamoto, H., Xie, D., Erickson, J.W., Lewis, M.S., Anderson, C.W., and Appella, E. (1997) Effect of phosphorylation on tetramerization of the tumor suppressor protein p53. J Protein Chem, 16(5), 553-556.

Scheffner, M., Nuber, U., and Huibregtse, J.M. (1995) Protein ubiquitination involving an E1-E2-E3 enzyme ubiquitin thioester cascade. Nature, 373(6509), 81-83.

Schon, O., Friedler, A., Bycroft, M., Freund, S.M., and Fersht, A.R. (2002) Molecular mechanism of the interaction between MDM2 and p53. J Mol Biol, 323(3), 491-501.

Schon, O., Friedler, A., Freund, S., and Fersht, A.R. (2004) Binding of p53-derived ligands to MDM2 induces a variety of long range conformational changes. J Mol Biol, 336(1), 197-202.

Sherr, C.J. (1998) Tumor surveillance via the ARF-p53 pathway. Genes Dev, 12(19), 2984-2991.

Shimizu, H., Burch, L.R., Smith, A.J., Dornan, D., Wallace, M., Ball, K.L., and Hupp, T.R. (2002) The conformationally flexible S9-S10 linker region in the core domain of p53 contains a novel MDM2 binding site whose mutation increases ubiquitination of p53 in vivo. J Biol Chem, 277(32), 28446-28458.

Shimizu, H., and Hupp, T.R. (2003) Intrasteric regulation of MDM2. Trends Biochem Sci, 28(7), 346-349.

Shimizu, H., Saliba, D., Wallace, M., Finlan, L., Langridge-Smith, P.R., and Hupp, T.R. (2006) Destabilizing missense mutations in the tumour suppressor protein p53 enhance its ubiquitination in vitro and in vivo. Biochem J, 397(2), 355-367.

Showalter, S.A., Bruschweiler-Li, L., Johnson, E., Zhang, F., and Bruschweiler, R. (2008) Quantitative lid dynamics of MDM2 reveals differential ligand binding modes of the p53-binding cleft. J Am Chem Soc, 130(20), 6472-6478.

Shvarts, A., Steegenga, W.T., Riteco, N., van Laar, T., Dekker, P., Bazuine, M., van Ham, R.C., van der Houven van Oordt, W., Hateboer, G., van der Eb, A.J., and Jochemsen, A.G. (1996) MDMX: a novel p53-binding protein with some functional properties of MDM2. Embo J, 15(19), 5349-5357.

Sionov, R.V., Coen, S., Goldberg, Z., Berger, M., Bercovich, B., Ben-Neriah, Y., Ciechanover, A., and Haupt, Y. (2001) c-Abl regulates p53 levels under

normal and stress conditions by preventing its nuclear export and ubiquitination. Mol Cell Biol, 21(17), 5869-5878.

Soussi, T., and May, P. (1996) Structural aspects of the p53 protein in relation to gene evolution: a second look. J Mol Biol, 260(5), 623-637.

Sternberger, L.A., and Sternberger, N.H. (1983) Monoclonal antibodies distinguish phosphorylated and nonphosphorylated forms of neurofilaments in situ. Proc Natl Acad Sci U S A, 80(19), 6126-6130.

Stevens, C., Pettersson, S., Wawrzynow, B., Wallace, M., Ball, K., Zylicz, A., and Hupp, T.R. (2008) ATP stimulates MDM2-mediated inhibition of the DNA-binding function of E2F1. Febs J.

Stoll, R., Renner, C., Hansen, S., Palme, S., Klein, C., Belling, A., Zeslawski, W., Kamionka, M., Rehm, T., Muhlhahn, P., Schumacher, R., Hesse, F., Kaluza, B., Voelter, W., Engh, R.A., and Holak, T.A. (2001) Chalcone derivatives antagonize interactions between the human oncoprotein MDM2 and p53. Biochemistry, 40(2), 336-344.

Stuhmer, T., Chatterjee, M., Hildebrandt, M., Herrmann, P., Gollasch, H., Gerecke, C., Theurich, S., Cigliano, L., Manz, R.A., Daniel, P.T., Bommert, K., Vassilev, L.T., and Bargou, R.C. (2005) Nongenotoxic activation of the p53 pathway as a therapeutic strategy for multiple myeloma. Blood, 106(10), 3609-3617.

Sudol, M., Bork, P., Einbond, A., Kastury, K., Druck, T., Negrini, M., Huebner, K., and Lehman, D. (1995a) Characterization of the mammalian YAP (Yes-associated protein) gene and its role in defining a novel protein module, the WW domain. J Biol Chem, 270(24), 14733-14741.

Sudol, M., Chen, H.I., Bougeret, C., Einbond, A., and Bork, P. (1995b) Characterization of a novel protein-binding module--the WW domain. FEBS Lett, 369(1), 67-71.

Sui, G., Affar el, B., Shi, Y., Brignone, C., Wall, N.R., Yin, P., Donohoe, M., Luke, M.P., Calvo, D., Grossman, S.R., and Shi, Y. (2004) Yin Yang 1 is a negative regulator of p53. Cell, 117(7), 859-872.

Sullivan, M.L., and Vierstra, R.D. (1991) Cloning of a 16-kDa ubiquitin carrier protein from wheat and Arabidopsis thaliana. Identification of functional domains by in vitro mutagenesis. J Biol Chem, 266(35), 23878-23885.

Takagi, M., Absalon, M.J., McLure, K.G., and Kastan, M.B. (2005) Regulation of p53 translation and induction after DNA damage by ribosomal protein L26 and nucleolin. Cell, 123(1), 49-63.

Tanimura, S., Ohtsuka, S., Mitsui, K., Shirouzu, K., Yoshimura, A., and Ohtsubo, M. (1999) MDM2 interacts with MDMX through their RING finger domains. FEBS Lett, 447(1), 5-9.

Tao, W., and Levine, A.J. (1999) Nucleocytoplasmic shuttling of oncoprotein Hdm2 is required for Hdm2-mediated degradation of p53. Proc Natl Acad Sci U S A, 96(6), 3077-3080.

Tateishi, K., Omata, M., Tanaka, K., and Chiba, T. (2001) The NEDD8 system is essential for cell cycle progression and morphogenetic pathway in mice. J Cell Biol, 155(4), 571-579.

Terzian, T., Suh, Y.A., Iwakuma, T., Post, S.M., Neumann, M., Lang, G.A., Van Pelt, C.S., and Lozano, G. (2008) The inherent instability of mutant p53 is alleviated by Mdm2 or p16INK4a loss. Genes Dev, 22(10), 1337-1344.

Toledo, F., Krummel, K.A., Lee, C.J., Liu, C.W., Rodewald, L.W., Tang, M., and Wahl, G.M. (2006) A mouse p53 mutant lacking the proline-rich domain rescues Mdm4 deficiency and provides insight into the Mdm2-Mdm4-p53 regulatory network. Cancer Cell, 9(4), 273-285.

Toledo, F., and Wahl, G.M. (2006) Regulating the p53 pathway: in vitro hypotheses, in vivo veritas. Nat Rev Cancer, 6(12), 909-923.

Toledo, F., and Wahl, G.M. (2007) MDM2 and MDM4: p53 regulators as targets in anticancer therapy. Int J Biochem Cell Biol, 39(7-8), 1476-1482.

Tortora, G., Caputo, R., Damiano, V., Bianco, R., Chen, J., Agrawal, S., Bianco, A.R., and Ciardiello, F. (2000) A novel MDM2 anti-sense oligonucleotide has anti-tumor activity and potentiates cytotoxic drugs acting by different mechanisms in human colon cancer. Int J Cancer, 88(5), 804-809.

Tsukamoto, S., Yoshida, T., Hosono, H., Ohta, T., and Yokosawa, H. (2006) Hexylitaconic acid: a new inhibitor of p53-HDM2 interaction isolated from a marine-derived fungus, Arthrinium sp. Bioorg Med Chem Lett, 16(1), 69-71.

Uhrinova, S., Uhrin, D., Powers, H., Watt, K., Zheleva, D., Fischer, P., McInnes, C., and Barlow, P.N. (2005) Structure of free MDM2 N-terminal domain reveals conformational adjustments that accompany p53-binding. J Mol Biol, 350(3), 587-598.

Uldrijan, S., Pannekoek, W.J., and Vousden, K.H. (2007) An essential function of the extreme C-terminus of MDM2 can be provided by MDMX. Embo J, 26(1), 102-112.

Vassilev, L.T. (2004) Small-molecule antagonists of p53-MDM2 binding: research tools and potential therapeutics. Cell Cycle, 3(4), 419-421.

Vassilev, L.T. (2005) p53 Activation by small molecules: application in oncology. J Med Chem, 48(14), 4491-4499.

Vassilev, L.T., Vu, B.T., Graves, B., Carvajal, D., Podlaski, F., Filipovic, Z., Kong, N., Kammlott, U., Lukacs, C., Klein, C., Fotouhi, N., and Liu, E.A. (2004) In vivo activation of the p53 pathway by small-molecule antagonists of MDM2. Science, 303(5659), 844-848.

Voges, D., Zwickl, P., and Baumeister, W. (1999) The 26S proteasome: a molecular machine designed for controlled proteolysis. Annu Rev Biochem, 68, 1015-1068.

Walerych, D., Kudla, G., Gutkowska, M., Wawrzynow, B., Muller, L., King, F.W., Helwak, A., Boros, J., Zylicz, A., and Zylicz, M. (2004) Hsp90 chaperones wild-type p53 tumor suppressor protein. J Biol Chem, 279(47), 48836-48845.

Wallace, M., Worrall, E., Pettersson, S., Hupp, T.R., and Ball, K.L. (2006) Dual-site regulation of MDM2 E3-ubiquitin ligase activity. Mol Cell, 23(2), 251-263.

Wang, X., Taplick, J., Geva, N., and Oren, M. (2004) Inhibition of p53 degradation by Mdm2 acetylation. FEBS Lett, 561(1-3), 195-201.

Wawrzynow, B., Zylicz, A., Wallace, M., Hupp, T., and Zylicz, M. (2007) MDM2 chaperones the p53 tumor suppressor. J Biol Chem, 282(45), 32603-32612.

Weber, J.D., Kuo, M.L., Bothner, B., DiGiammarino, E.L., Kriwacki, R.W., Roussel, M.F., and Sherr, C.J. (2000) Cooperative signals governing ARF-mdm2 interaction and nucleolar localization of the complex. Mol Cell Biol, 20(7), 2517-2528.

Weber, J.D., Taylor, L.J., Roussel, M.F., Sherr, C.J., and Bar-Sagi, D. (1999) Nucleolar Arf sequesters Mdm2 and activates p53. Nat Cell Biol, 1(1), 20-26.

Weinberg, R.L., Veprintsev, D.B., Bycroft, M., and Fersht, A.R. (2005) Comparative binding of p53 to its promoter and DNA recognition elements. J Mol Biol, 348(3), 589-596.

Weissman, A.M. (2001) Themes and variations on ubiquitylation. Nat Rev Mol Cell Biol, 2(3), 169-178.

White, D.E., Talbott, K.E., Arva, N.C., and Bargonetti, J. (2006) Mouse double minute 2 associates with chromatin in the presence of p53 and is released to facilitate activation of transcription. Cancer Res, 66(7), 3463-3470.

Willems, A.R., Goh, T., Taylor, L., Chernushevich, I., Shevchenko, A., and Tyers, M. (1999) SCF ubiquitin protein ligases and phosphorylation-dependent proteolysis. Philos Trans R Soc Lond B Biol Sci, 354(1389), 1533-1550.

Winter, M., Milne, D., Dias, S., Kulikov, R., Knippschild, U., Blattner, C., and Meek, D. (2004) Protein kinase CK1delta phosphorylates key sites in the acidic domain of murine double-minute clone 2 protein (MDM2) that regulate p53 turnover. Biochemistry, 43(51), 16356-16364.

Wu, X., Bayle, J.H., Olson, D., and Levine, A.J. (1993) The p53-mdm-2 autoregulatory feedback loop. Genes Dev, 7(7A), 1126-1132.

Xiong, Y., Hannon, G.J., Zhang, H., Casso, D., Kobayashi, R., and Beach, D. (1993) p21 is a universal inhibitor of cyclin kinases. Nature, 366(6456), 701-704.

Xirodimas, D.P., Chisholm, J., Desterro, J.M., Lane, D.P., and Hay, R.T. (2002) P14ARF promotes accumulation of SUMO-1 conjugated (H)Mdm2. FEBS Lett, 528(1-3), 207-211.

Xirodimas, D.P., Saville, M.K., Bourdon, J.C., Hay, R.T., and Lane, D.P. (2004) Mdm2-mediated NEDD8 conjugation of p53 inhibits its transcriptional activity. Cell, 118(1), 83-97.

Yano, T., Taura, C., Shibata, M., Hirono, Y., Ando, S., Kusubata, M., Takahashi, T., and Inagaki, M. (1991) A monoclonal antibody to the phosphorylated form of glial fibrillary acidic protein: application to a non-radioactive method for measuring protein kinase activities. Biochem Biophys Res Commun, 175(3), 1144-1151.

Yin, Y., Stephen, C.W., Luciani, M.G., and Fahraeus, R. (2002) p53 Stability and activity is regulated by Mdm2-mediated induction of alternative p53 translation products. Nat Cell Biol, 4(6), 462-467.

Yu, G.W., Allen, M.D., Andreeva, A., Fersht, A.R., and Bycroft, M. (2006a) Solution structure of the C4 zinc finger domain of HDM2. Protein Sci, 15(2), 384-389.

Yu, G.W., Rudiger, S., Veprintsev, D., Freund, S., Fernandez-Fernandez, M.R., and Fersht, A.R. (2006b) The central region of HDM2 provides a second binding site for p53. Proc Natl Acad Sci U S A, 103(5), 1227-1232.

Zacchi, P., Gostissa, M., Uchida, T., Salvagno, C., Avolio, F., Volinia, S., Ronai, Z., Blandino, G., Schneider, C., and Del Sal, G. (2002) The prolyl isomerase Pin1 reveals a mechanism to control p53 functions after genotoxic insults. Nature, 419(6909), 853-857.

Zhang, Y., Wolf, G.W., Bhat, K., Jin, A., Allio, T., Burkhart, W.A., and Xiong, Y. (2003) Ribosomal protein L11 negatively regulates oncoprotein MDM2 and mediates a p53-dependent ribosomal-stress checkpoint pathway. Mol Cell Biol, 23(23), 8902-8912.

Zhang, Y., and Xiong, Y. (2001) Control of p53 ubiquitination and nuclear export by MDM2 and ARF. Cell Growth Differ, 12(4), 175-186.

Zhao, J., Wang, M., Chen, J., Luo, A., Wang, X., Wu, M., Yin, D., and Liu, Z. (2002) The initial evaluation of non-peptidic small-molecule HDM2 inhibitors based on p53-HDM2 complex structure. Cancer Lett, 183(1), 69-77.

Zheng, H., You, H., Zhou, X.Z., Murray, S.A., Uchida, T., Wulf, G., Gu, L., Tang, X., Lu, K.P., and Xiao, Z.X. (2002) The prolyl isomerase Pin1 is a regulator of p53 in genotoxic response. Nature, 419(6909), 849-853.

Zhou, B.B., and Elledge, S.J. (2000) The DNA damage response: putting checkpoints in perspective. Nature, 408(6811), 433-439.

Zhou, B.P., Liao, Y., Xia, W., Zou, Y., Spohn, B., and Hung, M.C. (2001) HER-2/neu induces p53 ubiquitination via Akt-mediated MDM2 phosphorylation. Nat Cell Biol, 3(11), 973-982.

Zhou, R., Frum, R., Deb, S., and Deb, S.P. (2005) The growth arrest function of the human oncoprotein mouse double minute-2 is disabled by downstream mutation in cancer cells. Cancer Res, 65(5), 1839-1848.